Department of Chemistry

FERROCENIC METAL CHELATORS: SYNTHESIS, BIOLOGICAL AND ELECTROCHEMICAL STUDIES

By

Freddy MUNYOLOLO MUGANZA

A dissertation presented for the degree of

MASTER OF SCIENCE

In the subject

CHEMISTRY

Supervisors: Assoc.Professor Kelly Chibale and Assoc. Professor Allan T Hutton

January 2006

ABSTRACT

Resistance of *Plasmodium falciparum* (*P. falciparum*) to well-established drugs throughout the world has necessitated urgent alternative treatment for malaria. Iron chelation therapy was considered as a possible approach since iron has been found crucial in the metabolic pathways of *P.falciparum*.

A series of novel iron chelators were designed and synthesized based on thiosemicarbazone and/or ferrocenyl moieties. The novel compounds were characterized by NMR, infrared (IR) and mass spectroscopy as well as microanalysis and subjected to biological evaluation.

All the *N*-substituted ferrocenic thiosemicarbazones were evaluated against a chloroquine resistant W2 strain of the malaria parasite *P. falciparum* and enzymes (falcipains 2 & 3) derived from the same parasite. The intermediate thiosemicarbazone thioesters were also tested against different malaria parasite including chloroquine resistant (K1) and chloroquine sensitive (3D7) strains as well as against the causative agent of African trypanosomiasis, *Trypanosoma brucei* (*T. brucei*).

Of the intermediate thiosemicarbazone thioesters, compound **44y** a bipyridyl compound was the most active against both K1 and 3D7 strains with ED_{50} values of 0.18 μg/ml (0.625 μM) and 0.021 μg/ml (0.072 μM), respectively. However, this compound **44y** also showed similar toxicity to mammalian cells. A number of thiosemicarbazone thioesters displaying preferential potency against a chloroquine resistant (K1) strain were noted. For example, compounds **44a-h**, **44k-m**, **44s, 44u-v** were found to be more active against K1 than against the chloroquine sensitive (3D7) strain.

Against *T. brucei*, compound **44x** and **44y** were the most active with an ED_{50} of 0.12 μg/ml (0.52 μM) and 0.15 μg/ml (0.53 μM), respectively .

Within the synthesized *N*-substituted ferrocenic thiosemicarbazones, bipyridyl compound **42o** was found to be the most active against W2 strain with an IC_{50} of 0.11 μM compared to the rest but moderately active against the enzymes, FP-2 and FP-3, with IC_{50} values of 36.20 μM and 31.02 μM, respectively. Being a metal chelator, this *N*-substituted thiosemicarbazone could mechanistically also act as a metal-interactive cysteine protease inhibitor.

The electrochemical behaviour of these compounds was measured for correlation purposes between biological activities and electrochemical behaviour. The investigation showed no correlation.

ACKNOWLEDGEMENTS

First of all, I thank the ALMIGHTY GOD, the creator of the earth and the heavens, for keeping me alive up to now. His mercy and grace upon my life are immeasurable. Therefore I will always testify to his name and deeds as long as I am living. May all Glory and Honour go to Him.

GOD made this work possible for me through the assistance of his beloved sons such as my two enthusiastic supervisors, Associate Professor Kelly Chibale and Associate Professor Alan T. Hutton. Despite my background, they have been patient with me and so much helpful in terms of transferring knowledge to me. Besides science, they were giving me advice about social life. Then I understood their responsibilities to me as parents. I will never forget your contribution in my life.

My gratitude goes to my wife, Muganza Kajuru, who has been supportive during these two years of hard work and to my little baby boy Jamie Muganza Katale who is now eight months old. I say may the GOD of your father bless you with all the blessings; when you will be big enough remember these days.

Thanks to all the students in the chemistry laboratories, especially , Jamy Feng, Richard Gessner, Franck Chouteau, Natasha October, Linda Mbeki and Clare Muhanji. I also wish to thank Chitalu Musonda and Dawn Webber for all their help, guidance and knowledge. I could not have done this without your support. Thanks guys.

I would also like to thank Noel Hendricks and Pete Roberts for the NMR experiments, Tommy van der Merwe (University of the Witswatersrand) and Associate Professor Peter Smith (University of Cape Town, Pharmacology Department) for mass spectroscopy, Pierro Benincasa for microanalysis.

The laboratories of Professor Philip J. Rosenthal (University of California, San Francisco, USA) and Dr. Vanessa Yardley (London School of Hygiene and Tropical Medicine, UK) are gratefully acknowledged for the biological studies.

ABBREVIATIONS

DCM	Dichloromethane
DMSO	Dimethylsulfoxide
Et	Ethyl
EtOAc	Ethyl Acetate
MeOH	Methanol
eq	Equivalent
Hex	Hexane
Cp	Cyclopentadiene
Fc	Ferrocene
Fe	Iron
LR-MS	Low Resolution Mass Spectroscopy
HRMS	High Resolution Mass Spectroscopy
hrs	Hours
IC_{50}	Inhibitory concentration to inhibit 50% of enzyme activity or parasite growth
ED_{50}	Effective dose required to kill half the parasite population
IR	Infrared
C	Celcius
mmol	Millimole
μM	Micromolar
Me	Methyl
MS	Mass Spectroscopy
NMR	Nuclear Magnetic Resonance
P	*Plasmodium*
rt	Room Temperature
SAR	Structure-Activity Relationship
TLC	Thin Layer Chromatography
s	singlet

d	doublet
dd	doublet of doublets
t	triplet
td	triplet of doublets
Ar	Aromatic
m	multiplet
δ	chemical shift in part per million
cm^{-1}	wavelength unit
mp	melting point
m/z	mass to charge ratio
ppm	parts per million
R_f	Retention factor

TABLE OF CONTENTS

CHAPTER 1
INTRODUCTION

Malaria is one of the most significant infectious diseases in the world. It is endemic throughout the entire tropical region of the earth except for high mountain areas, deserts and a few islands.[1]
It has been reported that mortality from malaria is over one million persons worldwide each year and the most affected are children under five years old. The disease presents a public health problem for 2.4 billion people which represents over 40% of world population in 90 countries.[2]

1.1 Disease

Malaria is a protozoal disease caused by a parasite of the genus *Plasmodium*, spread to humans *via* bites by female mosquitoes, *Anopheles* (Fig.1.1).

Figure 1.1: Female anopheles mosquito[3]

Four species of *Plasmodium* are responsible for human malaria namely *P. vivax*, *P. malariae*, *P. ovale* and *P. falciparum*. Of these four strains, *P. falciparum* is the most deadly. This parasite is commonly found in tropical Africa, South America and South East Asia including the Indian Sub-continent, and claims more than 95 % of the malaria related deaths in these regions.[4]

Each year the number of patients who are suffering from malaria is around 300 million which is five times as many as the combined cases of tuberculosis, AIDS, measles and leprosy.[5-8]

The increase in malaria cases is due to many reasons including human migration, as well as land utilization especially plantation agriculture. This leads to contamination of the previously safe areas such as the highland areas of East Africa.[9] The map below shows that over 90% of the African continent is in danger from the disease.

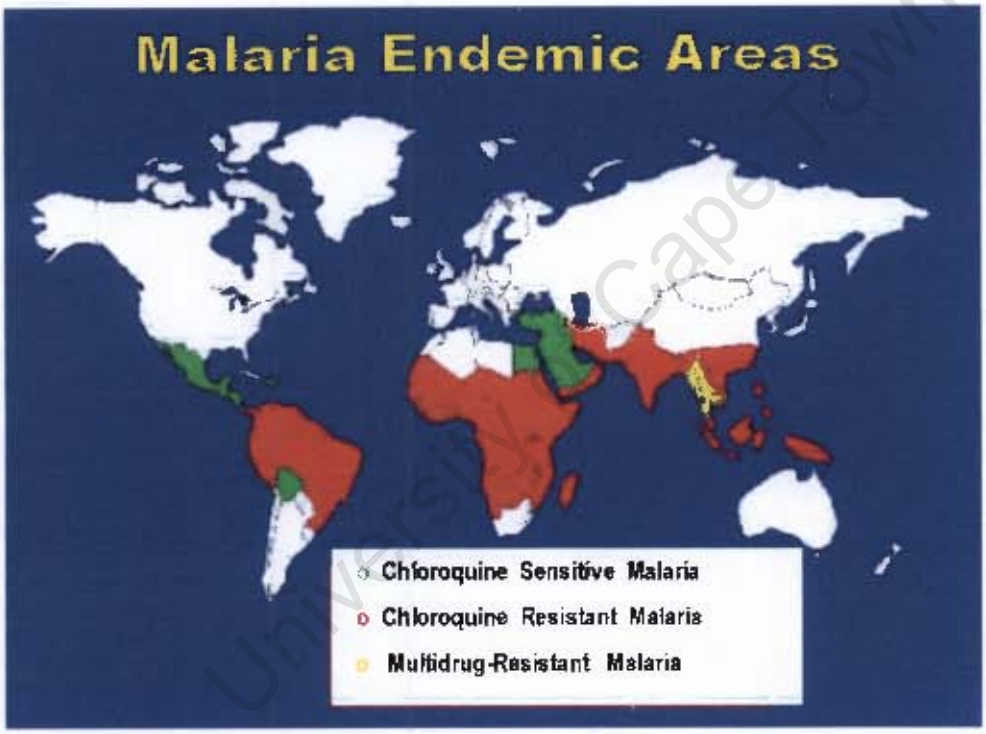

Figure 1.2: Malaria distribution in the World[10]

Other reasons for the disease proliferation include the multidrug resistance (MDR) that the parasite has developed towards the well-established drugs and insecticides. Currently, MDR is known to be the biggest drawback towards development of an effective chemotherapeutic agent. Knowledge of the life cycle of the malaria parasite could help in the understanding of the

methods of prevention, treatment, and research endeavours of this fatal desease.

1.1.1. Life cycle of the malaria parasite

The malaria parasite's life cycle shown in Fig.1.3, engages two hosts, human and mosquito. During a blood meal, the malaria-infected female *Anopheles* mosquito injects sporozoites into the human host **(1)**. Sporozoites infect liver cells **(2)** and mature into schizonts **(3)**, which rupture and liberate merozoites **(4)**. After this initial replication in the liver (exo-erythrocytic schizogony **A**), merozoites infect red blood cells **(5)** and the parasites go through asexual multiplication in the erythrocytes (erythrocyte schizogony **B**). The ring stage trophozoites mature into schizonts, which break releasing merozoites **(6)**. Various parasites differentiate into the sexual erythrocytic stage (gametocytes) **(7)**.

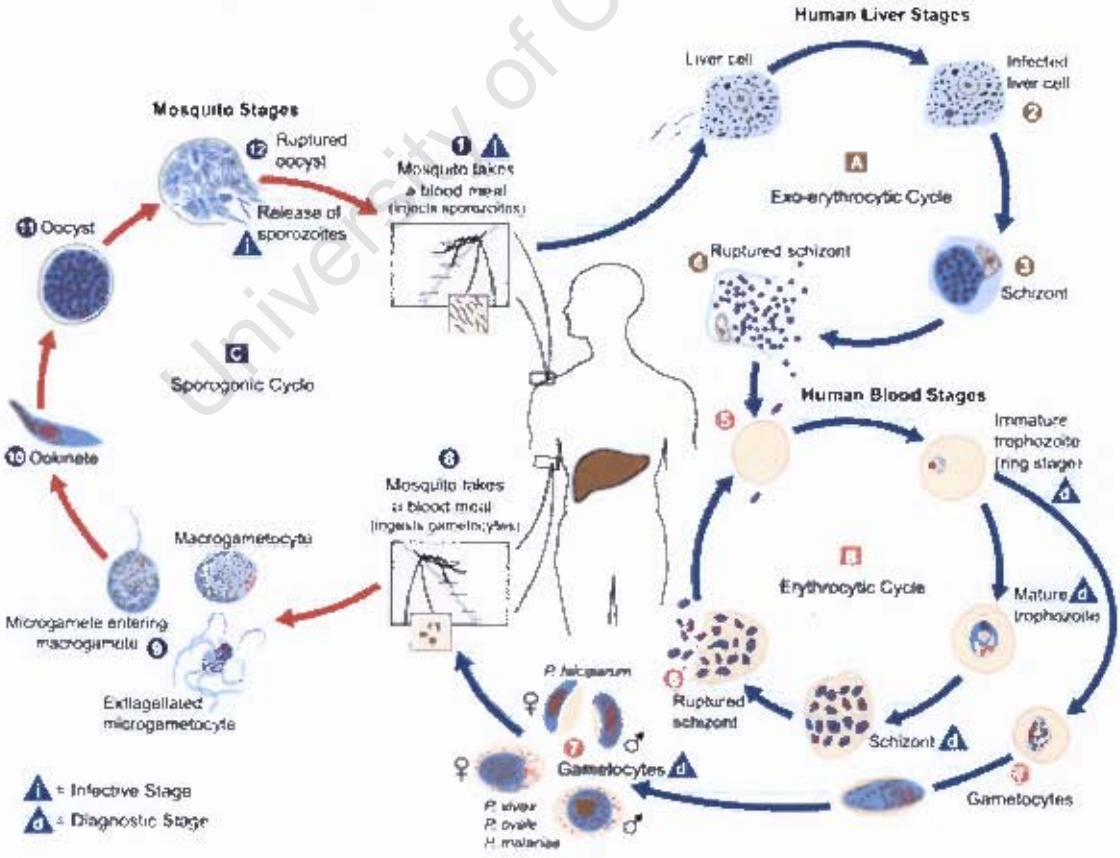

Figure 1.3: Life cycle of the malaria parasite[11]

Malaria symptoms such as chills, fevers, and nausea start at the blood stage. Moreover, it is at this stage that the young parasites, merozoites, attack erythrocytes and progressively break down human haemoglobin into amino acids and destroy the erythrocytes for its function.[12]

The gametocytes, male (microgametocytes) and female (macrogametocytes), are ingested by an *Anopheles* mosquito during a blood meal **(8)**. The parasites reproduce in the mosquito (sporogony cycle) **(C)**, while in the stomach the microgametes breakdown in the macrogametes generating zygotes **(9)**. The zygotes in turn become motile and extended (ookinetes) **(10)** and invade the midgut wall of the mosquito where they develop into oocysts **(11)**. The oocysts grow, rupture, and release sporozoites **(12)**, which make their way to the mosquito salivary glands. Inoculation of the sporozoites **(1)** into the new human host perpetuates the malaria life cycle.

One of the most significant stages in malaria is when the parasite breaks up the host haemoglobin into free amino acids which the parasite utilizes for growth and development.[12] Most of the current anti-malarial drugs target the parasite food vacuole which is a special organelle for the digestion of the host haemoglobin.[13]

1.1.2 Hemoglobin degradation in the food vacuole

Haemoglobin is an abundant protein (95%) found in the erythrocytes, which plays the role of transporting oxygen and removal of CO_2 from the tissues.[13] The degradation of haemoglobin in the food vacuole is believed to occur in a semi-ordered manner according to Fig. 1.4 & 1.5. A group of proteolytic enzymes, known as plasmepsins, falcipains and falcilysin are thought to mediate hemoglobin degradation.

Globin (Fig.1.4) is sequentially degraded into small entities (amino acids) which are utilized by the malaria parasites in their growth and

development processes.[12] The degradation occurs in a semi-ordered way such that there is a sequential action of different proteases.[14]

Figure 1.4 shows how host hemoglobin is metabolised by the parasite to get nutrients for development and growth. Hemoglobin is transported from the parasite cytoplasm into the food vacuole where an aspartic protease, plasmepsin-1 degrades it into globin fragments.

It has been shown that falcipain-2 and possibly falcipain-3 are also capable of digesting native hemoglobin and therefore participating in the initial cleavage of hemoglobin.[15,16] Other plasmepsins, plasmepsin-2 and plasmepsin-4, and the falcipains further degrade the globin fragments into polypeptides (up to 20 amino acids) which are further broken into small peptides (6 to 8 amino acids) by a metalloprotease, falcilysin. Small peptides are further degraded by aminopeptidases into amino acids outside the food vacuole (in the parasite cytoplasm).[17]

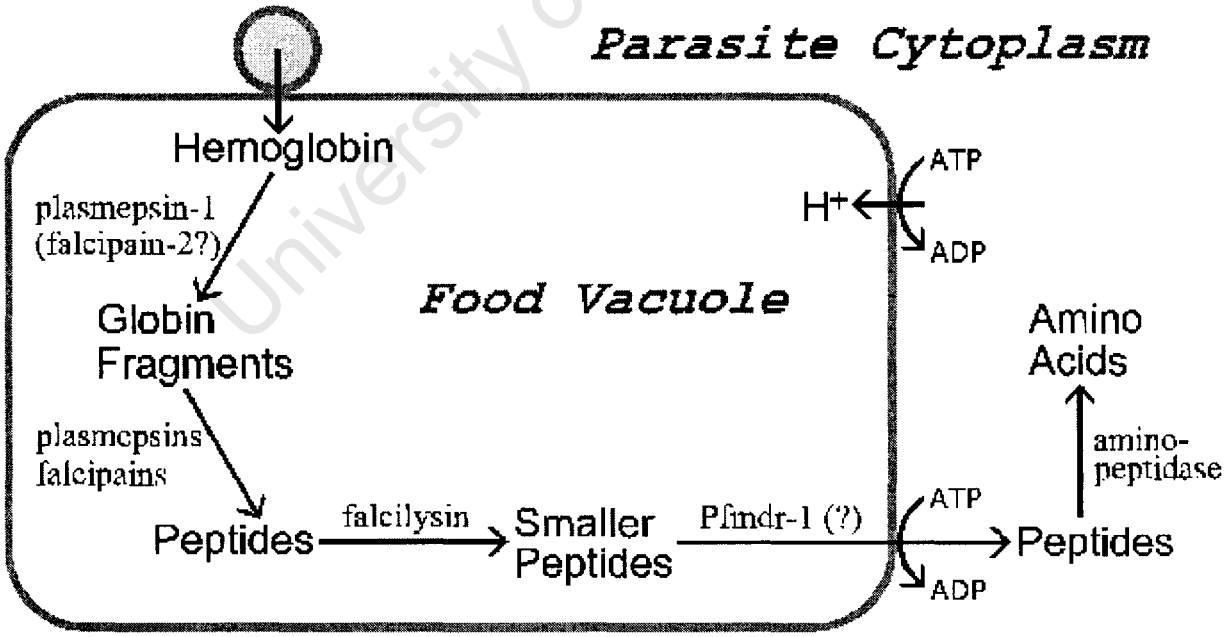

Figure 1.4. Digestion of host hemoglobin by proteases[13]

The other portion of the haemoglobin degraded product, heme, is converted to hemozoin (Fig. 1.5). This is a way for the parasite to protect

itself against the toxicity of heme. In the same vein, the parasite initiates degradation of heme by the following mechanisms: a) peroxides in the food vacuole, b) glutathione in its cytoplasm, c) heme oxygenase (this enzyme is only found in *P. berghei* and *P. knowlesi* but not in *P. falciparum*) in its cytoplasm.[18a] According to Tachezy,[18b] heme released from digested haemoglobin is rapidly sequestered into haemozoin; and the presence of heme oxygenase that mediates the release of iron in other cells was not found in *Plasmodium* spp. Elsewhere, it has been found that parasites that survived intracellularly in mammalians, such as *Leishmania* and malaria, could utilized mammalian holo-transferrin and / or holo-lactoferrin as sources of iron.[18c]

It has been proven that more than 95 % of heme is converted to hemozoin and the remainder is degraded as cited above.[18d]

Thus, considering the mechanism that the parasite has developed for its survival, most of the anti-malarial drugs are designed to target the food vacuole.[13]

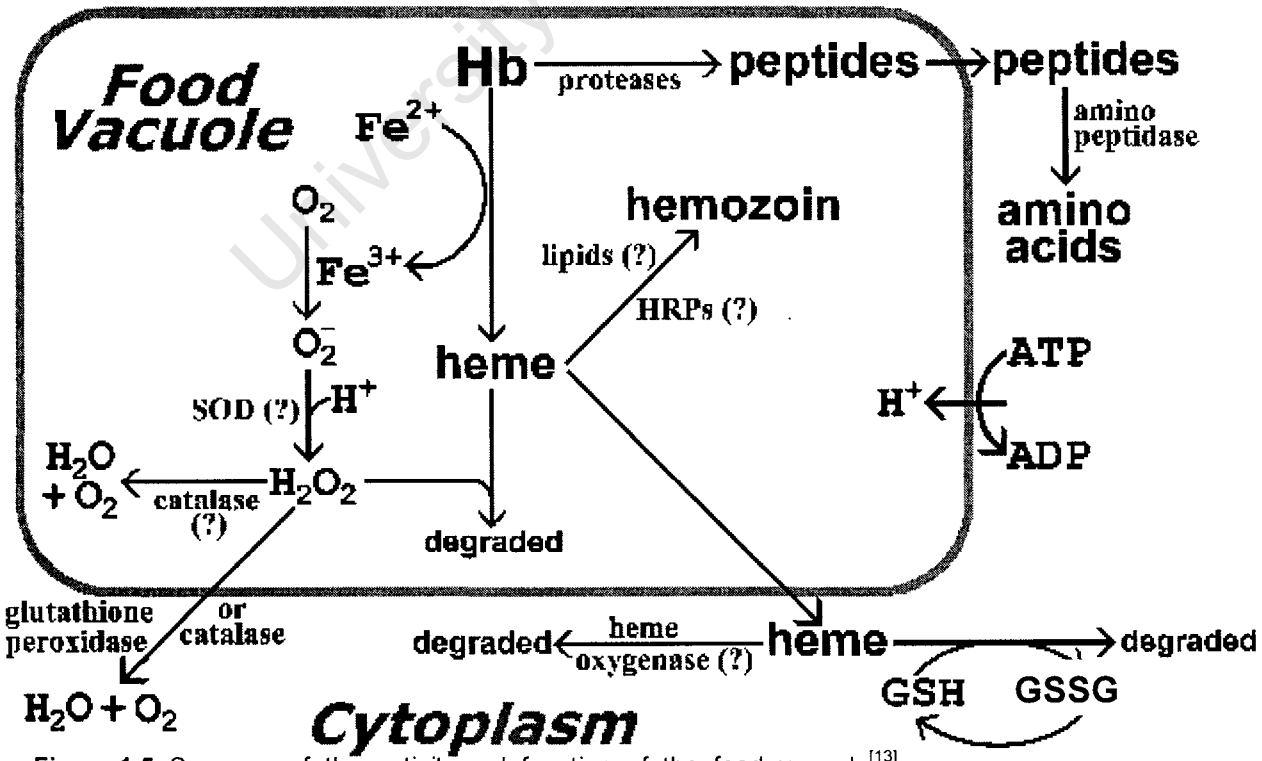

Figure 1.5. Summary of the activity and function of the food vacuole[13]

With regard to this current project, designing a compound that will target the food vacuole like the current drugs would be of great interest since such a drug could be able to prevent the detoxification of heme or inhibit any other detoxification processes or stop the parasite from replicating by inhibiting the hemoglobin degradation process.

1.2. Malaria Chemotherapy

The World Health Organisation (WHO) submitted at the World Health Assembly in 1955 an ambitious proposal for the eradication of malaria worldwide. Eradication efforts began and focused on house spraying with residual insecticides, anti-malarial drug treatment and surveillance. Success including eradication in nations with temperate climates and seasonal malaria transmission have been witnessed in some countries such as India and Sri Lanka where the number of cases was dramatically reduced. Other nations had negligible progression (such as Indonesia, Afghanistan, Haiti and Nicaragua). However, most of sub-saharan Africa was excluded completely from the eradication campaign at that time.[19]
Afterwards, the eradication campaign was abandoned due to many reasons including widespread resistance to available insecticides, drug resistance, wars, massive population movements, as well as difficulties in obtaining unceased funding from donor countries and lack of community participation.[19]

At present, chemotherapy remains the only keystone to malaria control.[20] Thus, in the battle to discover an effective chemotherapeutic agent, a number of drugs have been discovered. Unfortunately most of them are faced with resistance from the parasite, while others have serious side effects that make them unfavourable towards humans.
Some of the drugs that have been used for malaria control are discussed below, according to their structural classes.[21]

1.2.1. 4-Aminoquinolines

It is generally accepted that this category of anti-malarial drugs interfere with the detoxification of free heme, which is generated during hemoglobin degradation.[18a,22] There is evidence that 4-aminoquinoline drugs inhibit both malaria pigment (hemozoin) formation and the oxidative and glutathione-dependent heme degradation.[23] In this category of anti-malarial drugs, chloroquine **1** (Fig.1.6) is the most important due to it's great impact in the field of current anti-malarial drugs.

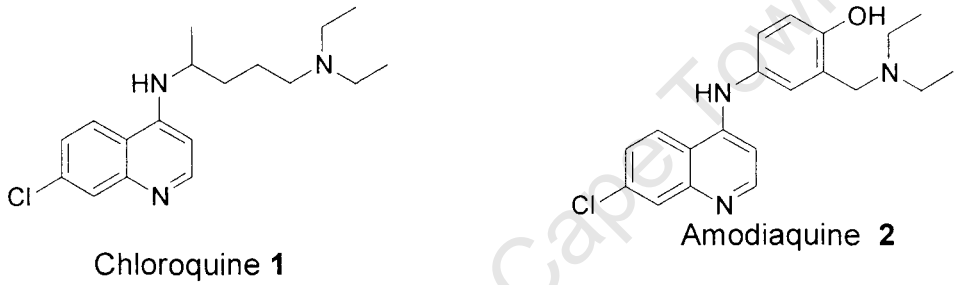

Figure 1.6: Chemical structures of chloroquine **1** and amodiaquine **2**

Chloroquine was discovered by a German scientist, Hans Andersag, in 1934 and was known by the name of resorchin at the time. It was not used at that time because it was considered to be toxic, until in 1946 when the drug was recognized by British and USA scientists. Since then, chloroquine has been the mainstay of anti-malarial chemotherapy.

Chloroquine is a very potent schizonticidal and an effective drug against the erythrocytic stage for all *Plasmodium* species. It is a weak uncharged base at neutral pH, while it is a di-cation at acidic pH. Based on this property chloroquine selectively accumulates inside lysosomes. The charged compound rapidly diffuses through the plasma and lysosomal membranes and, once charged the compound becomes trapped inside the acidic lysosomal (food vacuole) compartment of the parasite. Thus chloroquine

accumulates in the food vacuole to several orders of magnitude resulting from a concentration gradient.

Digestion of hemoglobin takes place inside the plasmodium food vacuole resulting in the generation of free haeme (ferriprotoporphyrin IX) which is insoluble and precipitates in the form of hemozoin in the food vacuole. Though not clearly known, it is postulated that chloroquine in the food vacuole interferes with pigment (hemozoin) formation and also the ferriprotoporphyrin-chloroquine complex is highly toxic to the parasite.[24a, 24b] These two are known chloroquine mechanisms in the food vacuole. Other mechanisms were proposed such as inhibition of heme-dependent protein synthesis,[25] prevention of iron release from hemoglobin[26] and inhibition of food vacuole cysteine proteases.[27,28]

Chloroquine effect on the parasite is so rapid comparatively to others and it is less toxic to the subject. This drug is admistrated to everyone even to pregnant women.[21] Its effect on the parasite is very rapid compared to other drugs. Sometimes patients can experience headaches, nausea, vomiting and gastrointestinal symptoms while taking the drug. In spite of the efficacy of chloroquine, the malaria parasite has developed resistance towards the drug. The first case was noted in the late 1950's from Colombia and Thailand. Reports of similar resistance patterns quickly followed from other countries in South America and South East Asia. The first clearly documented case of chloroquine-resistance *P. falciparum* was reported from Kenya in 1979 in a tourist.[29] Nowadays, chloroquine-resistant is prevalent in most *P. falciparum*-endemic areas of the world, causing the use of chloroquine for presumptive treatment of *P.falciparum* malaria or chemoprophylaxis to be inappropriate.[30]

Amodiaquine **2** (Fig.1.6) is another 4-aminoquinoline drug. It was introduced 40 years ago as an alternative to chloroquine **1** in the treatment and

prevention of uncomplicated malaria and some chloroquine-resistant strains.[30]

As with chloroquine, amodiaquine is an anti-malarial with schizonticidal activities. It is effective against the erythrocytic stages in all the *Plasmodium* species except mature gametocytes of *P. falciparum*.[31] It accumulates in the lysosomes and brings about loss of function and the parasite becomes unable to digest hemoglobin on which it depends. Various serious adverse effects were experienced with administration of the drug including nausea, vomiting, skin rash and pruritus. Its administration is not advisable to pregnant and breastfeeding women. Nowadays, amodiaquine is no longer recommended alone due to the risk of severe advert reactions such as agranulocytosis and hepatotoxicity.

1.2.2. 8-Aminoquinolines

Primaquine **3** and Tafenoquine **4** (Fig.1.7) belong to the 8-aminoquinoline class of anti-malarials. Primaquine is highly effective against the gametocytes of all malaria parasites and prevents spread of the disease to the mosquito from the patient. It is commonly used in areas with low or moderate malaria transmission.[21,32] It is also active against hypnozoites of the relapsing malarial parasites, *P. vivax* and *P. ovale*.[33] It reported to be active against asexual blood stages of *P. falciparum* in Thailand.[32,34]

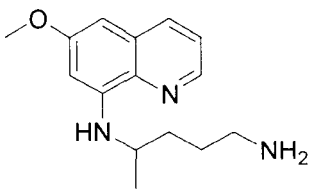

Primaquine **3**

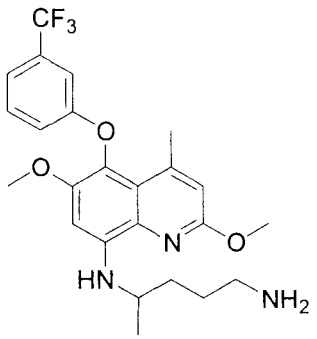

Tafenoquine **4**

Figure 1.7. Chemical structures of primaquine **3** and tafenoquine **4**

The mechanism of action of primaquine is not clear yet but it was suggested that it may act by generating reactive oxygen species or by interfering with the electron transport in the parasite.[21]

Primaquine is tolerable at therapeutic dosage but at higher dosages it may cause occasional epigastric distress and abdominal cramps, mild anemia, cyanosis, methemoglobinemia in some patients. Toxicological concerns have led to restrictions in the use of primaquine.[35] For this drug there is no specific antidote and treatment is only symptomatic.

Tafenoquine **4** (Fig.1.7) is a long-acting 8-aminoquinoline anti-malarial with a half-life of 2 weeks. The drug is used by short-time visitors to malaria areas to prevent the risk of *P.falciparum* malaria infections.[36] It is frequently used for treating multidrug-resistant *P.falciparum*, and in combination with artemisinin derivatives gives good results.

The major disadvantage of 8-aminoquinoline drugs is that patients with deficiency of glucose 6-phosphate dehydrogenase (G6PD) are not advised to take the drug because they are likely to develop hemolytic anemia on taking usual doses (up to 0.25mg/kg/day and 15mg/day/adult).[37]

1.2.3. Aryl Amino Alcohols

Quinine **5** (Fig.1.8) is the chief constituent of the tree *cinchona ledgenaria* (known as "fever bark") found in South America. Quinine was isolated in 1820 from the cinchona tree by Pelletier and Caventou.[21] Nowadays, quinine is obtained entirely from natural sources due to difficulties in synthesis.

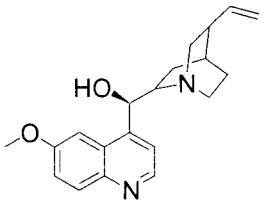

Quinine **5**

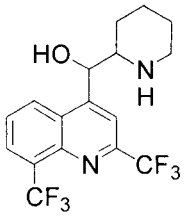

Mefloquine **6**

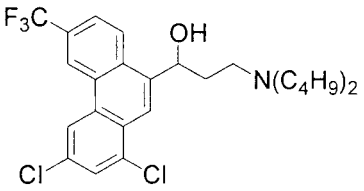

Halofantrine **7**

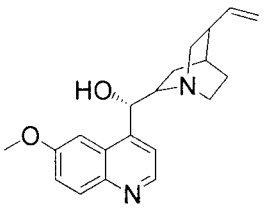

Quinidine **8**

Figure 1.8: Chemical structures of quinine **5** ,mefloquine **6**, halofantrine **7** and quinidine **8**

Quinine, like chloroquine is a schizonticidal drug. Besides its schizonticidal activity against the 4 *Plasmodium* species, it also has gametocytocidal activity against *P. vivax* and *P.malariae*.[21]

Quinine is less effective, less tolerable and more toxic than chloroquine. Toxicity of quinine results from repeated doses while adverse effects including tinnitus, progressive loss of auditory acuity, blurred vision, photophobia, rashes, sweating, nausea have been reported in larger doses. Massive hemolysis and hemoglobinuria can occur, especially in pregnant women or on repeated use. This drug is only recommended in places where severe *P.falciparum* malaria resistance towards chloroquine has been reported. It is used as an intravenous formulation in severe malaria when patients are unable to tolerate oral medication.

Mefloquine **6** (Fig.1.8) was discovered during the Vietnam war as a result of research into newer anti-malarials to protect American soldiers. It is chemically related to quinine. It is a potent long-acting blood schizonticide active against *P.falciparum* resistant to 4-aminoquinolines. It is also highly active against *P.vivax* and *P.malariae*, and most probably *P. ovale*.

Mefloquine is not gametocytocidal, and is not active against the hepatic stages of malaria parasites.[32] In terms of the mode of action, mefloquine has been found to produce swelling of the *P.falciparum* food vacuole and it also may act by forming toxic complexes with free heme that end up damaging the parasite membrane and other plasmodial components.[21] Mefloquine is recommended as a prophylactic drug for travelers to areas with significant risk of chloroquine-resistant *P.falciparum* malaria.

Neuropsychiatric adverse reactions have been reportedly associated with mefloquine use including affective disorders, anxiety disorders, hallucinations, sleep disturbances, toxic encephalopathy, convulsions and acute brain syndrome.[38-40] The drug is not recommended to persons with an allergies to it, of severe neuropsychiatric disease and to persons performing activities requiring fine coordination and spatial discrimination (e.g. air pilots and machine operators).

Halofantrine **7** (Fig.1.8) is a blood schizonticidal against all malaria parasites. It is active against *P.falciparum* infections that are resistant to chloroquine **1**.[21] The drug is not recommended to people with a history of heart disease.[41]

Quinidine **8** (Fig.1.8) is a diastereoisomer of quinine with similar anti-malarial properties. It is slightly more effective than quinine but has a greater cardiosuppressant effect.[42] With respect to the toxicity and drug interaction, quinidine's reactions are similar to those of quinine. Quinidine is a useful

drug for parenteral treatment of severe malaria and may be used instead of quinine in patients with uncomplicated malaria.

1.2.4. Folate Antagonists

This category of anti-malarials affects the synthesis and utilization of folate. Proguanil **10** and pyrimethamine **11** (Fig.1.9) act by inhibiting dihydrofolate reductase, which is necessary for the synthesis of tetrahydrofolate, a precursor in the parasite DNA synthesis.[43,44] Sulphonamides (e.g. sulfadoxine **12**) and sulphones (e.g. dapsone **9**) (Fig.1.9) inhibit folate synthesis by competing for dihydropteroate synthetase with *para*-aminobenzoic acid.[43]

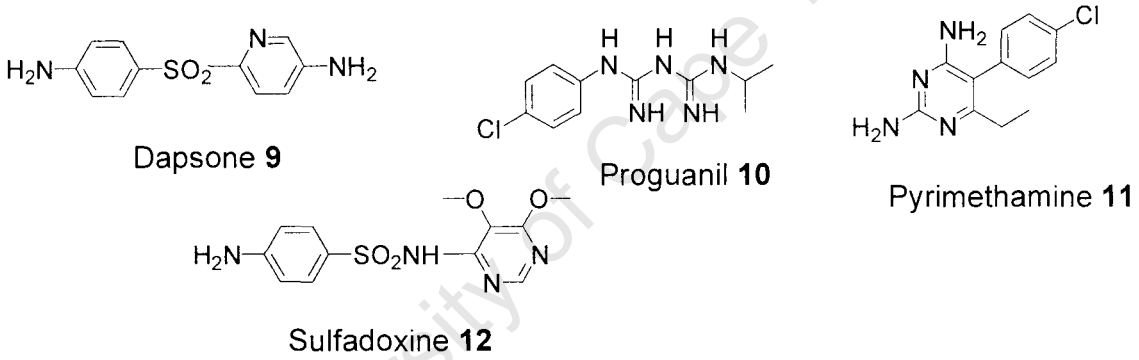

Figure 1.9: Structures of Folate antagonist anti-malarials.

Proguanil is a well tolerated drug that is commonly used in combination with chloroquine due to its low efficacy if used as a monotherapeutic agent.[45]

These folate antagonists act on erythrocytic *P.falciparum* by a mop up system after treatment with quinine in an acute attack of chloroquine resistant *P.falciparum* malaria parasites. Large doses of pyrimethamine-dapsone cause hemolytic anaemia and aglanulocytosis.[43,46]

1.2.5. Naphthoquinones

Atovaquone **14** (Fig.1.10) is a naphthoquinone derivative that is structurally analogous to coenzyme Q (ubiquinone) found in the mitochondrial electron transport chain. This drug disturbs parasite biochemical processes by acting against ubiquinol-cytochrome c oxido-reductase, inhibiting electron transport and collapsing mitochondrial membrane potential.[47]

A combination of atovaquone and chloroproguanil **13** (Fig.1.10) is used both for treatment and prophylaxis of malaria, and it has been proven to be highly efficacious in the treatment of uncomplicated malaria in areas with chloroquine-resistant or multidrug-resistant strains.[21]

Chloroproguanil **13** Atovaquone **14**

Figure 1.10: Chemical structures of chloroproguanil **13** and atovaquone **14**

1.2.6. Antimicrobials

Certain antimicrobial drugs are useful in the treatment of drug resistant *P.falciparum* malaria. They act relatively slowly and for that reason they are applied as prophylactics or combined with faster acting drugs like quinine or pyrimethamine for effective cure.

Tetracycline **15** (Fig.1.11) is a bacteriostatic agent, which supposedly acts by inhibiting protein synthesis by binding to the 30s ribosome subunit.[21]

Another antimicrobial, doxycycline **16** (Fig.1.11) is the most frequently used in anti-malarial chemotherapy, either alone as a prophylactic or in combination with quinine or artesunate for treatment of multidrug-resistant *P.falciparum*.[45]

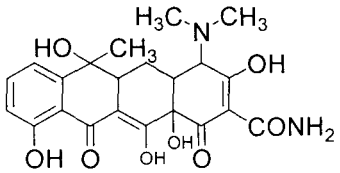

Tetracycline **15**

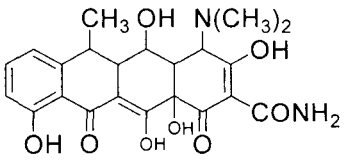

Doxycycline **16**

Figure 1.11: Chemical structures of tetracycline **15** and doxycycline **16**

1.2.7. Endoperoxides

Artemisinin **17** (Fig.1.12) an endoperoxide anti-malarial and its derivatives (artemether **18**, artesunate **19** and arteether **20**) (Fig.1.12) are the most effective new drugs.

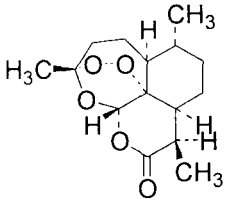

Artemisinin **17**

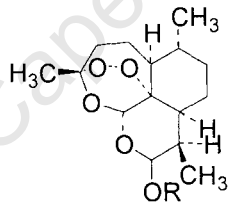

18 R = CH_3 Artemether
19 R = $COCH_2CH_2COONa$ Artesunate
20 R = CH_2CH_3 Arteether

Figure 1.12: Chemical structures of artemisinin **17** and its derivatives **18**, **19**, **20**

Artemisinin was isolated in 1971 from the Chinese medicinal herb *artemisia annua* used in the treatment of fevers in China.[21]

Artemisinin derivatives have been developed for the treatment of cerebral malaria as well as for the control of multidrug-resistant *P. falciparum*.[21] The artemisinins are active against the sexual parasite stages (gametocytes), which are responsible for the infection of the *anopheles* mosquito and for transmission of the disease,[47] and they are also effective against the chloroquine-resistant strains of *P.falciparum*.[21] However, these expensive drugs are associated with high incidences of recrudescent infection if used alone, therefore it is suggested that the combination with other anti-malarial drugs might bring maximum efficacy. In

one of the controversial mechanisms, the biological activity of artemisinins is believed to depend on the cleavage of the peroxide bond after contact with Fe^{II} heme inside the food vacuole (Fig.1.5), thus generating free radicals that can alkylate the heme molecule.[48] A number of other mechanisms for artemisinin and related compounds have been proposed.[49]

1.2.8. Iron Chelators

Desferrioxamine (DFO) **21** (Fig.1.13) is the only iron chelator that is used against malaria *in vivo*. It is a naturally occurring trihydroxamic acid, a siderophore produced by *Streptomyces pilosus*.[50]

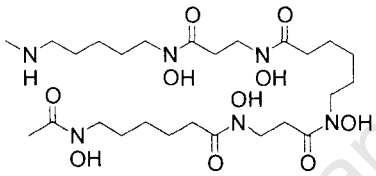

Desferrioxamine **21**

Figure 1.13. Structure of desferrioxamine **21**

When given as a single agent, DFO suppresses the growth of *P. falciparum* in parasitized erythrocytes by chelating a pool of iron associated with the parasite.[51] DFO could also enhance the host immune response.[50] The clear mode of action of DFO is still debatable. Some side effects are associated with this drug such as kidney function decrease, fever (pyrexia), blood disorders, asthma, hearing disturbances and visual disturbances.[43]

Based on the above succinct description of different drugs, their mode of actions and the associated drawbacks, it gives a clear image that there is not yet an effective drug that would tackle this health threatening disease, malaria, to effectively replace chloroquine. Therefore, doors are still open for any potential drug that will be effective, accessible and also that will eradicate malaria or reduce drug resistance problems.

REFERENCES

[1] http://www.scienceafrica.co.za/**2002**/august/malaria.htm: last accessed October 2005.

[2] World Health Report; WHO: Geneva, **2000**.

[3] www.revue.ch/swisskids/img/anopheles k. jpg: last accessed May 2006.

[4] Westling, J; Yowell, CA; Major, P; Erickson, JW; Dame, JB, *Exp. Parasitol.,* **1999,** *87*, 185.

[5] WHO. *Weekly Epidemiol. Rep.*, **1996**, *3*, 17.

[6] WHO.*Weekly Epidemiol. Rep.*, **1996**, *4*, 25.

[7] WHO. *Weekly Epidomil. Rep.*, **1996**, *5*, 37.

[8] Winstanley, PA, *Parasitol.Today*, **2000**, *16*, 146.

[9] http://sprojects.mmi.mcgill.ca/tromped/disease/malaria/geographical.htm: last accessed October 2005.

[10] http://www.traveldoctor.co.uk/malaria.htm: last accessed October 2005.

[11] http://www.tiscali.co.uk/lifestyle/healthfitness: last accessed October 2005.

[12] Zeigler, J; Linck, R; Wright, DW; *Curr.Med.Chem.*, **2001**, *8*, 171.

[13] http://www.tulane.edu. : last accessed October 2005.

[14] Klemba, M; Goldberg, DE, *Ann.Rev.Biochem.*, **2002**, *71*, 275.

[15] Shenai, BR; Sijwali, PS; Singh, A; Rosenthal, PJ, *J.Biol.Chem.,* **2000**, *275*, 29000.

[16] Sijwali, PS; Shenai, BR; Singh, A; Rosenthal, PJ, *Biochem.J.,* **2001**, *360,* 481.

[17] Curley, GP; O'Donovan, SM; McNally, J; Mullaly, M; O'Hara, H; Troy, A; O'Callaghan, SA; Dalton, JP, *J.Euk.Microbiol.*, **1994**, *41*, 119.

[18] a) Ginsburg, H; Ward, SA; Bray, PG, *Parasitol.Today,* **1999**, *15*, 466 b) Tachezy, *Parasitol. Today*, **1999**, *15*, 207 c) Wilson, ME; Britigan, BE, *Parasitol.Today*, **1998**, *14*, 348 d) Timothy, J.E; Jill, MC; Joanne, E; Giovanni, RH; Helder, MM; Skhumbuzo, N; Sewell, BT; Smith, PJ; Taylor, D; van Schalkwyk, DA; Walden, JC, *Biochem. J*, **2002**, *365*, 343.

[19] http://www.cdc.gov/malaria/history

[20] White, *Treatment of malaria*, NEJM, **1996**, *335*, 800.

[21] http://www.malariasite.com,

[22] Sanchez, CP; Lanzer, M, *Curr.Opin.Infect.Dis,* **2000**, *13*, 653.

[23] Foley, M; Tilley, L, *Pharmacol.Ther.,* **1998**, *79*, 55.

[24] a) Dorn, A; Stoffel, R; Matile, H; Bubendorf, A; Ridley, R, *Nature*, **1995**, *374*, 269. b) Slater, AFG; Cerami, A, *Nature*, **1992**, *355*, 167.

[25] Surolia, N; Padmanaban, G, *Proc.Natl.Acad.Sci.USA* 88, **1991**, 4786.

[26] Gabay, T; Krugliak, M; Shalmiev, G; Ginsburg, H, *Parasitology*, **1994**, *108*,371.

[27] Rosenthal, PJ, *Exp.Parasitol.,* **1995**, *80*, 272.

[28] Gluzman, IY; Francis, SE; Oksman, A; Smith, CE; Duffin, KL; Goldberg, DE, *J.Clin.Invest.,* **1994**, *93*, 1602.

[29] Kean, BH, *JAMA*, **1979**, *241*, 395.

[30] Olliaro, P; Cattani, J; Wirth, D, *JAMA*, **1990**, *263*, 2729.

[31] O'Neill, PM; Bray, PG; Hawley, SR; Ward, AS; Park, BK, *Pharmacol.Ther.* , **1998**, *77,* 29.

[32] http://www.WHO.int/malaria

[33] PukrittayaKamee, S; Vanijanonta, S; Chantra, A; Clemens, R; White, NJ, *J.Infect. Dis.*, **1994**, *169*, 932.

[34] Wilairatana, P; Silachamroon, U; Krudsood, S; Singhasivanon, P; Treeprasertsuk, S, Bussaratid, V; Phumratanaprapin, W; Srivilirit, S; Looareesuwan, S, *Am.J.Trop.Med.Hyg.*, **1999**, *61*,973.

[35] Jochen, W; Regina, O; Hassan, J; Martin, S, *Angew. Chem. Int. Ed.*, **2003**, *42*, 5274.

[36] Cowman, AF, *Int. J. Parasitol.,* **2001**, *31*, 871.

[37] Brueckner, RP; Ohrt, C; Brai, JK; Milhous, W;In Antimalarial Chemotherapy, (Ed.: P.J. Rosenthal), Humana Press, Totowa, NJ, **2001**, 123.

[38] Havaldar, PV; Mogale, KD, *Paed. Infect. Dis.*, **2000**, *19*, 166.

[39] Potasman, I *et al.*, *J. Travel Med.*, **2000**, *7*, 5.

[40] Phillips-Howard, PA; ter Kuile, FO, *Drug safety*, **1995**, *12*, 370.

[41] Report no WHO/CDS/RBM/**2001**, *33* (WHO, Geneva, **2001**)

[42] WHO technical report series, **1990**, no 805.

[43] Nwanyanwu, OC; Ziba, C; Kazembe, PN; Gamadzi, G; Gondwe, J;

Redd, SC, *Ann.Trop.Med.Parasitol.*, **1996**, *90*, 589.

[44] WHO technical report series, **1987**.

[45] Kain, KC; Shanks, GD; Keystone, JS, *Clin.Infect.Dis.*, **2001**, *33*, 226.

[46] Baseo, LK; Ringwald, P, *Ann. J.Trop.Med.Hyg.*, **1998**, *58*, 374.

[47] Vaidya, AB, Atovaquone-Proguanil combination.In Antimalarial Chemotherapy: *Mechanism of Action, Resistance and New directions in Drug Discovery*. Rosenthal, P.J. Ed; Humana Press Inc., Totowa, **2001**, pp.203.

[48] Anne, R; Francoise, B. V; catherine, C; Bernard, M, PNAS no 9048, ref. 05-00972, 5 Sepember **2005**.

[49] Haynes, RK, *Angew. Chem. Int. Ed.*, **2005,** *44*, 2064.

[50] Gavino, F; Guido, C, *Coord. Chem. Reviews,* **1999**, *184*, 291.

[51] Loyevsky, M; Godeuk, VR; In antimalarial Chemotherapy: *Mechanism of Action, Resistance and New directions in Drug Discovery*. Rosenthal, P.J. Ed; Humana Press Inc., Totowa, **2001**.

CHAPTER 2

IRON CHELATORS AS ANTI-MALARIALS

2.1. Iron

Iron is the second most abundant metal on the earth's surface, falling closely behind aluminium and in near equivalent concentration to calcium and sodium.[1] The concentration of iron (Fe) in the human body is estimated to be about 40-50 mg/ kg for men and less than that for women. Most of this (about 80%) is located in the oxygen transport storage proteins hemoglobin and myoglobin.[2]

Iron is a critically important metal for a wide variety of cellular events.[2] It is an essential element for the growth of almost all microorganisms, with the notable exception of non- pathogenic lactobacilli.[3] It is used in the catalysis of DNA synthesis and in a variety of enzymes concerned with electron transport and energy metabolism.[1] It also plays a role in the reduction of ribonucleotide[4,5] to deoxyribonucleotide which is the rate-limiting step for DNA synthesis, and the activity of the enzyme ribonucleotide reductase (RR) is iron-dependent. The iron centre in RR stabilizes a tyrosyl radical within its R2 subunit.[4,5]

Molecules with nitrogen, oxygen and sulfur donor atoms avidly bind Fe. The Fe-N bonds in the porphyrin ring of heme proteinase are key to their function as efficient oxygen transport and storage molecules.[6] Additionally, Fe plays a role in activation and decomposition of peroxides.[1]

Like all living organisms, malaria parasites need iron for vital cell functions and it has been found that Fe (III), Fe^{3+}, is the one involved in the intra-erythrocyte growth and development of the human malaria parasite.[7,8]

Egan *et al* [9] have shown that *P. falciparum* trophozoites contain 61 ± 2% of the iron within parasitized erythrocytes, of which 92 ± 6% is located within the food vacuole. Of this, 88 ± 9% is in the form of hemozoin.

The acquisition of iron by the intra-erythrocyte parasite has been suggested as follows: The merozoite enters the erythrocyte by attaching to sialic acid residues on the red blood cell surface.[10] Within the red blood cell, the parasite first appears as a ring form and matures into a trophozoite. The parasite, by some process, enhances the host red blood cell permeability[11] and then the trophozoite ingests the host cell cytoplasm, including hemoglobin, by means of a cytostome to get nutrients[8] or may take up molecules from the outer medium directly *via* the parasitophorous duct.[12] Once taken up into the parasite, host cytoplasm is transported in vesicles to the food vacuole (site of primary hemoglobin proteolysis) where aspartic proteases (plasmepsin I and II) cleave the hemoglobin into small peptides.[13]

2.2. Potential Sources of Fe for the Malaria Parasite

Iron being important to almost all microorganisms including the malaria parasites, one has to ask: where do parasites get iron from?. Although there are some doubts about the source of iron for the parasite growth, some researchers think that there is a possibility that a small amount of heme degraded in a controlled way in the food vacuole could release Fe for the metabolic processes of the parasite.[14] This is just a small amount of Fe that the parasite might use in the process. There is less information on the means by which protozoa, including malaria parasites, acquire iron to sustain their growth. Some potential sources of iron for the parasite use are discussed below.

2.2.1. Plasma transferrin-bound iron

Some studies suggested that plasma transferrin (iron transport protein) may be one of the sources of Fe for the parasite. Through clinical studies, it has been found that the protection of Fe deficiency against human malaria and increased Fe uptake through daily nutrition improved responsiveness to malaria infection[15-17] and the expression of transferrin receptors by mature parasitized red blood cells has been reported.[18, 19]
Later, however, some clinical and experimental evidence proved that human Fe does not affect malaria infection[20] and no transferrin receptors exist on parasitized erythrocyte.[20, 21]

Many arguments have arisen about transferrin being amongst the sources of Fe for the parasite but the overall evidence indicates that transferrin Fe is not taken up by the parasitized red blood cells.[22,23]

2.2.2. Erythrocyte Ferritin

It has been found that the mature erythrocyte is incapable of synthesizing its own ferritin, Fe storage protein, but it contains some residual ferritin which was produced during the earlier erythroblast phase.[24] This residual ferritin was found to contain about 4.5 μM Fe if fully concentrated.[19]

The acquisition of Fe by the parasite within the parasitophorous vacuole from ferritin in the cytoplasm of the erythrocyte is not yet experimentally proven. Nevertheless ferritin traces have been detected in subjects deficient in Fe[25] and the possibility exists for the parasite to take up iron from ferritin across the parasitophorous vacuole membrane and parasite plasma membrane, or through the process of cytostosomal ingestion and transport to the food vacuole.

In contrast to early statements, Fe deficiency was found to be associated with low red blood cell ferritin concentrations[25] without inhibition of intra-erythrocytic parasite growth.[22]

2.2.3. Host hemoglobin

A great portion of the amino acids that are necessary for protein synthesis comes from the host hemoglobin catabolism process which is mainly used by the intraerythrocytic parasite.[13,26,27] The heme released from the process is known to contain significant amounts of Fe and might be available for the parasite's metabolic needs, if liberated.[28]

While evidence that the parasite uses the Fe derived from host heme is missing, it is likely that a small amount of heme in the food vacuole is degraded to liberate Fe for the metabolic processes of the parasite.[13]
Elsewhere, it was proven that the parasite might also utilize a non-heme source of Fe.[20, 29]

2.2.4. Intra-erythrocyte iron pool

Some studies done on hemolysates of rat cells parasitized with *P.berghei* have revealed that there is a labile pool of Fe that is chelatable by preincubation of the intact cells with an Fe chelator such as DFO (Desferrioxamine).[22] Elsewhere, two studies have shown that there is no inhibition of the plasmodial growth when Fe chelator agents were introduced into the cytoplasm of erythrocytes specifically but not into the parasite compartment within the parasitophorous vacuole.[25,29] It is possible that the parasite uses both host labile iron and host hemoglobin iron as a source of Fe. Therefore the abrogation of only one will not prevent parasite growth.
Since the source of Fe for the parasite is not yet well-known, the fact remains though that the malaria parasite needs Fe for its growth and

development like all living organisms.[2,30] Many enzymes of the intra-erythrocytic malaria parasite are Fe-dependent. The table below (Table 1) shows a list of different malaria parasite enzymes that are Fe-dependent and their respective pathways.

Table 2.1: Fe-dependent enzymes and their metabolic pathways

Metabolic pathway	Enzymes	Reference
DNA synthesis	Ribonucleotide reductase	31, 32
Pyrimidine synthesis	Dihydrorotate dehydrogenase	33, 34
Glycolysis	Glycolytic enzyme	35, 36
Pentose phosphate shunt	Pentose phosphate shunt enzyme	37
CO_2 fixation	Phosphoenol pyruvate carboxykinase	31
Proteolysis of hemoglobin	Proteolytic enzymes	38
Heme synthesis	δ-aminolevulinate	39
Mitochondrial electron Transport	Cytochrome oxidase	34, 40, 41

2.3. Iron Chelators

Fe chelators have been used to remove excess Fe in the body in thalassemia patients because the human body has no efficient ways to excrete excess Fe accumulated.[42] Fe chelators display other interesting medicinal properties apart from removal of Fe from the body including anti-cancer properties,[43] photoprotective properties,[44] anti-asthma properties,[45] anti-HIV properties in conjunction with HIV-protease or reverse transcriptase inhibitors[46] anti-hydroxyl radical formation,[47] anti-neurodegenerative properties[43,47,48] as well as anti-malarial properties.[14,43]

As far as this Msc project is concerned, focus will be placed on iron chelators as antimalarial agents.

In the process of finding a way of eliminating malaria or decreasing its fatality, researchers have hypothesized that depriving the malaria causative agent, *P. falciparum*, of Fe might have some implications in the metabolic pathways of the parasite regarding the role of Fe in malaria parasite growth and proliferation.[32,49] Therefore, inhibiting the parasite could be one of the routes to effective antimalarial therapy.

2.3.1. Mode of inhibition of malaria parasites by antimalarial iron chelators

There are two known major modes by which Fe chelators deprive malaria parasites of Fe, therefore inhibiing the parasite growth.[50]

i) Withholding Fe from malaria parasite metabolism. The mechanism of antimalarial action of this class of iron chelators appears to be the sequestration of iron for plasmodium replication. This class of molecules with this mode of action include the following: hydroxamate siderophores (e.g. DFO), catecholamide and catecholate siderophores (e.g.Gamma Amino Butyric Acid), α-ketohydroxypyridinones (e.g. Deferiprone), dihydrocoumarins (e.g. Daphnetin), and bis-cyclic imides (Dexrazoxane) (Fig.2.1).

The anti-plasmodial action of DFO is related to its interference with DNA synthesis presumably *via* inhibition of ribonucleotide reductase, RR.[32, 51] Eukaryotic ribonucleotide reductase, including the *P. falciparum* enzyme, contains two α and two β- subunits.[52] The two dimers α_2 and β_2 are known as protein B1 and protein B2 respectively. B2 contains an essential tyrosyl radical that is stabilized by an adjacent dinuclear iron centre and is thought to initiate the radical–based reaction of ribose into deoxyribose.[4,5] The intracellular Fe in the labile Fe pool is in equilibrium with the Fe in the dinuclear Fe centre.[53] DFO chelates the intracellular Fe, which indirectly impacts on the dinuclear iron centre. Thus, it inhibits ribonucleotide reductase and cell growth as well as prevents the

regeneration of Fe radical centre.[54] This leads to the DNA synthesis inhibition and eventually the death of the parasite could occur.

ii) Complexing with Fe to form a complex that is toxic to the parasite. This class of compounds seem to have an antiparasitic effect other than the withholding of iron. Agents that inhibit parasite growth by forming toxic complexes with Fe are represented by 8-hydroxyquinoline (Fig. 2.1). It appears that the 8-hydroxyquinoline-Fe complex is formed extracellularly, which subsequently enters the parasitized red blood cell to produce a rapid lethal free radical-mediated intracellular reaction.

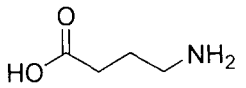

GABA: gamma amino butyric acid

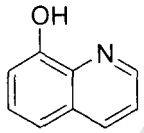

8-hydroxyquinoline

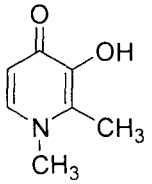

Deferiprone: (1,2-dimethyl 3-hydroxypyrid-4-one)

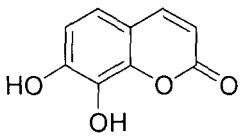

Daphnetin
:(7,8-dihydroxycoumarin)

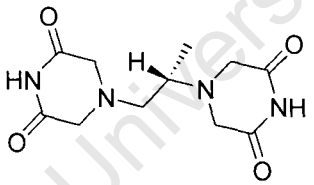

Dexrazoxane :(S) -4,4'-(1-methyl-1,2-ethanediyl) *bis*-2,6-piperazinedione

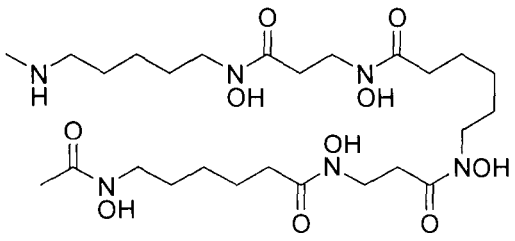

DFO: Desferrioxamine

Figure 2.1 : Structures of antimalarial iron chelators.

Further examples of other antimalarial iron chelators have been reported.[50]

REFERENCES

[1] Alvin, LC., *Oxygen society Education Prog.*, Department of Chemistry, Duke University.

[2] Liu, ZD; Hider, RC, *Coord. Chem. Reviews*, **2002**, *232*, 151.

[3] Wilson, ME; Britigan, BE, *Parasitol. Today*, **1998**, *14*, 348.

[4] Thelander, L; Reichard, P, *Annu. Rev. Biochem.*, **1979**, *48*, 13.

[5] Thelander, L; Graslund, A; Thelander, M, *Biochem.Biophys.Res. Comm.*,**1983**, *110*, 859.

[6] Lovejoy, DB; Richardson, DR, *Curr. Med. Chem.* **2003**, *10*, 1035.

[7] Mishra, RC; Tripathi, R; Katiyar, D; Tewari, N; Singh, D; Tripathi, RP, *Bioorg. Med. Chem.*, **2003**, *11*, 5363.

[8] Aikawa, M, *Principles and Practice of malariology*, pp 97-130, Wernsdorfer, W.H. and McGregor I.(eds.) Churchill Livingstone, Edinburg.

[9] Egan, TJ ; Combrinck, JM; Egan, J; Hearne, GR; Marques, HM; Ntenteni, S; Sewell, BT; Smith, PJ; Taylor, D; van Schalkwyk, DA; Walden, JC, *Biochem. J.*, **2002**, *365*, 343.

[10] Hudson-Taylor, DE; Dolan, SA; Klotz, FW; Fujioka, H; Aikawa, M; Koonin, EV; Miller, LH, *Mol. Microbiol.*, **1995**, *15*, 463.

[11] Cabantchik, ZI, *Blood Cells*, **1990**, *16*, 421.

[12] Pouvelle, B; Spiegel, R; Hsiao, L; Howard, RJ; Morris, RL; Thomas, AP; Taraschi, TF, *Nature*, **1991**, *353*, 73.

[13] Kolakovich, KA; Gluzman, IY; Duffin, KL; Goldberg, DE, *Mol. Biochem. Parasitol.*, **1997**, *87*, 123.

[14] Mabeza, GF; Loyevsky, M; Gordeuk, VR; Gunter, W, *Pharmacol. Ther.*, **1999**, *81*, 53.

[15] Murray, MJ; Murray, AB; Murray, MB; Murray, CJ, *Br. Med. J.*, **1975**, *2*, 1113.

[16] Oppenheimer, JL; Mac Farlane, SB; Moody, JB; Harrison, C, *Trans. R. Soc.Trop. Med. Hyg.*, **1986**, *80*, 818.

[17] Murray, MJ; Murray, AB; Murray, MB; Murray, CJ, *Lancet*, **1975**, *1*, 653.

[18] Haldar, K; Henderson, CL; Cross, GA, *Proc. Natl. Acad. Sci. USA*, **1986**, *83*, 8565.

[19] Gaby, T; Ginsburg, H, *Exp. Parasitol.*, **1993**, *77*, 261.

[20] Pollack, S; Schnelle, V, *Br. J. Haematol.*, **1988**, *68*, 125.

[21] Sanchez-Lopez, R; Halder, K, *Mol. Biochem. Pharmacol.*, **1992**, *63*, 273.

[22] Hirshko, C; Peto, TE, *J. Exp. Med.*, **1988**, *168*, 375.

[23] Peto, TE; Thompson, JL, *Br. J. Haematol.*, **1986**, *63*, 273.

[24] Cazzola, M; Arioso, P; Barosi, G; Bergamaschi, G; Dezza, L; Ascari, E, *Br. J. Haematol.*, **1983**, *53*, 659.

[25] Scott, MD; Ranz, A; Kuypers, FA; Lubin, BH; Meshnick, SR, *Br.J. Haematol.*, **1990**, *75*, 598.

[26] Gamboa de Dominguez, N; Rosenthal, PJ , *Blood*, **1996**, *87*, 4448.

[27] Francis, SE ; Barnejee, R; Golberg, DE, *J. Biol. Chem.*, **1997**, *272*, 14961.

[28] Rodriguez, MH; Jungery, MH, *Nature*, **1986**, *324*, 388.

[29] Loyevsky, M; Lytton, SD; Mester, BL; Shanzera, A; Cabantchik, ZI, *J. Clin.Invest.*, **1993**, *91*, 218.

[30] Cabantchi, ZI, *Parasitology today*, **1995**, *11*, 74.

[31] Wrigglesworth, JM; Baum, H, *Iron in biochemistry and medicine II*, **1980**, pp 29- 86, Jacobs, A and Worwood, M (eds.) Academic Press, New York .

[32] Raventos-Suarez, C; Pollack, S; Nagel, RL, *Am. J. Trop. Med. Hyg.*, **1982**, *31*, 919.

[33] Bezkorvainy, A, *Biochemistry of non-heme iron.* Plenum Press, New York and London, **1980.**

[34] Scheibel, LW; Sherman, IW, *Malaria principles and practice of malariology*, **1988**, pp 219-252, Wernsdorfer, W and McGregor, I (eds.) Churchill Livingstone, New York..

[35] Scheibel, LW; Adler, A; Trager, W, *Proc. Natl. Acad. Sci.* USA, **1979**, *76*, 5303.

[36] Scheibel, LW; Adler, A, *Mol. Pharmacol.*, **1980**, *18*, 320.

[37] Bailey-Wood, R; Blayney, MT; Muir, JR; Jacobs, A, *Br. J. Exp. Pathol.*, **1975**, *56*, 193.

[38] Cook, L; Grant, PT; Kermack, WO, *Exp. Parasitol.*, **1961**, *11*, 372.

[39] Bonday, ZQ; Taketani, S; Gupta, PD; Padmanaban, G, *J. Biol. Chem.*,

1997, *272*, 21839.

[40] Moormann, AM; Hossler, PA; Meshnick, SR, *Mol. Biochem. Parasitol.*, **1999**, *98*, 279.

[41] Pradines, B; Ramiandrasoa, F; Basco, LK; Bricard, L; Kunesh, G; Le-Bras, *J. Antimicrob. Agents Chemother.*, **1996**, *40*, 2094.

[42] Tim, FT; Regis, LT; Wanren, L; Yingsheng, W; Khashayar, K; Michael, S, *Curr. Med. Chem.*, **2003**, *10*, 983.

[43] Voest, EE; Vreugdenhil, G; Marx, JJ, *Ann. Intern. Med.*, **1994**, *120*, 490.

[44] http://opi.health.ufl.edu/file/feb26-2002post.pdf

[45] Steele, V E; Holmes, CA; Hawk, ET; Kopelovich, L; Lubet, RA; Crowell, JA; Sigman, CC; Kelloff, GJ, *Cancer Epidemiol. Biomarkers Prev.*, **1999**, *8*, 467.

[46] Asbeck, BSV; Marx, JJM, *W00112168A2*, **2001.**

[47] Galey, JP, *Mini Rev. Med. Chem.*, **2001**, *1*, 233.

[48] Mandel, S; Youdim, MB, *J. Neurol.*, **2000**, *247*, 95.

[49] Cabantchik, ZI; Glickstein, H; Golenser, J; Loyevsky, M; Tsafack, A, *Acta Haematol.*, **1996**, *95*, 70.

[50] Loyevsky, M; Gordeuk, VR, *Antimalarial chemotherapy, Mechanisms of action, Resistance, and New directions in Drug discovery*, Rosenthal, P. J. ed. Humana Press, **2001**, pp 307.

[51] Atkinson, CT; Bayne, MT; Gordeuk, VR; Brittenham, GM; Aikawa, M, *Am. J.Trop.Med.Hyg.*, **1999**, *45*, 593.

[52] Rubin, H; Salem, HS; Li, LS; Yang, FD; Mama, S; Wang, ZM; Fischer, A; Hamann, CS; Cooperman, BS, *Proc. Natl. Acad. Sci. USA 40*, **1993**, 9280.

[53] Niroshini, MG; Aaron, BW; Gregory, IG; Fiona, HF; Jennifer, A, *Chemistry and Biology*, **2003**, *10*, 677.

[54] Nyholm, S; Mann, GJ; Johansson, AG; Bergeron, PT; Graslund, A; Thelander, L, *J. Biol. Chem.*, **1993**, *268*, 26200.

CHAPTER 3
FERROCENIC COMPOUNDS IN CHEMOTHERAPY– AIMS AND OBJECTIVES OF THIS RESEARCH

3.1. Introduction

Ferrocenic compounds are those containing the ferrocene moiety **22** (Fig.3.1) within their structure. Ferrocene comprises two cyclopentadienide ligands coordinated to Fe in the +2 oxidation state; it was reported for the first time in 1952.[1,2] The suggested structure of ferrocene was provided by Wilkinson[3] and Fischer[4] separately afterwards. The name ferrocene was given by Woodward due to its resemblance to benzene in terms of reactivity.[5]

22

Figure 3.1: Structure of ferrocene **22**

The discovery of this new organometallic compound has brought about the starting point for modern organometallic chemistry,[1] and the growth of bioorganometallic chemistry which links classical organometallic chemistry to biology, medicine, and molecular biotechnology.[6-8]

Today ferrocene and its derivatives are popularly used in various biological applications and for conjugation with biomolecules because of ferrocene's unique properties such as low reported toxicity,[9,10] stability in aqueous and aerobic media, high lipophilicity ($\log P_{octanol/water}$= 3.28), accessibility of its large variety of derivatives and also its favorable electrochemical

properties.[11] Ferrocene itself is reported to exhibit anti-anemic properties.[12,13]

3.2 Ferrocenic Compounds

3.2.1 Ferrocenic Compounds as Antimycobacterial Agents

The ferrocenyl diamines **23** and **24** (Fig.3.2) have been synthesized as potential inhibitors of *Mycobacterium tuberculosis*, the causative agent of tuberculosis.[14] Out of the compounds synthesized, ferrocenyl diamines **23** and **24** were shown to possess greater activities with the most active compound having an IC_{50} value of 8 µg/ml against *M. tuberculosis* H37Rv strain.[14]

Replacement of the ferrocenyl moieties in **23** and **24** to generate the phenyl-substituted diamines **25** and **26** (Fig.3.2) resulted in a four-fold decrease in activity against *Mycobacterium tuberculosis in vitro* (IC_{50} >64 µg/ml).[14]

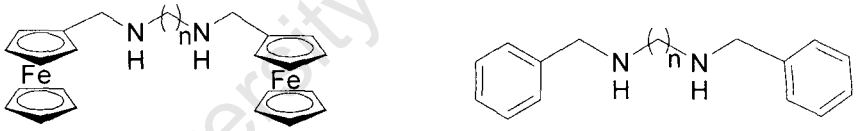

23: n= 2
24: n=3

25: n=2
26: n=3

Figure 3.2: Chemical structures of ferrocenyl diamines **23** and **24**, and their phenyl derivatives

This suggests an important role for ferrocene in the antimycobacterial activity of diamines **23** and **24**.

3.2.2. Ferrocenic compounds as Antifungal Agents

Fluconazole **27** (Fig.3.3) is a triazole antifungal agent which inhibits specific steps in fungal sterol biosynthesis. It has been shown to be effective

particularly against opportunistic yeasts of the genus *Candida*.[15] *Candida* species (i.e. *C. albians*, *C. glabrata, C. parapsilosis, C. krusei*) are the fifth most common isolates in hospital environments. Fluconazole is considered to be a useful agent for managing patients at risk of these infections.[16] However, this drug has encountered resistance from fungi.[17,18]

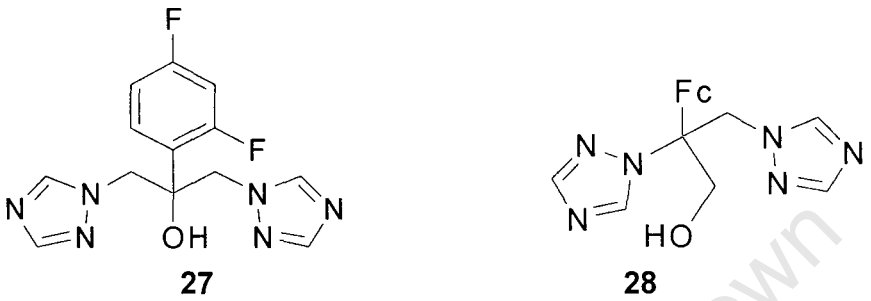

27 **28**

Fc= ferrocene

Figure 3.3: Fluconazole **27** and ferrocene-fluconazole **28**

Ferrocene-fluconazole (**28**) is a derivative of fluconazole in which the aromatic ring was replaced by a ferrocenyl group. The introduction of ferrocene in fluconazole resulted in a reversal effect on the resistance of the fungi. This was assumed to be an effective way of overcoming fluconazole resistance in the yeast.[16]

3.2.3. Ferrocenic Compounds as Anticancer Agents

Tamoxifen **29** (Fig.3.4) is a drug used in the treatment of hormone-dependent breast cancers *via* its active metabolite, 4-hydroxytamoxifen **30** (Fig.3.4),[19a, 19b] which is considered as the archetypical SERM (Selective Estrogen Receptor Modulator). Replacement of the aromatic ring on tamoxifen **29** and 4-hydroxytamoxifen **30** with a ferrocenyl moiety gives ferrocifen **31** and hydroxyferrocifen **32** respectively.

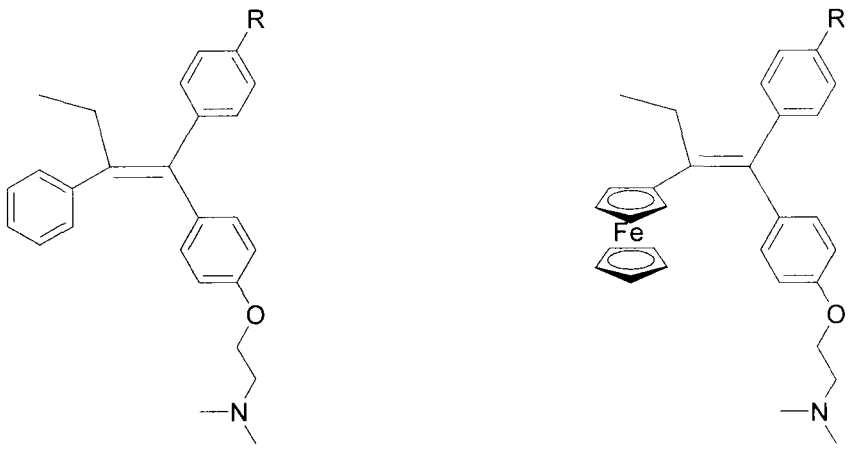

29: R= H : Tamoxifen

30: R= OH: Hydroxytamoxifen

31: R=H

32:R= OH

Figure 3.4: Structures of tamoxifen **29**, hydroxytamoxifen **30** and their ferrocene derivatives **31** and **32**, respectively.

It has been shown that hydroxyferrocifen **32** displays superior activity compared to its phenyl counterpart, compound **32**. Hydroxyferrocifen has shown antiproliferative effects on both hormone-dependent (MCF7) and independent (MDA-MB231) breast cancer cell lines *in vitro* whereas its phenyl counterpart **30** is active only against hormone-dependent cell lines.[20]

3.2.4. Ferrocenic Compounds as Antimalarial Agents

The antimalarial activities of ferrocenic compounds has been the most studied to date. Several well-established antimalarial drugs have been coupled covalently to a ferrocene entity resulting in general improvement in activity.[21]

The well-established drug, chloroquine, has experienced varying degrees of resistance from the parasite.[22-24] In the process of overcoming this

resistance, new approaches have been developed including the incorporation of a ferrocenyl group into a chloroquine molecule. This has led to the development of Ferroquine **33.** This compound **33** (Fig.3.5), a 4-aminoquinoline derivative in which the two methylene groups in the side chain of chloroquine have been replaced by a Ferrocenyl moiety, has been synthesized and found to be active against both chloroquine-resistant and sensitive strains of the malaria parasite at low concentrations, *in vitro*.[21] ferroquine is currently in pre-clinical development.

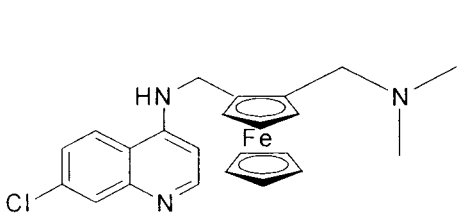

33

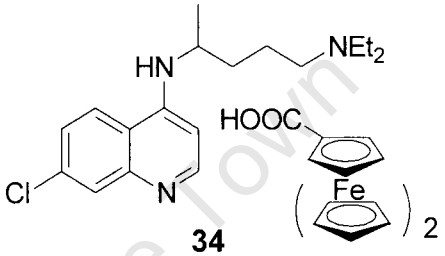

34

Figure 3.5: Structures of ferroquine **33** and chloroquine ferrocene carboxylic acid salt **34**

The efficacy of chloroquine decreased when the ferrocene entity was not covalently bound to the chloroquine (as in ferroquine), as exemplified by compound **34**. (Fig.3.5)

The low antiplasmodial activity of **34** amongst others demonstrated that the ferrocene molecule needs to be bound covalently to chloroquine to reverse chloroquine-resistance in the parasites, and that ferrocene by itself does not have significant anti-malarial activity.[21]

In the process of looking for other ways of incorporating ferrocene into the structure of chloroquine, compound **35** (Fig. 3.6) was synthesized and found to reverse chloroquine resistance in the malaria parasite (HB3, Dd2, FG1, FG3 and FG4) strains. The enhancement of activity was attributed to

increased cellular accumulation and also increased lipophilicity brought about by the presence of the substituted ferrocene.[22]

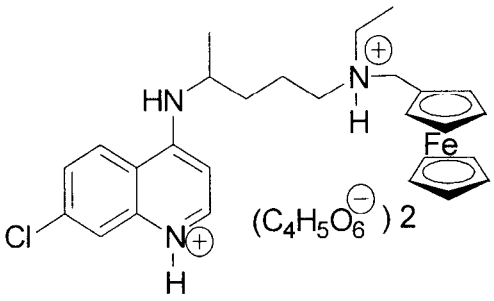

35

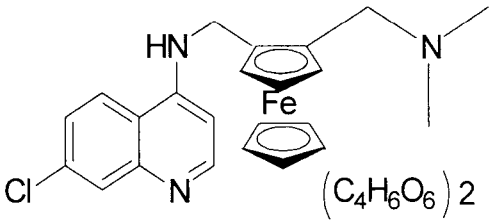

36

Figure 3.6: Ferrocene derivative salt **35** and ferroquine salt **36**

A salt derivative of ferroquine was synthesized in order to investigate if the solubility has an impact on the antimalarial activity of the ferroquine. The inhibitory concentration (IC_{50}) of both the ferroquine salt **36** (Fig.3.6) and ferroquine **33** were similar.[21]

The strategy for the synthesis of new ferrocene-chloroquine analogues particularly replacing the carbon chain of chloroquine by a ferrocenyl moiety was also extended to the anti-malarial amino-alcohols such as mefloquine and quinine. This led to new analogues of quinine and mefloquine **37** and **38** respectively (Fig.3.7).[23]

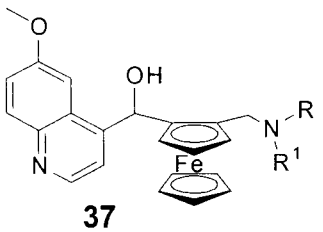

37

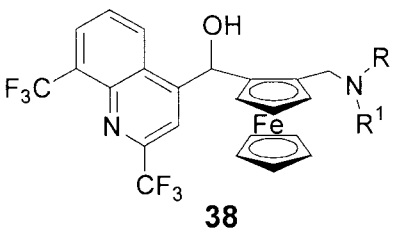

38

Figure 3.7: Structures of ferrocenic quinine **37** and ferrocenic mefloquine **38** analogues

Ferrocenic quinine analogue **37** is an amino-alcohol derivative in which the quinuclidinyl group was replaced by a substituted ferrocenyl moiety and ferrocenic mefloquine analogue **38**, is also an amino-alcohol derivative in which the piperidinyl group of mefloquine was replaced by the ferrocenyl moiety and unfortunately these compounds were found to have lower antimalarial activity than mefloquine or quinine on all *P. falciparum* strains used.[23]

Other ferroquine analogues were synthesized in which Fe of the ferrocenyl moiety was replaced by ruthenium (Ru) (structures shown in Figure 3.8) and tested against the malaria parasite resistant K1 strain and sensitive D10 strain. Compared to ferrocene, these ruthenocenes did not show essential difference in terms of the antimalarial activity.[24]

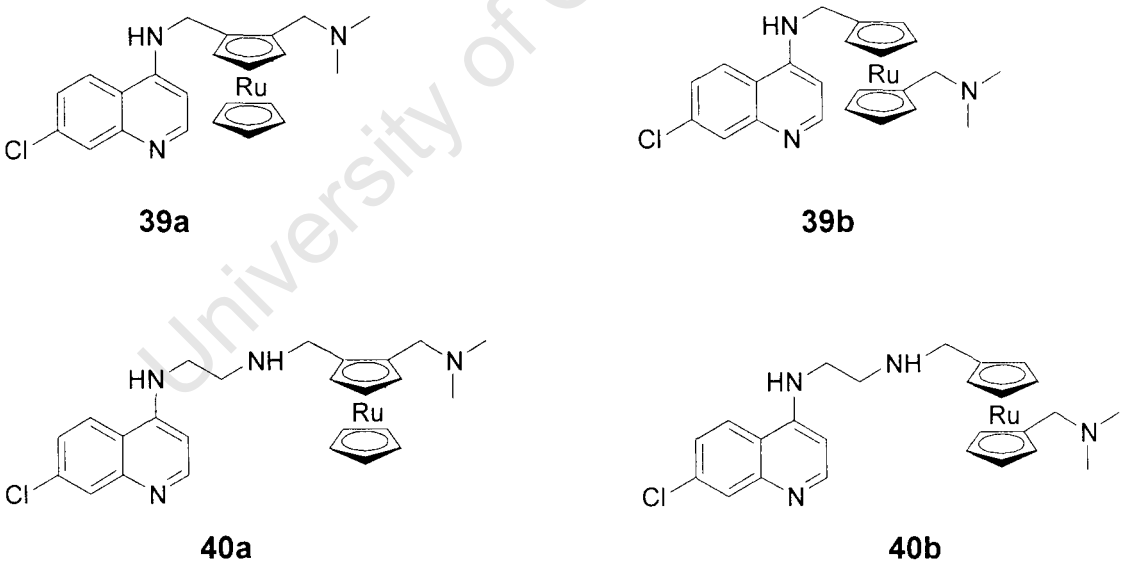

Figure 3.8: Chemical structures of ferroquine analogues **39a-b**, **40a-b**.

The probable mechanism of ferroquine on malaria parasite has been to some extent studied and discovered to be likely similar to that of chloroquine **1** and possibly involves hematin as the drug target and

inhibition of hemozoin formation.[25] The lipophilic character of ferrocenyl moiety present in ferroquine has been found to be one of the contributors to activity of the compound. This physical property presumably allows the toxic drug to be maintained within the vacuole.[25]

Moreover, ferrocene has been proposed to block PfCRT (*P. falciparum* Chloroquine Resistance Transporter) through its lipophilic properties like a resistance reversing agent.[25] PfCRT is a transmembrane protein which localizes to the parasite digestive vacuole, the site of chloroquine action.

3.3 Aims and Objectives of this Msc Dissertation

3.3.1 Objectives

The overall objective of this Msc project was to incorporate a ferrocene unit into the structure of metal (iron) chelating thiosemicarbazones and to study the electrochemical behaviour of the resulting molecules with a view to exploring any correlation between redox behaviour and antiparasitic activity.

3.3.2 Specific aims and rationale of the project

1. Synthesis and structure activity relationship study of new ferrocenic metal chelating thiosemicarbazones **41** and **42** (Fig. 3.9) as potential antiprotozoal agents.

   Thiosemicarbazones were selected due to their known multiple biological activities including antibacterial and antiviral,[26,27] anticancer,[28] antiplasmodial[29] and antitrypanosomal[30] properties.

   The known lipophilicity of ferrocene was envisaged to render ferrocenic thiosemicarbazones lipophilic. Lipophilicity is important in the antimalarial properties of iron chelators since the iron withheld

by chelators from *P.falciparum* most likely resides within the parasitic compartment of the malaria infected red blood cell. Thus, chelators have to cross the malaria parasite membranes to reach to the presumed site of action where selectivity is required for iron compared to other endogenous metals.[31]

2. Biological evaluation, in collaboration with appropriate laboratories, of the synthesized thiosemicarbazones against both chloroquine-sensitive and chloroquine resistant strains of the causative agent *P.falciparum* as well as against *Trypanosoma brucei*, the causative agent for African sleeping sickness or trypanosomiasis.

3. Electrochemical (cyclic voltammetric) evaluation of the synthesized ferrocenic thiosemicarbazones.

   The ferrocenyl group is particularly well-behaved electrochemically, providing a reversible one-electron couple. Thus we reasoned that studying the electrochemical behaviour of the synthesized ferrocenic thiosemicarbazones in conjunction with biological activity evaluation might provide insight into possible correlation between redox behaviour and biological activity. If correlation between redox behaviour and biological activity could be established, cyclic voltammetry might be used as an analytical pre-selection tool for compounds to proceed for biological evaluation.

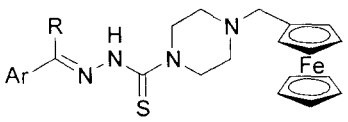

41

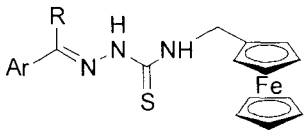

42

Figure 3.9: General classes of Ferrocenic Thiosemicarbazones

REFERENCES

[1] Kealy, TJ; Pauson, PL, *Nature*, **1951**, *168*, 1039.

[2] Miller, SA; Tebboth, JA; Tremaine, JF, *J. Chem. Soc.*, **1952**, 632.

[3] Wilkinson, G; Rosenblum, M; Whiting, MC; Woodward, RB, *J. Am.Chem. Soc.*, **1952**, *74*, 2125.

[4] Fischer, EO; Pfab, WZ, *Naturforsch*, **1952**, *7b*, 377.

[5] Woodward, RB; Rosenblum, M; Whiting, MC, *J. Am. Chem. Soc.*, **1952**, *74*, 3458.

[6] Jaouen, G; Vessières, A; Butler, IS, *Acc. Chem. Res.*, **1993**, *26*, 361.

[7] Fish, RH; Jaouen, G, *Organometallics*, **2003**, *22*, 2166.

[8] Metzler-Nolte, N, *Angew. Chem., Int. Ed.,* **2001**, *40*, 1040.

[9] Yeary, RA, *Toxicol. Appl. Pharmacol.*, **1969**, *15*, 666.

[10] Sun, JD; dahl, AR; Gillett, NA; Barr, EB; Crews, ML; Eidson, AF; Bechtold, WE; Burt, DG; Dieter, MP; Hobbs, CH, *Fundam. Appl. Toxicol.*, **1991**, *17*, 150.

[11] van Staveren, DR; Metzler-Notle, Nils, *Chem. Rev.*, **2004**, *104*, 5931.

[12] Köpf-Maier, P; Köpf, H., *Chem. Rev.*,**1987**, *87*, 1137.

[13] Köpf-Maier, P; Köpf, H, *Struct.Bond.*, **1988**, *70*, 105.

[14] Razafimahefa, D; Ralambomanana, D.; Hammouche, L; Pélinski, L; Lauvagie, S; Bebear, C; Brocard, JS; Maugein, J, *Bioorg. & Med. Chem. Lett.*, **2005**, *15*, 2301.

[15] Terrell, CL, *Maya Clin. Proc.*, **1999**, *74*, 78.

[16] Biot, C; Nadine, F; Maciejewski, L; Brocard, JS; Poulain, D, *Bioorg. Med. Chem. Lett.* , **2000**, *10*, 839.

[17] Vanden Bossche, H; Warnock, DW; Dupont, B; Kerridge, D; Sen Gupta, S; Improvisi, L; Marichal, P; Odds, FC; Provost, F; Ronin, O, *J. Med. Vet. Mycol.*, **1994**, *32*, 189.

[18] Dupont, B, *Curr. Opin. Infect. Dis.*, **1995**, *8*, 424.

[19] a) Jordan, VC, *Tamoxifen for the treatment and prevention of Breast cancer*; PR: New York, **1999**. b) Hillard, E; Vissières, A; Thouin, L; Jaouen, G; Amatore, C, *Angew. Chem. Int. Ed.*, **2006**, *45*, 285.

[20] Top, S; Tang, J; Vessiere, A; Carrez, D; Provot, C; Jaouen, G, *Chem.*

Commun., **1996**, 955.

[21] Biot, C, *Curr. Med. Chem.-Anti-Infective agents*, **2004**, *3*, 135.

[22] Biot, C; Delhaes, L; Abessolo, H; Domarle, O; Maciejewski, LA; Mortuaire, M; Delcourt, P; Deloron, P; Camus, D; Dive, D; Brocard, JS, *J. Organomet. Chem.*, **1999**, *589*, 59.

[23] Biot, C; Delhaes, L; Maciejewski, LA; Mortuaire, M; Camus, D; Dive, D; Brocard, JS, *Eur. J. Med. Chem.*, **2000**, *35*, 707.

[24] Beagley, P; Blackie, MAL; Chibale, K; Clarkson, C; Moss, JR; Smith, PJ, *J. Chem. Soc., Dalton Trans.*, **2002**, *23*, 4426.

[25] Biot, C; Taramelli, D; Forfar-Bares, I; Maciejewski, LA; Boyce, M; Nowogrocki, G; Brocard, JS; Basilico, N; Olliaro, P; Egan, TJ, *Molecular Pharmaceutics*, **2005**, *2,* 185.

[26] Mishra, V; Pandeya, SN; Pannecouque, C; Witvrou, M ; De Clercq, E, *Arch. Pharm.* (Weinheim), **2002**, *335*, 183.

[27] Condit, RC ; Easterly, R ; Pacha, RF; Fathi, Z; Meis, RJ, *Virology*, **1991**, *185*, 857.

[28] Finch, RA; Liu, MC; Cory, AH; Cory, JG; Santorelli, AC, *Adv. Enzyme Regul.*, **1999**, *39*, 3.

[29] Klayman, DC; Bartosevich, JF; Griffin, TS; Mason, CJ; Secovill, JP, *J. Med. Chem.*, **1979**, *22*, 855.

[30] Greenbaum, DC; Mackey, Z; Hansell, E; Doyle, P; Gut, J; Caffrey, CR; Lehrman, J; Rosenthal, PJ; McKerrow, JM; Chibale, K, *J. Med. Chem.*, **2004**, *47*, 3212.

[31] Chiyanzu, I; Clarkson, C; Smith, PJ; Lehrman, J; Gut, J; Rosenthal, PJ; Chibale, K, *Bioorg. Med. Chem.*, **2005**, *13*, 3249.

CHAPTER 4
RESULTS AND DISCUSSION

4.1. Introduction

In this chapter the synthesis and characterization of ferrocenic thiosemicarbazones and their intermediates are detailed. This is followed by electrochemical studies of selected ferrocenic thiosemicarbazones. The biological results of both the intermediate thiosemicarbazide thioesters and target ferrocenic compounds are presented and discussed.

4.2. Chemistry

4.2.1 Retrosynthetic analyses

The *N*-substituted ferrocenic thiosemicarbazones **41** and **42** could be made from two different methods as depicted in schemes 4.1 – 4.4.

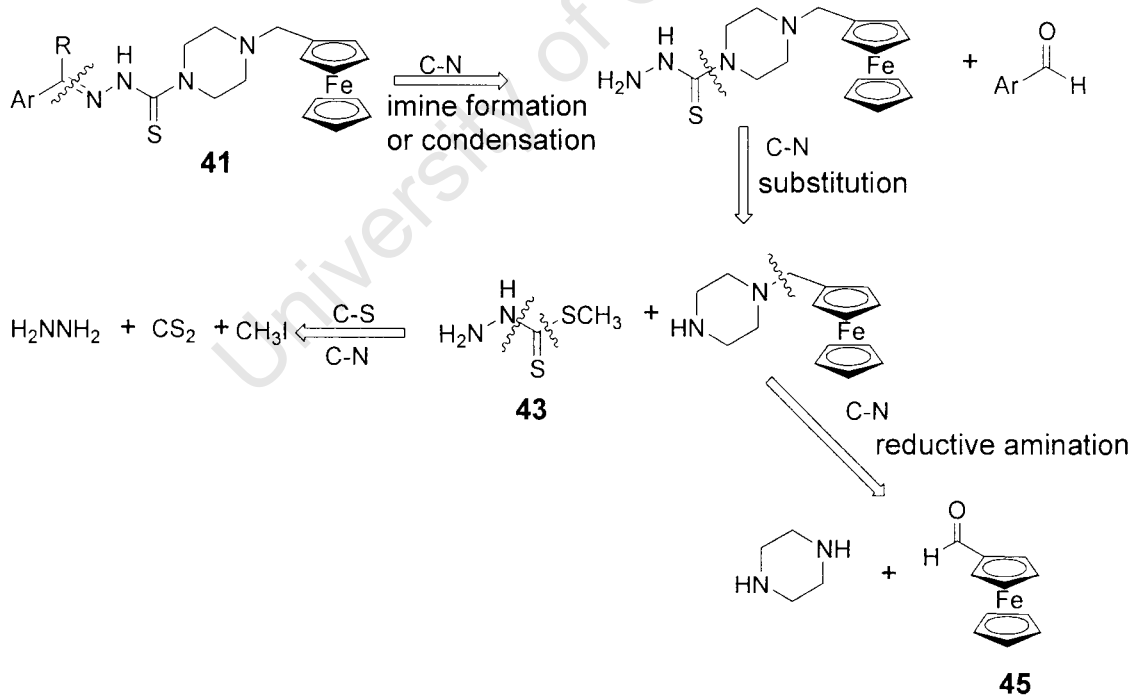

Scheme 4.1:Retrosynthetic analyses of *N*-substituted ferrocenic thiosemicarbazone (Meth. 1)

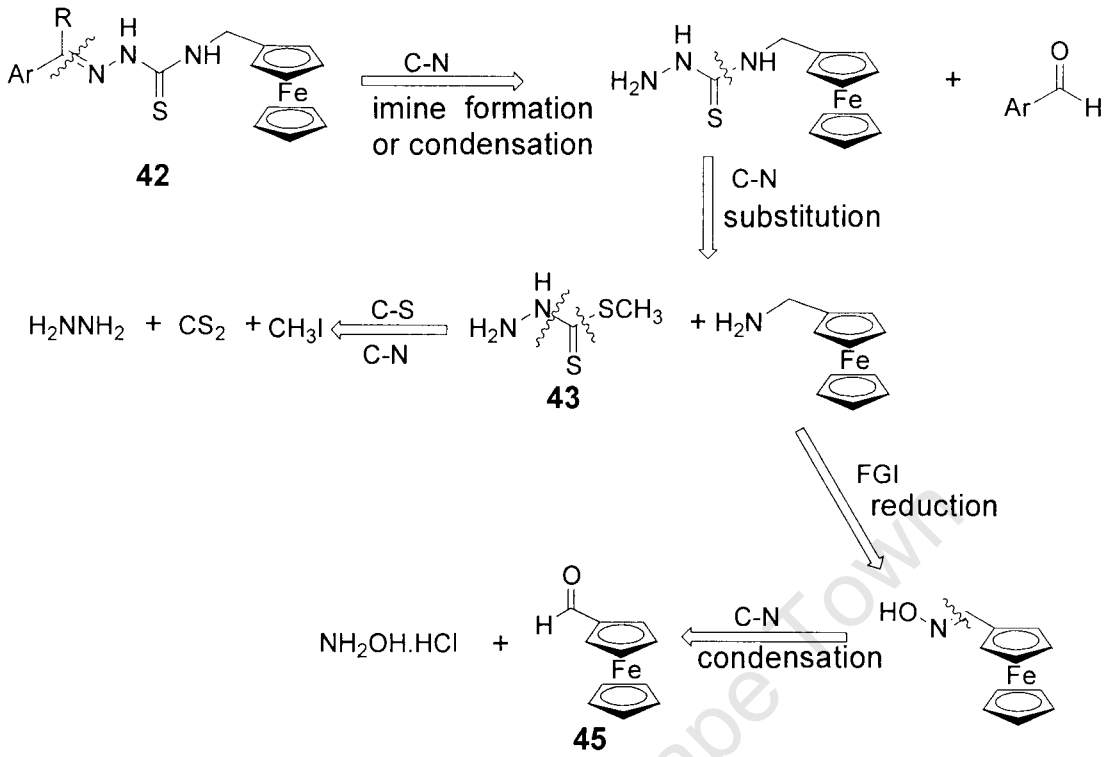

Scheme 4.2:Retrosynthetic analyses of *N*-substituted ferrocenic thiosemicarbazone (Meth. 1).

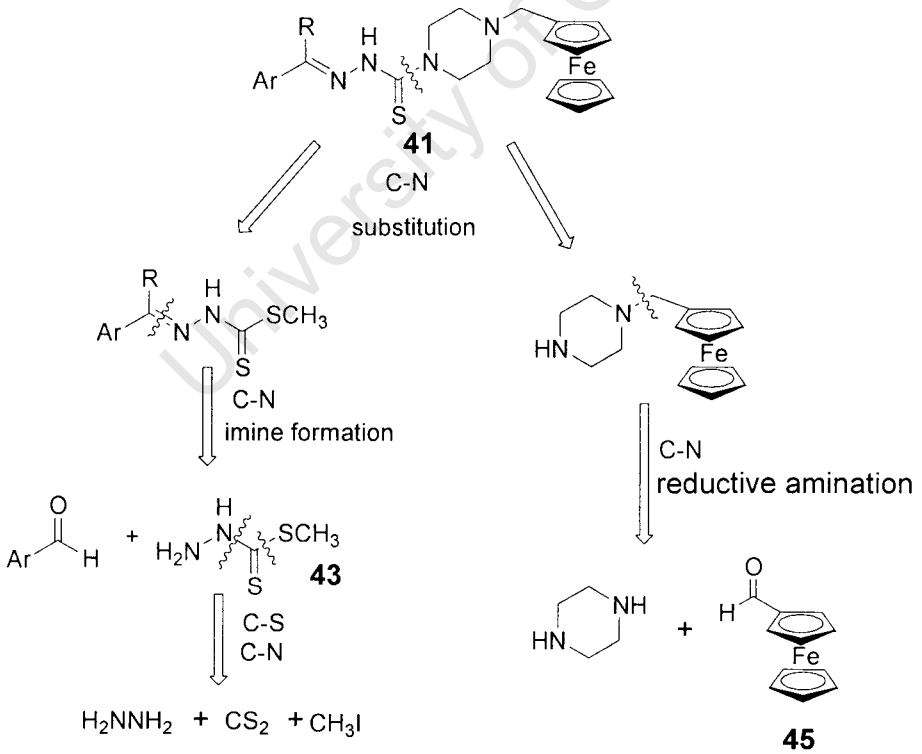

Scheme 4.3:Retrosynthetic analyses of *N*-substituted ferrocenic thiosemicarbazone (Meth. 2)

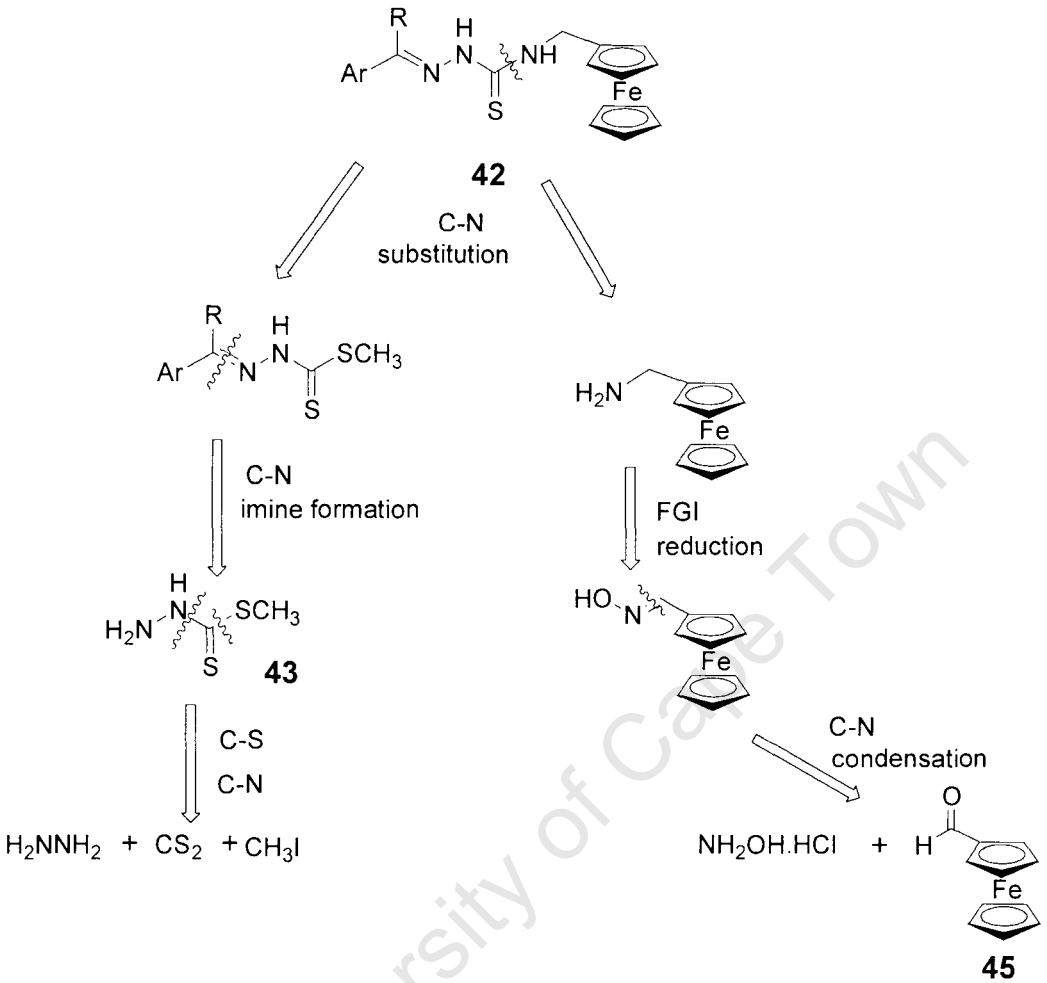

Scheme 4.4: Retrosynthetic analyses of *N*-substituted ferrocenic thiosemicarbazone (Meth. 2).

The retrosynthetic analyses depicted in schemes 1 and 2 identify ferrocene carboxaldehyde **45**, piperazine and hydrazine thioester **43** as key starting materials. Method 2 as depicted in scheme 4.3 and 4.4 was judged to be more convenient as we were interested in evaluating the biological activities of the intermediate thioester.

4.2.2 Synthesis of thiosemicarbazone thioesters

The substituted thiosemicarbazone thioesters were synthesized from a condensation reaction of substituted carbonyl compounds (commercially

available) and synthesized hydrazine thioester **43**, scheme 4.5. Compound **43** was synthesized from commercially available hydrated hydrazine (NH_2NH_2), carbon disulphide (CS_2) and methyl iodide (CH_3I) according to a literature protocol.[1]

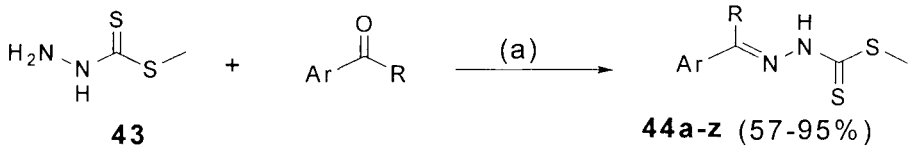

43 **44a-z** (57-95%)

Scheme 4.5: Reagents and conditions: (a) CH_3OH, ambient temperature, 20 h.

^{1}H NMR spectroscopy was used to confirm the proposed structures of thiosemicarbazone thioesters in all cases. The ^{1}H NMR of synthesized compounds showed a singlet integrating for 3 hydrogens at *ca* δ= 2.6 ppm corresponding to the S*CH*$_3$ group (Fig. 4.1 and Fig. 4.2). A singlet was observed at *ca* δ= 2.3 ppm for methyl ketone-derived thiosemicarbazone thioesters integrating for 3 hydrogens corresponding to the methyl group (Fig.4.2).

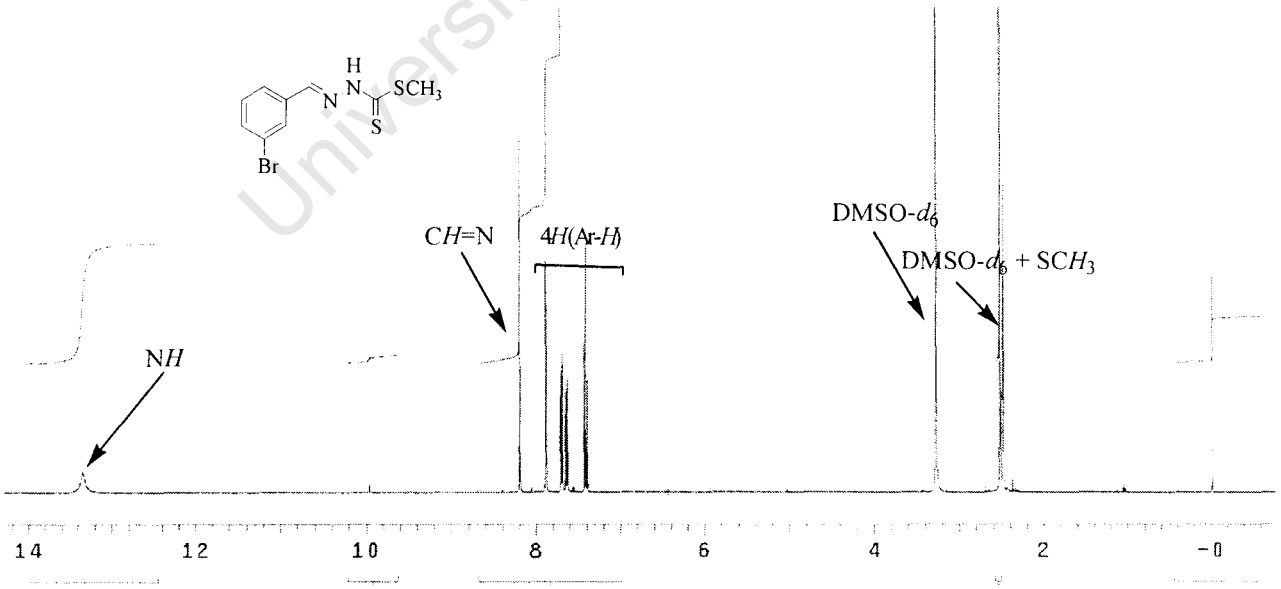

Figure.4.1: ^{1}H NMR spectrum of **44c** a typical aldehyde-derived thiosemicarbazone thioester In DMSO-d_6.

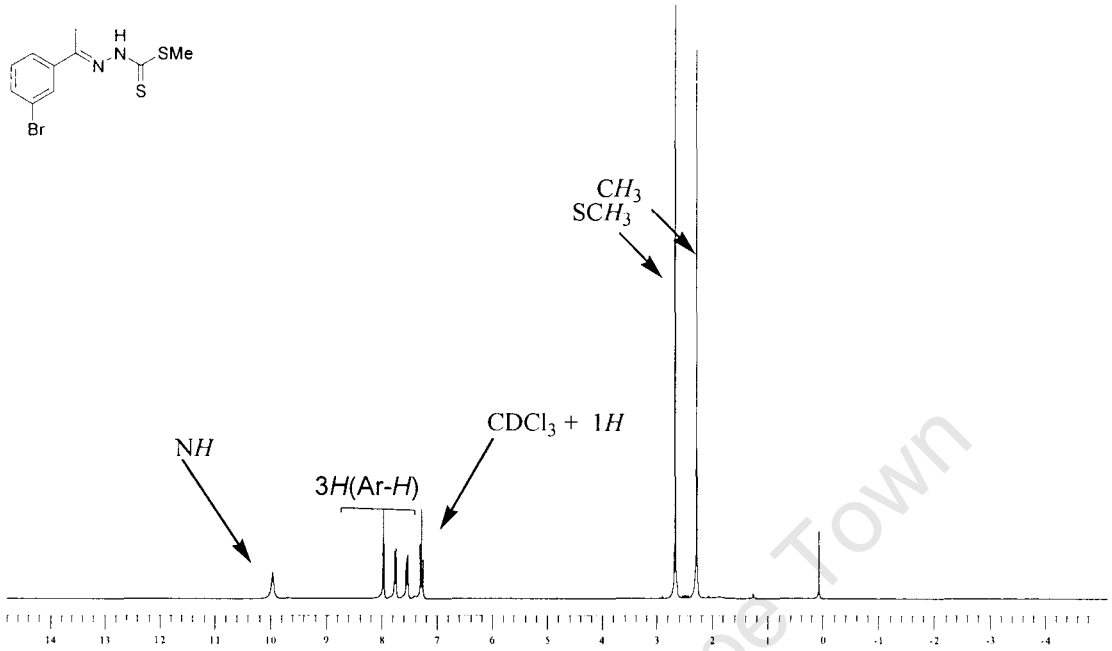

Figure 4.2: ^{1}H NMR spectrum of **44a** a typical ketone-derived thiosemicarbazone thioester in $CDCl_3$

The ^{13}C NMR data confirmed the exact number of carbon present in the synthesized molecule. At around 198 ppm, for most of them, the peak for thione carbon which confirmed the successful synthesis of the thiosemicarbazone thioester was observed. The infrared analyses showed, for all the thiosemicrabazone thioesters, absorbance peaks at around 3020, 1420, 1213 and 770, 666 characteristics of amine (N-H), imine (N=C), thione (C=S) and aromatic protons (C-H), respectively.

The mass spectrommetry value, for each thiosemicarbazone thioester, was consistent with the calculated molecular weight for each synthesized molecule.

The ^{1}H NMR spectrum of the 2-acetylpyridine-derived thiosemicarbazone thioester (Fig. 4.4) showed a mixture of geometrical isomers in deutero-chloroform ($CDCl_3$) as described in the literature.[2] The literature suggested that there are at least three isomeric forms (*Z, E'* and *E*). The *E'* isomer (Fig. 4.3) involves C=N-N=C(S^-)N conjugation. In deutero-chloroform the intensity of *E'* is lower. It has been observed that in deutero-DMSO (DMSO-d_6) a single hydrogen-bonded isomer is observed and that must be *E'*.

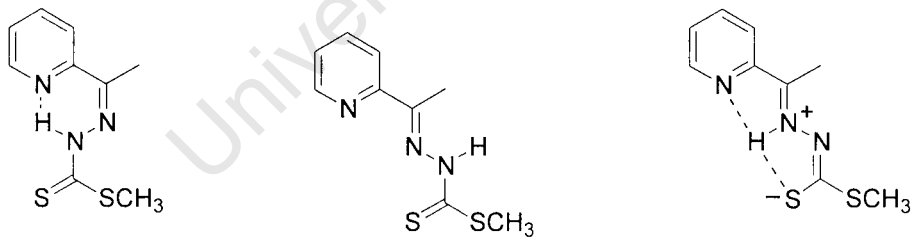

" *Cis*" (*Z*) "*Trans*" (*E*) "*Trans*" (*E'*)

Figure 4.3: *Z, E* and *E'* possible geometrical conformation of 2-acetylpyridine derived thiosemicarbazide thioester.

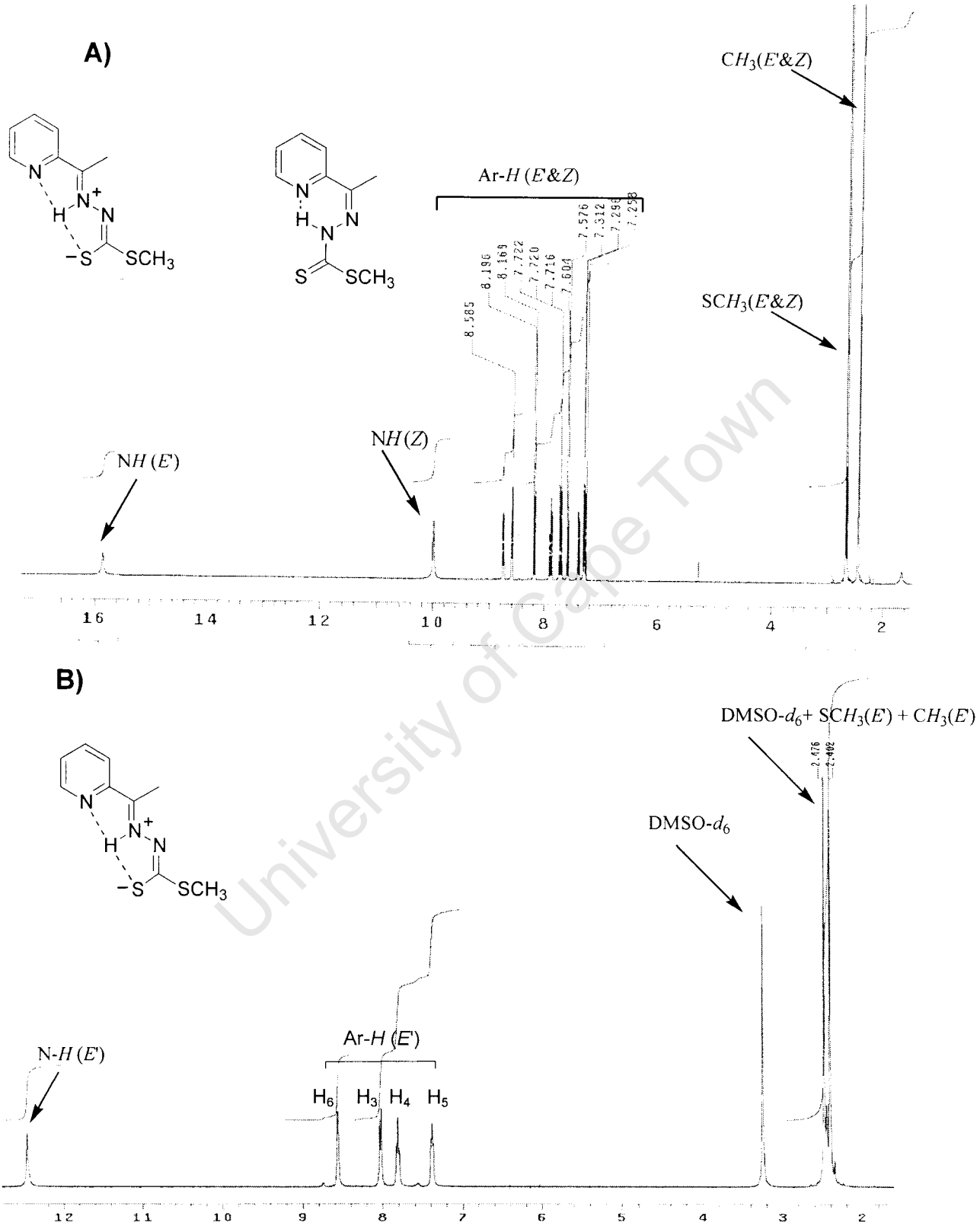

Fig. 4.4 : ^{1}H NMR spectra of 2-acetylpyridine thiosemicarbazone thioester in $CDCl_3$ (A) and in DMSO-d_6 (B).

Table 4.1: Isolated yields of thiosemicarbazone thioesters

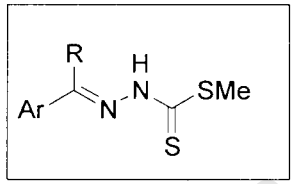

Compounds	Ar	R	% yield	Compounds	Ar	R	% yield
44a	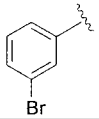	CH_3	80	**44g**	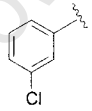	H	64
44b		H	71	**44h**	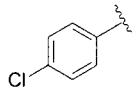	H	80
44c	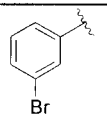	H	71	**44i**	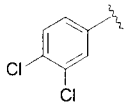	CH_3	92
44d	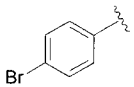	H	57	**44j**	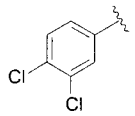	H	88
44e	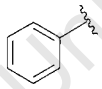	H	71	**44k**	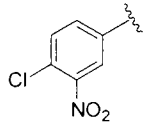	H	88
44f	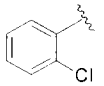	H	63	**44l**	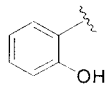	H	84

Table 4.1: Isolated yields of thiosemicarbazone thioesters (continued).

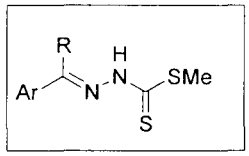

Compounds	Ar	R	% yield	Compounds	Ar	R	% yield
44m	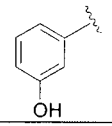	H	94	**44t**	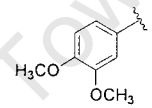	H	77
44n	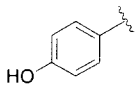	H	95	**44u**	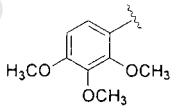	H	82
44o	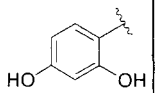	H	75	**44v**	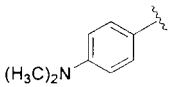	H	94
44p	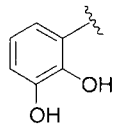	H	57	**44w**	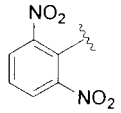	H	92
44q	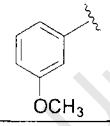	H	85	**44x**	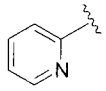	CH_3	64
44r	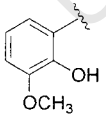	H	64	**44y**	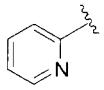	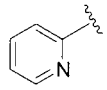	86
44s	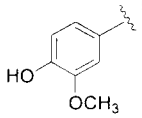	H	77	**44z**	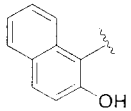	H	92

4.2.3 Synthesis of ferrocenylmethyl amines 47 and 48, and synthesis of *N*- substituted ferrocenic thiosemicarbazones

This synthesis was carried out *via* two different methods. The first method involved the synthesis of ferrocene amine **47** which was synthesized from ferrocene carboxaldehyde **45** and hydroxylamine hydrochloride ($NH_2OH.HCl$) to generate ferrocene oxime **46**[3] in 80% yield. Compound **46** was further reduced to ferrocene amine **47** using $LiAlH_4$[3] in 76 % yield (Scheme 4.6a').

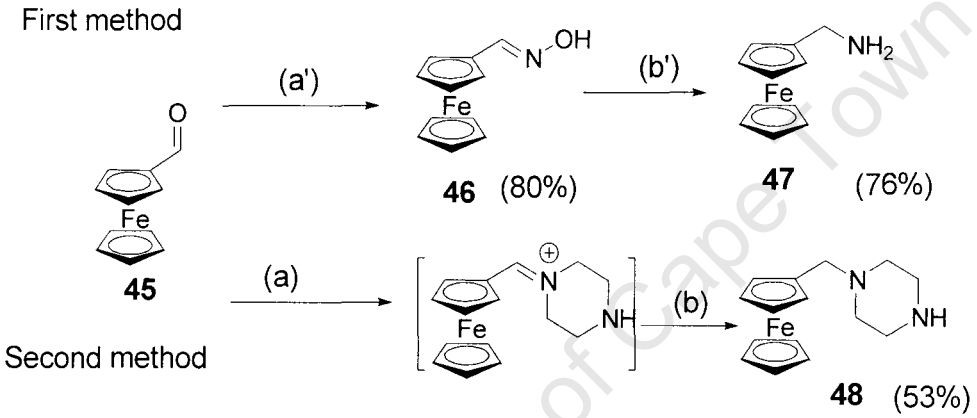

Reagents and conditions: a') $NH_2OH.HCl$, NaOH, C_2H_5OH b') $LiAlH_4$, THF, reflux.
a) Piperazine, CH_3OH b) $NaBH_3CN$

Scheme 4.6: Chemical synthesis of ferrocenyl methyl amines, **47** and **48**

The second method involved the synthesis of the piperazine-based ferrocenylmethyl amine **48** *via* reductive amination.[4] Thus, ferrocene carboxaldehyde was reacted with piperazine to generate an iminium ion *in situ*, which was subsequently reduced using $NaCNBH_3$ to give the target compound **48** in 53% yield.

The ^{1}H NMR spectrum of **46** showed a singlet at δ= 8.0 ppm corresponding to one proton of the azomethine and a broad singlet at δ= 7.5 ppm due to the OH group of the oxime which disappeared after reduction to **47**.

The ^{1}H NMR spectrum of **47** showed a singlet at 3.54 ppm integrating for two (CH_2) protons. In addition to this, the broad singlet observed at 7.5 ppm in the ^{1}H NMR spectrum of **46** and assigned to the OH group of the oxime disappeared. The ^{1}H NMR data of both **46** and **47** were consistent with the literature.[3]

The synthesis of thiosemicarbazones[5] was a straight forward substitution reaction between selected ketone and/or aldehyde-derived thiosemicarbazone thioesters in MeOH under reflux. The results are presented in Table 4.2.

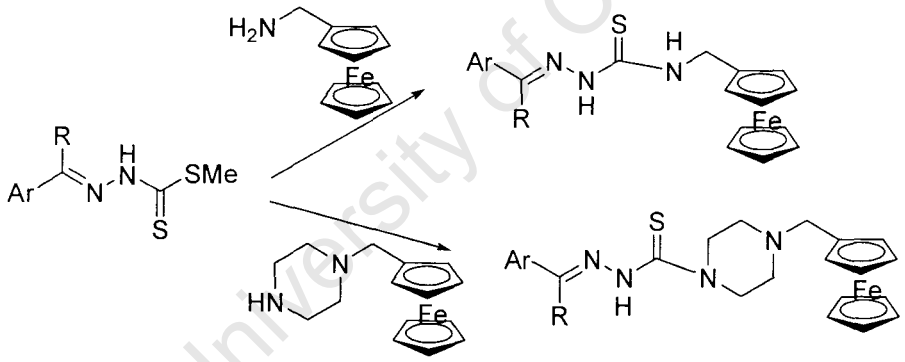

Scheme 4.7 : Reagents and conditions: CH_3OH, reflux, 24 h.

Table 4.2: Isolated yields of synthesized *N*-substituted Ferrocenic Thiosemicarbazones

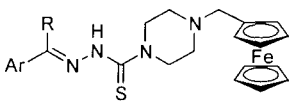

41 a-b

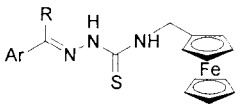

42 a-o

Cmpd	Ar	R	% yield	Cmpd	Ar	R	% yield
41a	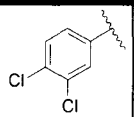	CH_3	44	**42h**	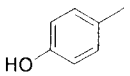	H	6
41b	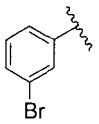	CH_3	26	**42i**	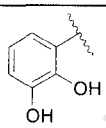	H	13
42a		H	27	**42j**	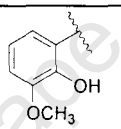	H	24
42b	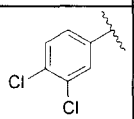	H	76	**42k**	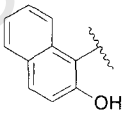	H	9
42c	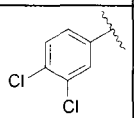	H	45	**42l**	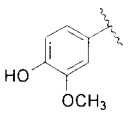	H	28
42d	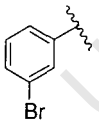	H	38	**42m**	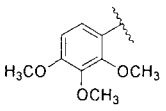	H	23
42e	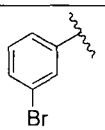	H	22	**42n**	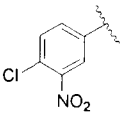	H	39
42f	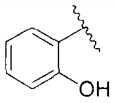	H	31	**42o**	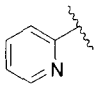		54
42g	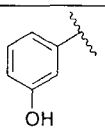	H	52				

The ^{1}H NMR spectrum of a representative *N*-substituted ferrocenyl methyl thiosemicarbazone **42c** is shown in Fig.4.5. A doublet at *ca* δ= 4.5 ppm integratimg for the two methylene protons of ferrocenylmethyl group and a triplet at *ca* δ= 8.5 ppm integrating for one proton of the adjacent N*H* group are some of the key spectroscopic indicators. Disappearance of the singlet at *ca* δ= 2.5 ppm due to the S*CH*$_3$ protons from the thiosemicarbazone thioester precursor, provided further evidence of the expected product.

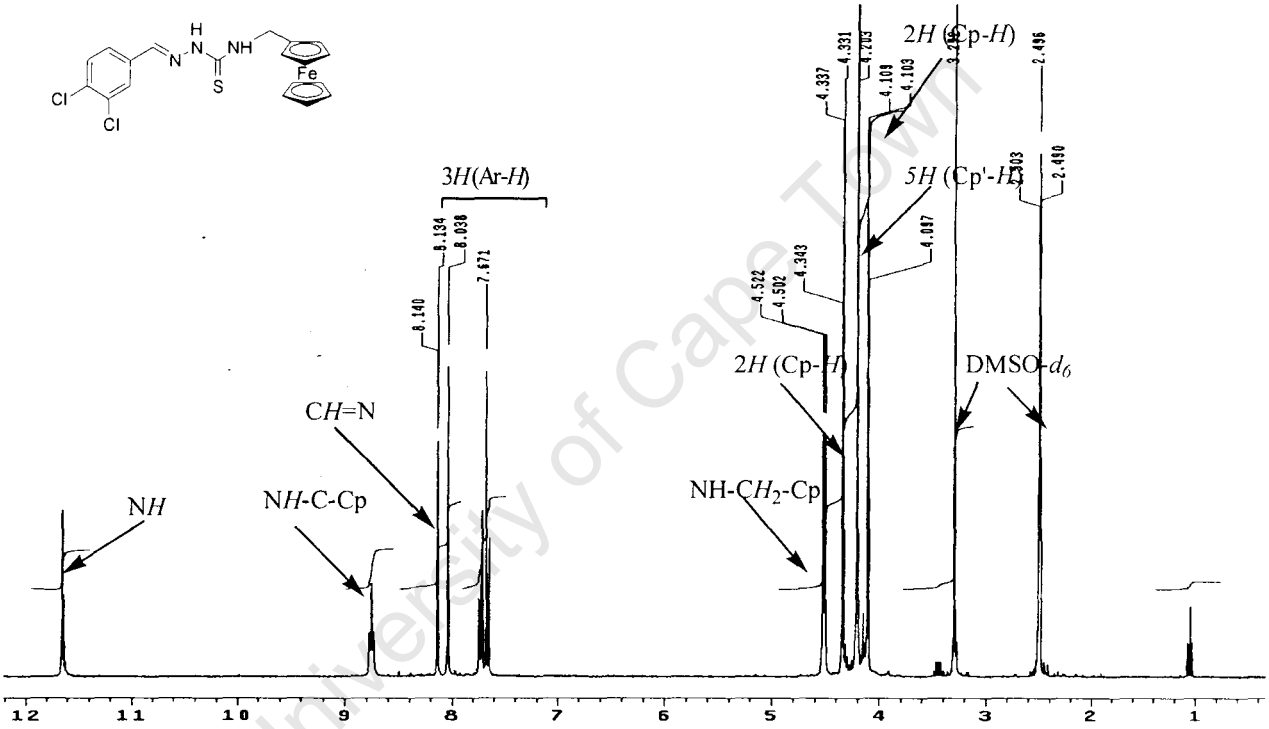

Figure 4.5: ^{1}H NMR spectrum of **42c** in DMSO-d_6

On the other hand, the ^{1}H NMR spectra of piperazine-based thiosemicarbazones exemplified by **41a** (Fig.4.6) showed disappearance of the broad peak at *ca* δ= 7.5 ppm and the singlet at *ca* δ= 2.5 ppm assigned to the N-*H* of the ferrocene piperazine **48** and S*CH*$_3$ proton of the thiosemicarbazone thioester respectively. These data helped to confirm that the target molecule had been successfully synthesized.

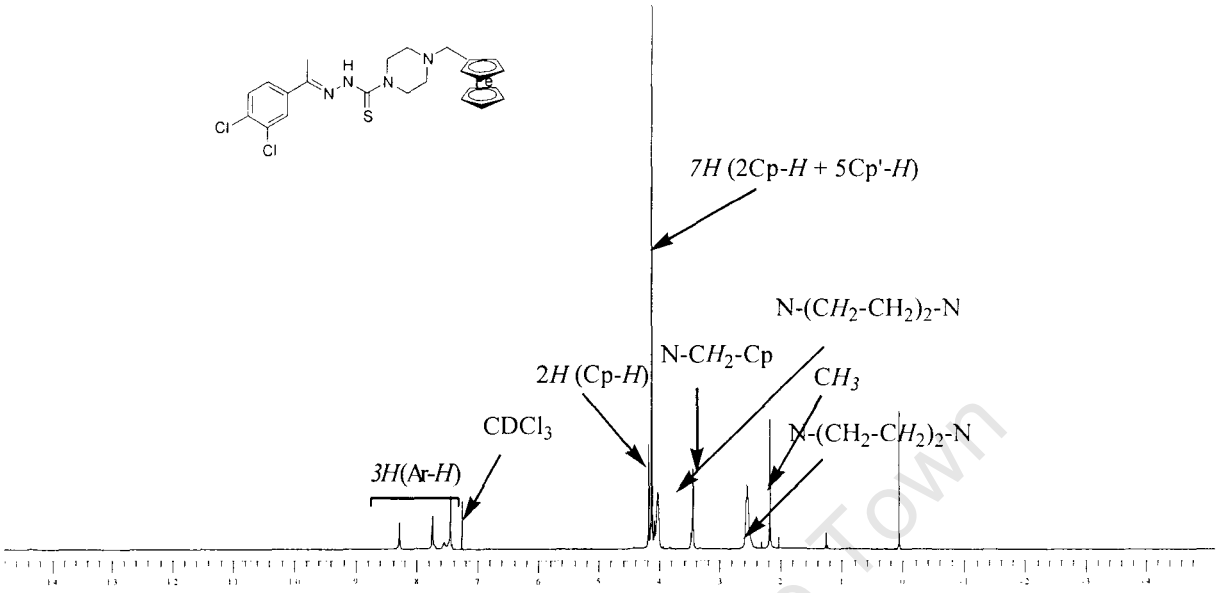

Figure 4.6: ^{1}H NMR spectrum of **41a** in $CDCl_3$

Some specific spectral features that were observed with both aldehyde and ketone-derived thiosemicarbazones are as follows:

For aldehyde-derived thiosemicarbazones: five Cp protons appeared as a singlet at *ca* δ= 4.2 ppm and other four Cp protons appeared differently in pairs as triplets at *ca* δ= 4.3 ppm and 4.1 ppm, respectively (exemplified by compound **42c**) in Figure 5, on the other hand only two protons appeared at *ca* δ= 4.2 ppm and seven protons at *ca* δ= 4.1 ppm, both as singlets for all ketone-derived thiosemicarbazones ,exemplified by compound **41a** in Figure 4.6.

The ^{13}C NMR, infrared absorbance peaks and the mass spectrometry confirmed the synthesis of the ferrocenic thiosemicarbazones.

The thiosemicarbazone and their ferrocenic analogues were successfully synthesized with generally good yield.

4.3 Electrochemistry

4.3.1 Cyclic voltammetry

Cyclic voltammetry was developed from the discovery of polarography in 1922 by the Czech chemist, Jaroslav Heyrovsky, for which he received a Nobel Prize in chemistry in 1959.[6] In the 1960s and 1970s, after going through a number of difficulties related to the routine use of the technique, significant progress was made in establishing the theory, methodology, and instrumentation of voltammetric techniques.[6]

There are various types of voltammetric techniques, such as polarography, pulse methods, preconcentration and stripping techniques, as well as cyclic voltammetry. The common characteristic of all voltammetric techniques is that they involve the application of potential (E) to an electrode and the monitoring of the resulting current (i) flowing through the electrochemical cell.

Cyclic voltammetry is the most widely used technique for acquiring qualitative information about electrochemical reactions, and is a sensitive electrochemical method which permits the collection of excellent data at low concentration of electroactive substances.[7]

Over the last twenty years, cyclic voltammetry has become a popular tool in different fields such as in organic chemistry, where it is used to study different biosynthetic pathways[8] and to study chemically generated free radicals.[9] It has also been widely used in inorganic chemistry to assess the effects of ligands on oxidation/reduction potential of the central metal ion in coordination and organometallic complexes and multinuclear clusters.[10] On the other hand, physical and biological chemists use this technique for many purposes, such as for studying oxidation and reduction processes in different media, adsorption processes on surfaces, electron

transfer and reaction mechanisms, kinetics of electron transfer processes, and transport, speciation and thermodynamic properties of solvated species.[6]

Cyclic voltammetry consists of cycling the potential of an electrode, which is immersed in an unstirred solution (the reason for this will be detailed later in this section, pp.60) of an electroactive species, and measuring the resulting current. The potential of the working electrode is controlled against a reference electrode such as saturated calomel electrode (SCE) or a Ag/Ag^+ electrode. The controlling potential which is applied across these two electrodes are considered to be an excitation signal which is a linear potential scan with a triangular waveform as shown in Fig. 4.7 .

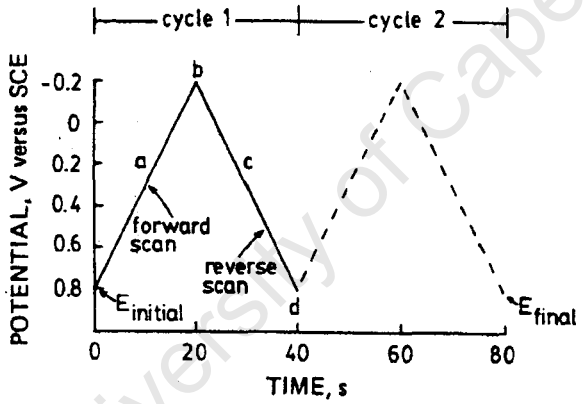

Figure 4.7 : Typical excitation signal for cyclic voltammetry - a triangular potential waveform with switching potentials at 0.8 and –0.2 V *versus* SCE.[11]

The triangular potential excitation signal sweeps the potential of the working electrode back and forth between two designated values (switching potentials) at a constant scan rate. Because the potential varies linearly with time, the horizontal axis can be thought of as a time axis. The response signal to the potential excitation is the measured current (*i*). The plot of the current (*i*) *versus* the potential (*E*) results in a voltammogram. A

typical electrochemical cell for CV and resulting voltammogram are illustrated in Fig. 4.8 below.

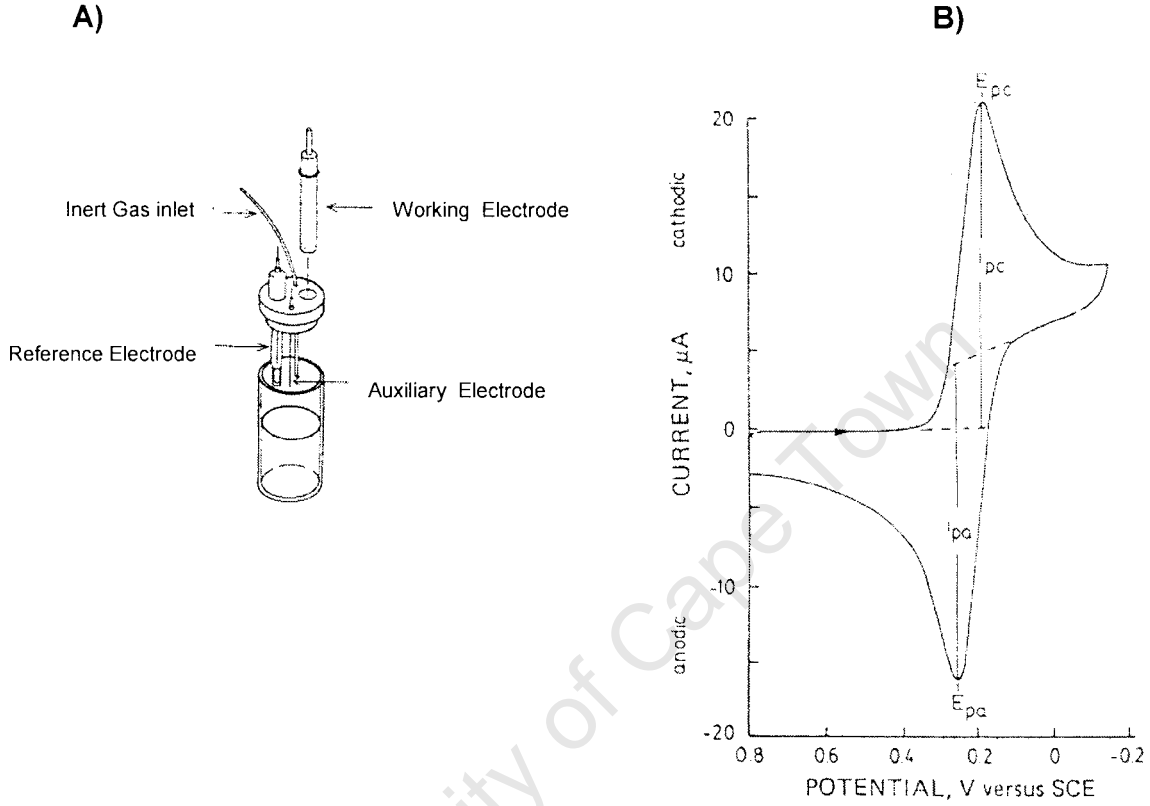

Figure 4.8: A) Typical electrochemical cell for cyclic voltammetry. In this work the reference electrode was Ag/Ag^{+}, the auxiliary electrode was Pt wire and the working electrode was a Pt disc.[11]
B) Typical cyclic voltammogram.[11]

Modern potentiostats utilize a three–electrode configuration that includes a working electrode, a reference electrode and an auxiliary electrode, as shown in Fig. 4.8A. The potentiostat applies the desired potential between a working electrode and a reference electrode. The applied potential controls the concentration of the redox species at the electrode surface and the rate of the reaction.[6] The working electrode is the electrode at which the electrolysis of interest takes place. The current required to sustain the

electrolysis at the working electrode is provided by the auxiliary electrode. The auxiliary electrode is usually a platinum wire that is placed directly into the solution. This arrangement prevents large currents from passing through the reference electrode that could change its potential. Before the experiment oxygen is removed from the solution by bubbling with nitrogen gas to avoid any traces of oxygen that could give rise to a redox reaction.

The measurements are plotted using computer software to produce a cyclic voltammogram (Fig. 4.8B). The important parameters that may be obtained from a cyclic voltammogram are the magnitudes of the peak potentials (E_{pc}, E_{pa}) and peak currents (i_{pc}, i_{pa}) of the cathodic and anodic peaks, respectively. E_{pa}, E_{pc}, i_{pc}, and i_{pa} give qualitative information about electroactive compounds, ie the information about the reversibility or irreversibility of the electrochemical reaction and the number of electrons exchanged during the process.[11]

The peak separation between potentials E_{pa} and E_{pc} (ΔE) can be used to determine the number of electrons transferred in a reversible system by the following relationship $\Delta E = 59/n$ mV (n being the number of electrons transferred).[12] The half-wave potential, $E_{1/2}$, for a reversible couple is centered between E_{pa} and E_{pc} and is close to the formal reduction potential, $E^{o'}$, for the electroactive species.

An electrochemical reaction is termed reversible if the electron transfer process is fast compared with other processes such as diffusion and is irreversible if the electrochemical reaction is due to a slow electron transfer rate with the working electrode,[6,12] the latter being manifested by an increase of the potential peak separation (ΔE). For a reversible couple the ratio of the peak currents, i_{pa} and i_{pc}, is unity.

It should be noted that the higher (more positive) the half-wave potential, $E_{1/2}$, which is the average of E_{pc} and E_{pa}, the easier the electroactive compound is reduced at the working electrode or the more difficult it is to oxidize.[8]

There are three general mass-transport processes by which species may be brought to an electrode surface: by migration of charged ions in an electric field; by convection, which is due to motion of the solution or the electrode; and by diffusion under the influence of a concentration gradient.

Migration is not desirable in electrochemical reactions since it depends directly on the transferred number of ions in solution and the electrical potential gradient in the vicinity of the electrode surface.[9] Thus migration may increase or oppose diffusion. In order to minimize the effects of migration, some innocuous salt (supporting electrolyte) is added into the solution with at least 100-fold greater concentration than the electroactive species.

Convection results from stirring, density gradients or temperature gradients. Thus to ensure movement of the electroactive species by diffusion only, measurements in cyclic voltammetry are made on unstirred, thermally insulated solutions.

Diffusion, the movement of chemical species under the influence of a concentration gradient, is of great importance in voltammetric techniques.[7] The species (ions or molecules) will move from a high concentration area to a low concentration area in order to minimize or eliminate concentration differences which were established as soon as electrolysis began. The rate of diffusion is proportional to the gradient of the concentration in the solution. Thus, the situation when the rate of reaction is controlled by the

rate of diffusion rather than the rate of the reaction itself is called diffusion control, and that is the requirement of all voltammetric techniques.

4.3.2 Electrochemical behaviour of *N*-substituted ferrocenic thiosemicarbazones

Cyclic voltammograms of various ferrocene derivatives were obtained in acetonitrile solution and compared to the parent ferrocene. It is noted that a fully reversible one-electron wave will have a peak separation of 59 mV, theoretically.[6] A reversible redox reaction is observed when both species, reduction and oxidation, rapidly exchange electrons with the working electrode; whereas a quasi-reversible redox reaction which some authors do not differentiate from irreversible redox reaction, is caused by a slow electron exchange of the redox species with the working electrode and resulting a greater peak potential than reversible redox reaction. However, in practice it is difficult to reach that figure and our peak separations ranged from 70–120 mV. In addition, it is required that the anodic and cathodic peak currents are of similar magnitude for reversibility.

Ferrocene itself (Fc) is known to be electrochemically stable, providing a reversible one-electron couple (Fig.4.9), the half-wave potential of which can change depending on the environment around the ferrocenyl group.

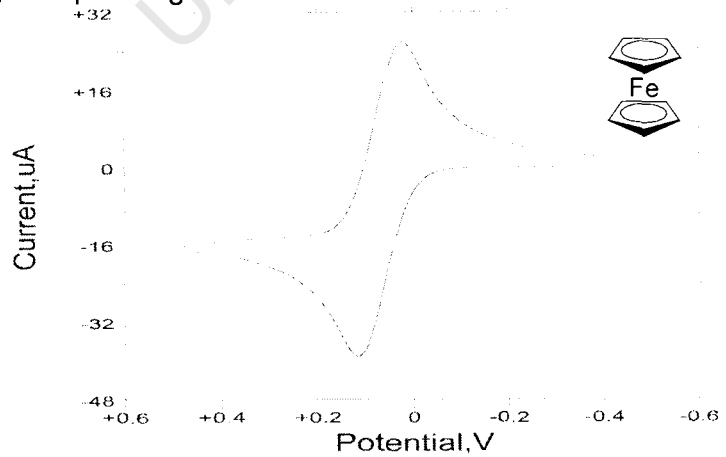

Figure 4.9: Cyclic voltammogram of ferrocene

The three intermediates, **45, 46** and **48** (Scheme 4.6, pp 51) preserved the shape of the ferrocene voltammogram with a one-electron couple; the $E_{1/2}$ values differed (Table 4.3), while the ΔE values are smaller than that of Fc itself, though still in the range expected for a one-electron process.

Table 4.3: Electrochemical data for ferrocene derivatives

Cmpd	ΔE_p	$E_{1/2}$[a] ($E_{1/2}$ *vs* Fc)[b]
22	126	78 (00)
45	78	359 (281)
46	80	182 (104)
48	67	90 (12)

[a] Measured *vs* Ag/Ag^+ reference electrode

[b] Relative to Fc/Fc^+ reference couple

These intermediates, **45** and **46**, showed one reversible redox couple (see example in Fig. 4.10B) with $E_{1/2}$ values (referenced to the Fc/Fc^+ couple) of 281 mV and 104 mV, respectively, and are more difficult to oxidize than ferrocene. However, the voltammogram of **47** and **48** (Fig.4.10A) showed different picture, with two reversible redox couples at $E_{1/2}$(P1) = – 37 mV (ΔE (P1) = 79 mV) and $E_{1/2}$ (P2) = 140 mV (ΔE (P2)= 56 mV) for compound **47** (Table 4) and an irreversible oxidation peak was observed at around 500mV for compound **48**. It appears that the amine group also underwent redox reaction, reversible for compound **47** but irreversible for compound **48** (might be because of the primary and secondary character of the amine on compound **47** and compound **48**, respectively).

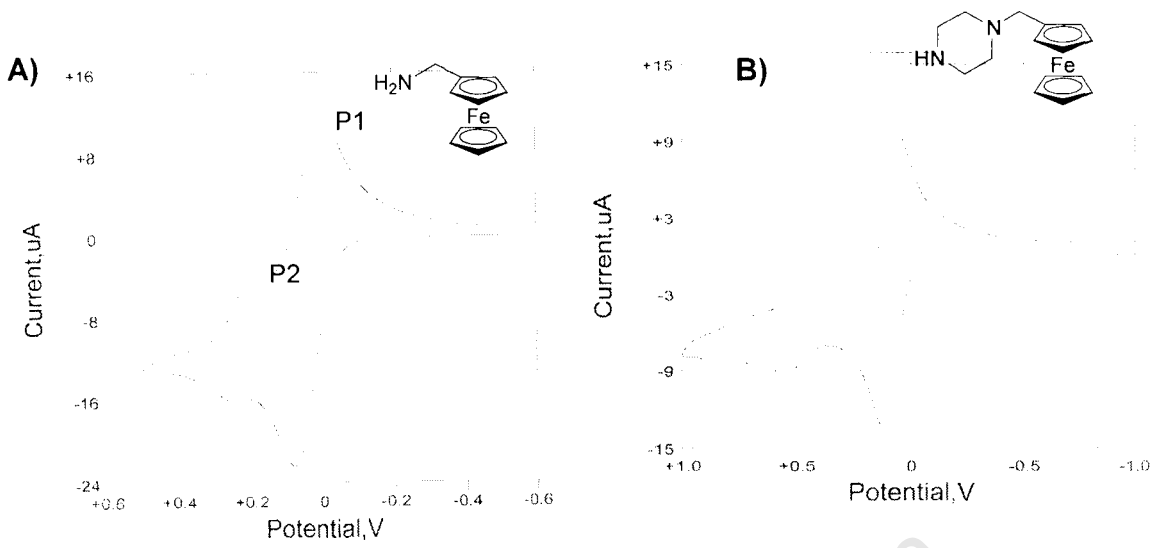

Figure 4.10: Cyclic voltammograms of A) **47** and B) **48**

Table 4.4: Ferrocene amine **47** electrochemical data

Cmpd	I_{pa}/i_{pc}		E_{pa} (Cmpd *vs* Fc)		E_{pc} (Cmpd *vs* Fc)		ΔE_p (Cmpd *vs* Fc)		$E_{1/2}$[a] ($E_{1/2}$ *vs* Fc)[b]	
	P1	P2	P1	P2	P1	P2	P1	P2	P1	P2
22	1		141 (00)		15 (00)		126 (00)		78 (00)	
47	1.3	1.2	80 (-61)	246 (105)	1 (-14)	190 (175)	79 (-47)	56 (-70)	41 (-37)	218 (140)

[a] Measured *vs* Ag/Ag^+ reference electrode.

[b] Relative to Fc/Fc^+ reference couple.

i_{pa}, anodic peak current; i_{pc}, cathodic peak current; E_{pa}, anodic peak potential; E_{pc}, cathodic peak potential; ΔE_p, potential peak separation; $E_{1/2}$, half-wave potential.

P1 is the peak resulting from the ferrocenyl moiety and P2 the peak resulting from the secondary amine group. The amine substituent rendered the ferrocene moiety slightly easier to oxidize compared with parent ferrocene. The introduction of thiosemicarbazide thioester into ferrocene-amine **47** to give compound **42b** ($E_{1/2}$ value of 21 mV relative to Fc / Fc^+) blocked the amine moiety from undergoing redox reaction (Fig. 4.11B).

Table 5 depicts the electrochemical data of the piperazine-derived thiosemicarbazones. The data show that the two synthesized piperazine-derived compounds exhibit a quasi-reversible reaction with i_{pa}/ i_{pc} greater than unity. The presence of two peaks (exemplified by compound **41a**, Fig. 11A) must be due to amine group (piperazine ring) which undergoes redox reaction in addition to the ferrocene moiety. The ferrocenyl peak is labeled P1 and P2 probably arises from the piperazine moiety which may have undergone reduction, because the corresponding compound without that moiety, **42b**, showed only one redox couple (Fig. 11B); but this is not yet experimentally proven. The $E_{1/2}$ values of compounds **41a** and **41b** are (P1) 19 mV, (P2) 160 mV and (P1) 22 mV, (P2) 200 mV relative to Fc/Fc^{+}, respectively.

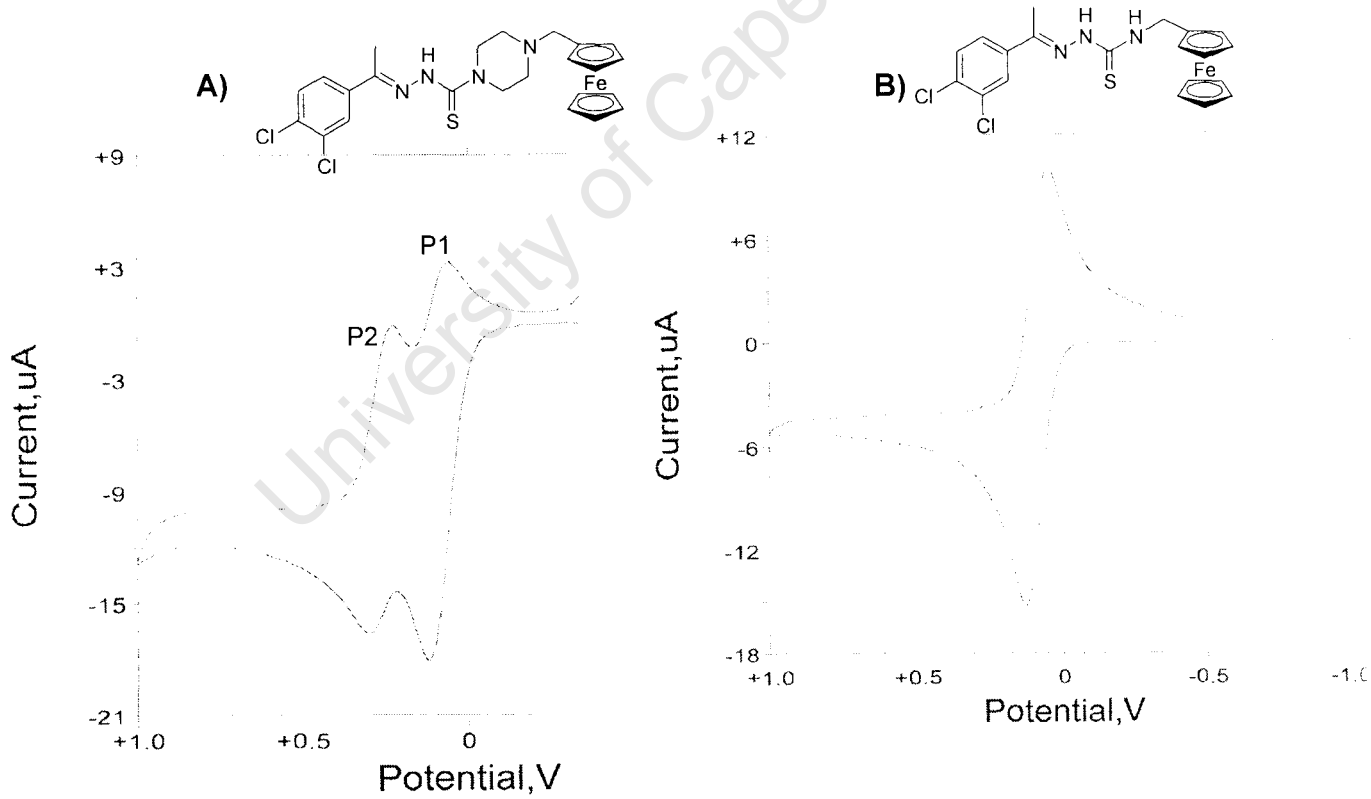

Figure 4.11: Cyclic voltammograms of A) **41a** and B) **42b**

Table 4.5: Electrochemical data for *N*- substituted ferrocenic piperazine-derived thiosemicarbazones

Cmpd	i_{pa}/i_{pc}		E_{pa} (Cmpd *vs* FC)		E_{pc} (Cmpd *vs* Fc)		ΔE_p (Cmpd *vs* Fc)		$E_{1/2}$[a] ($E_{1/2}$ *vs* Fc)[b]	
	P1	P2	P1	P2	P1	P2	P1	P2	P1	P2
22	1		118 (00)		23 (00)		95 (00)		71 (00)	
41a	4	4	120 (2)	299 (18)	60 (37)	231 (208)	60 (-35)	68 (-43)	90 (19)	231 (160)
41b	4	9	127 (9)	59 (-59)	320 (197)	221 (198)	68 (-27)	99 (4)	93 (22)	271 (200)

[a] Measured *vs* Ag/Ag^+ reference electrode

[b] Relative to Fc/Fc^+ reference couple

i_{pa}, anodic peak current; i_{pc}, cathodic peak current; E_{pa}, anodic peak potential; E_{pc}, cathodic peak potential; ΔE_p, potential peak separation; $E_{1/2}$, half-wave potential.

With the exception of five compounds (**42f**, **42j**, **42k**, **42m** and **42o**), all the *N*-substituted ferrocenic thiosemicarbazones (Table 4.6) show reversible electrochemistry, with the transfer of one electron.

Table 4.6: Electrochemical data for *N*-substituted ferrocenic thiosemicarbazones

Cmpd	i_{pa}/i_{pc}	E_{pa} (Cmpd *vs* Fc)	E_{pc} (Cmpd *vs* Fc)	ΔE_p (Cmpd *vs* Fc)	$E_{1/2}$[a] ($E_{1/2}$ *vs* Fc)[b]
22	1	117 (00)	24 (00)	93 (00)	71 (00)
42a	1.1	127 (10)	48 (24)	79 (-14)	88 (17)
42b	1.2	131 (14)	52 (28)	79 (-14)	92 (21)
42c	1.2	141 (24)	28 (4)	113 (20)	85 (14)
42d	1.2	120 (3)	42 (18)	78 (-15)	81 (10)
42e	1.2	135 (18)	32 (8)	103 (10)	84 (13)
42f	1.5	146 (29)	29 (5)	117 (24)	86 (15)
42g	1.1	123 (6)	43 (19)	80 (-7)	83 (12)
42h	1.2	120 (3)	47 (23)	73 (-20)	84 (13)
42i	1.1	130 (13)	63 (39)	67 (-26)	97 (26)
42j	1.5	126 (9)	31 (7)	95 (2)	79 (8)
42k	2.3	154 (37)	27 (3)	127 (34)	90 (19)
42l	1.1	126 (9)	42 (18)	84 (-9)	84 (13)
42m	3.6	144 (27)	12 (-12)	131 (38)	78 (9)
42n	1.2	131 (34)	45 (21)	86 (-7)	88 (17)
42o	2.4	150 (33)	7 (-17)	143 (50)	79 (8)

[a] Measured *vs* Ag/Ag^+ reference electrode

[b] Relative to Fc/Fc^+ reference couple

i_{pa}, anodic peak current; i_{pc}, cathodic peak current; E_{pa}, anodic peak potential; E_{pc}, cathodic peak potential; ΔE_p, potential peak separation; $E_{1/2}$, half-wave potential.

The two ketone-based ferrocenic thiosemicarbazone (compounds **42b** and **42d**) have $E_{1/2}$ values of 21 mV and 10 mV relative to Fc/Fc^+, respectively.

All the aldehyde-derived ferrocenic thiosemicarbazones have $E_{1/2}$ values that range from 8 mV–26 mV relative to Fc/Fc^+. Amongst these, compounds

42j and **42o** have the smallest values of $E_{1/2}$ (8 mV); these are the easiest to oxidize compared to the others.

The electrochemical behaviour of the synthesized molecules were observed and discussed. Most of the synthesized molecules had shown a one electron reversible redox reaction except the piperazine-based thiosemicarbazones which showed a quasi-reversible redox reaction.

4.4 Biological results and discussion

4.4.1. Introduction

As already mentioned, one of the main objectives was to evaluate the antiplasmodial activities of the synthetic ferrocenic thiosemicarbazone metal chelators. Their biological properties and electrochemical behaviour compared to establish whether they were correlated.

It is useful at this point to explain a number of general points about biological testing and to describe some terms. The ED_{50} and IC_{50} values used in this section to express biological activity give the same information. IC refers to inhibitory concentration and is usually used when the assay is carried out by measuring the inhibitory activity of a certain compound. ED refers to the effective dose and is used when the actual number of parasites are counted.

Practically, the IC_{50} value is the drug concentration required to cause the measured parameter to fall to 50% of its initial value. The ED_{50} value is the dosage of the drug required to kill half the parasite population or to inhibit 50% of the enzyme activity. The lower the two values, the greater the efficacy of the drug.

Cytotoxicity refers to the toxicity of a compound towards mammalian cells. An ideal drug would show toxicity or efficacy towards the parasite

and low or no toxicity towards mammalian cells. All the biological activity tests were done in duplicate.

4.4.2 Results

4.4.2.1 *In vitro* testing of thiosemicarbazone thioesters against K1 and 3D7 strains

The *in vitro* activities of synthesized thiosemicarbazone thioesters against *P.falciparum* the chloroquine resistant (CQR) K1 strain and the chloroquine sensitive (CQS) 3D7 strain are shown in Table 4.7.

Table 4.7: *In vitro* activities of synthesized thiosemicarbazone thioesters against *P.falciparum* on chloroquine resistant (CQR) K1strain and chloroquine sensitive (CQS) 3D7 strain.

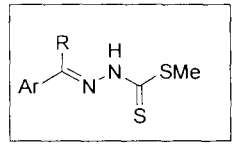

Cmpd	Ar	R	*P.falciparum* K1 (CQR) ED_{50}, µg/ml (µM)	*P.falciparum* 3D7 (CQS) ED_{50}, µg/ml (µM)	Cytot. µg/ml (µM)	Cmpd	Ar	R	*P.falciparum* K1 (CQR) ED_{50}, µg/ml (µM)	*P.falciparum* 3D7 (CQS) ED_{50}, µg/ml (µM)	Cytot. µg/ml (µM)
Chloroquine	-	-	0.09(0.28)^{C1} / 0.76(2.37)^{C2}	0.002(0.006)^{C1} /0.001(0.003)^{C2}	-	**44c**		H	4.9 (16.95)	15.9 (55.01)	93.6 (323.87)
Artesunate	-	-	0.001 (0.002)	0.015(0.036)^{A1} / 0.0003 (0.0007)^{A2}	-	**44d**	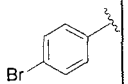	H	3.8 (13.14)	5.6 (19.37)	>300 (>1038.06)
Cycloguanil	-	-	0.213(0.846)	0.01(0.039)	-	**44e**	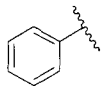	H	2.98 (14.19)	5.4 (25.71)	92.94 (440)
44a		CH_3	0.03 (0.099)	4.74 (15.64)	97.55 (321.94)	**44f**	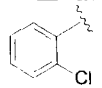	H	7.09 (28.93)	20.9 (85.30)	99.84 (407.5)
44b		H	10.4 (35.98)	21.0 (72.66)	61.5 (212.80)	**44g**	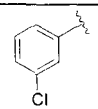	H	6.0 (24.48)	12.7 (51.83)	29.4 (120)

C1 and C2: ED_{50} values of chloroquine as control drug in 1st and 2nd experiment respectively, A1 and A2: ED_{50} values of artesunate as control drug in 1st and 2nd experiment respectively.

Table 4.7 :*In vitro* activities of synthesized thiosemicarbazone thioesters against *P.falciparum* on chloroquine resistant (CQR) K1 strain and chloroquine sensitive (CQS) 3D7 strain. (Continued)

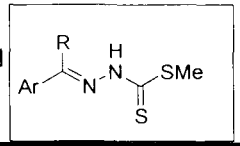

Cmpd	Ar	R	*P.falciparum* K1 (CQR) ED_{50}, µg/ml(µM)	*P.falciparum* 3D7 (CQS) ED_{50}, µg/ml(µM)	Cytot. µg/ml (µM)	Cmpd	Ar	R	*P.falciparum* K1 (CQR) ED_{50}, µg/ml(µM)	*P.falciparum* 3D7 (CQS) ED_{50}, µg/ml(µM)	Cytot. µg/ml (µM)
44h	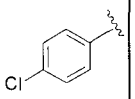	H	5.70 (23.26)	10.7 (43.67)	186.03 (759.30)	**44n**	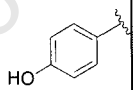	H	3.71 (16.41)	1.61 (7.12)	47.77 (211.37)
44i	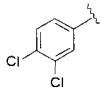	CH_3	6.9 (23.54)	2.3 (7.84)	19.41 (66.24)	**44o**		H	3.35 (13.84)	1.4 (5.78)	9.00 (37.19)
44j	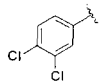	H	5.14 (18.42)	0.95 (3.40)	293.94 (1053.54)	**44p**	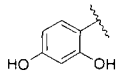	H	2.3 (9.50)	1.4 (5.78)	120.98 (499.91)
44k	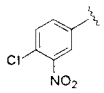	H	4.9 (16.95)	10.7 (37.02)	53.7 (185.81)	**44q**		H	5.63 (23.45)	5.31 (22.12)	120.98 (504.08)
44l		H	3.4 (15.04)	4.0 (17.69)	51.2 (226.54)	**44r**	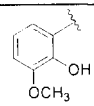	H	2.93 (11.44)	1.86 (7.26)	11.66 (45.54
44m		H	1.21 (5.35)	20.85 (92.25)	11.23 (49.69)	**44s**	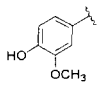	H	5.27 (20.58)	8.4 (32.81)	45.57 (178.00)

Table 4.7 : *In vitro* activities of synthesized thiosemicarbazone thioesters against *P.falciparum* on chloroquine resistant (CQR) K1 strain and chloroquine sensitive (CQS) 3D7 strain. (Continued)

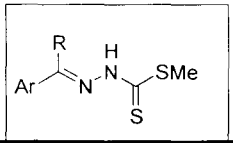

Cmpd	Ar	R	*P.falciparum* K1 (CQR) ED_{50}, µg/ml(µM)	*P.falciparum* 3D7 (CQS) ED_{50}, µg/ml(µM)	Cytot. in µg/ml (µM)	Cmpd	Ar	R	*P.falciparum* K1 (CQR) ED_{50}, µg/ml(µM)	*P.falciparum* 3D7 (CQS) ED_{50}, µg/ml(µM)	Cytot. µg/ml (µM)
44t	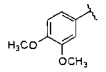	H	8.25 (30.55)	5.89 (21.81)	127.91 (473.74)	**44x**		CH_3	0.48 (2.13)	0.001 (0.004)	<0.3 (<1.04)
44u	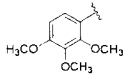	H	6.87 (22.9)	8.94 (29.8)	6.41 (21.36)	**44y**			0.18 (0.625)	0.021 (0.072)	<0.3 (<1.33)
44v	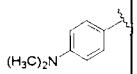	H	6.12 (24.18)	7.45 (29.44)	91.54 (361.81	**44z**	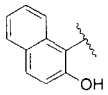	H	1.10 (3.98)	0.8 (2.89)	4.29 (15.54)
44w	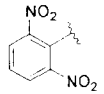	H	1.95 (6.5)	0.61 (2.03)	3.87 (12.9)	-	-	-	-	-	-

As indicated earlier the preparation of the selected thiosemicarbazone analogues was dictated by the well reported anti-malarial properties of thiosemicarbazones.[13,14]

Bipyridyl ketone-derived thiosemicarbazone thioester **44y** showed lower activity against 3D7 strain compared to the corresponding methyl ketone-derived **44x**, but was more active against K1 strain than compound **44x**.

Compound **44a** showed greater activity against both K1 and 3D7 strains compared to the corresponding aldehyde-derived thiosemicarbazone thioester **44c**. The result against K1 for compound **44a** is particularly noteworthy for in significance.

Within the aldehyde-derived thiosemicarbazone thioesters, there were compounds with bromine as a substituent at either the *ortho*, *meta* or *para* position on the aromatic ring. The compound with bromine at the *para* position (compound **44d**) showed slightly higher to comparable activity against K1 strain than the *meta* (compound **44c**) substituted compound but higher (almost 2-fold) activity than the *ortho* brominated compound **4b**. The activity was preserved against both strains when changing the substituent from bromine to chlorine. However, when a hydroxyl group was substituted instead of halogen, the *meta* position (compound **44m**) became more active against K1 than the *ortho* and *para* positions. Compared to its corresponding fused bicyclic aldehyde-derived thiosemicarbazone thioester compound **44z** which showed greater activity against both K1 and 3D7 strains with ED_{50} values of 1.1 µg/ml (3.98 µM) and 0.8 µg/ml (2.89 µM) respectively, compound **44l** showed weaker activity. Comparing compounds that are similar (**44h** and **44d**) with respect to substitution at the *para* position, the general order of activity against both K1 and 3D7 strains was H > Br > Cl.

Considering singly halogenated and singly hydroxylated compounds, compound **44m** showed the greatest activity against K1 strain with an

ED_{50} value of 1.21 µg/ml (5.35 µM), whereas **44n** showed the greatest activity against 3D7 strain with an ED_{50} value of 1.61 µg/ml (7.12 µM).

Considering the mono chlorinated compounds **44f, 44g** and **44h** *versus* the bis chlorinated compound **44j**, the latter was the most active against both K1 and 3D7 strains with ED_{50} values of 5.14 µg/ml (18.42 µM) and 0.95 µg/ml (3.40 µM), respectively. Changing the hydrogen atom on the azomethine carbon to methyl group resulted in a loss of activity against both K1 and 3D7 strains (compound **44i**).

In the series of compounds (**44o**, **44p** and **44r**) that all had a hydroxyl group in the *ortho* position with various additional substituents, either *meta* or *para*, compound **44p** which had hydroxyl groups at both the *ortho* and *para* positions showed the greatest activity against both K1 and 3D7 strains with ED_{50} values of 2.3 µg/ml (9.5 µM) and 1.4 µg/ml (5.78 µM), respectively.

Within the *meta* alkoxylated aldehyde-derived thiosemicarbazone thioester series (**44q**, **44r**, **44s**, **44t** and **44u**), compound **44r** showed the greatest activity against both K1 and 3D7 strains with ED_{50} value of 2.93 µg/ml (11.44 µM) and 1.86 µg/ml (7.26 µM), respectively. Changing the position of the substituent from *ortho* to *para* on the aromatic ring resulted in a loss of activity against both strains (compound **44s** and compound **44t**). Substitution at both the *ortho* and *para* positions did not restore the activity (compound **44u**).

Consideration of all the thiosemicarbazone thioesters showed that compound **44y** was the most active against both K1 and 3D7 strains with ED_{50} values of 0.18 µg/ml (0.625 µM) and 0.021 µg/ml (0.072 µM) respectively.

Finally a number of compounds (**44a-h**, **44k-m**, **44s** and **44u-v**) were found to be more active against the resistant (K1) strain than against the

sensitive (3D7) strain. This preferential potency against a chloroquine resistant strain for the aforementioned compounds is noteworthy. For the compounds (**44i-j**, **44n-r**, **44t**, **44w-z**) that were more active against 3D7 strain than against K1 strain, the stronger pyridyl chelators (**44x** and **44y**) displayed an even greater potency against 3D7 strain compared to the others (**44i-j**, **44n-r**, **44t**, **44w** and **44z**).

4.4.2.2 *In vitro* testing of thiosemicarbazone thioesters against *Trypanosoma brucei*

It is evident from the *in vitro* studies of thiosemicarbazone thioesters against *T.brucei* (Table 4.8) that thioester **44x** was generally the most active compared to other compounds with an ED_{50} value of 0.12 µg/ml (0.53 µM). The presence of a pyridine moiety on the azomethine carbon resulted in comparable activity as seen for compound **44y** with an ED_{50} value of 0.15 µg/ml (0.52 µM).

Table 4.8: *In vitro* activities of synthesized thioesters against *T. brucei*

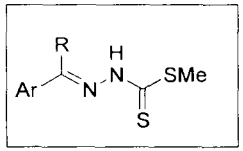

Cmpd	Ar	R	ED_{50} µg/ml (µM)	Cytot. µg/ml (µM)	Cmpd	Ar	R	ED_{50} µg/ml (µM)	Cytot. µg/ml (µM)
Pentamidine	-	-	0.0006 (0.0017)	-	**44f**	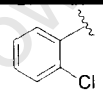	H	4.50 (18.36)	99.8 (407.34)
44a	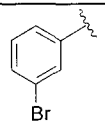	CH_3	4.37 (14.42)	97.6 (322.11	**44g**	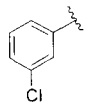	H	6.22 (25.38)	29.4 (120)
44b		H	5.62 (19.44)	61.5 (212.8)	**44h**	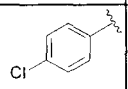	H	7.46 (30.20)	186.0 (759.18)
44c		H	1.82 (6.29)	93.6 (323.8)	**44i**	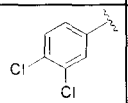	CH_3	4.35 (14.84)	19.4 (66.21)
44d	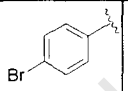	H	5.48 (18.96)	<300 (>1038)	**44j**	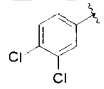	H	4.40 (15.77)	293 (1053.40)
44e		H	6.11 (29.09)	92.9 (442.38)					

Table 4.8: *In vitro* activities of synthesized thioesters against *T. brucei* (continued).

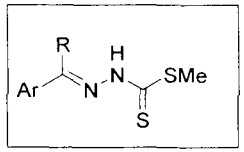

Cmpd	Ar	R	ED_{50} µg/ml (µM)	Cytot. µg/ml (µM)	Cmpd	Ar	R	ED_{50} µg/ml (µM)	Cytot. µg/ml (µM)
44k	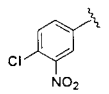	H	7.72 (26.71)	53.7 (185.8)	**44s**	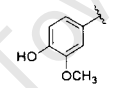	H	5.51 (21.52)	45.6 (178.1)
44l		H	0.77 (3.40)	51.2 (226.5)	**44t**	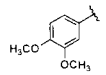	H	7.48 (27.70)	127.9 (473.7)
44m		H	2.96 (13.09)	11.2 (49.55)	**44u**	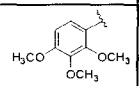	H	12.54 (41.8)	6.4 (21.33)
44n	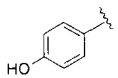	H	3.25 (14.38)	47.8 (211.5)	**44v**	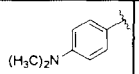	H	5.24 (20.71)	91.5 (361.6)
44o		H	2.15 (8.88)	90 (371.9)	**44w**	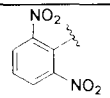	H	4.89 (16.3)	3.9 (13)
44p	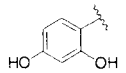	H	>30 (>123.96)	2.6 (10.74)	**44x**		CH_3	0.12 (0.53)	<3 (<13.3)
44q	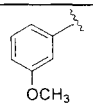	H	6.43 (26.79)	121.0 (504.1)	**44y**			0.15 (0.52)	<0.3 (<1.04)
44r	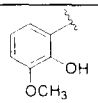	H	1.50 (5.85)	11.7 (45.70)	**44z**	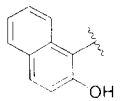	H	>30 (>108.69)	4.3 (15.57)

The dichloro substituted methyl ketone-derived thiosemicarbazone thioester **44i** showed greater activity against *T.brucei* than its corresponding dichloro substituted aldehyde-derived thiosemicarbazone thioester **44j**. The former had an ED_{50} value of 4.35 µg/ml (14.84 µM).

Within the aldehyde-derived thiosemicarbazone thioester series in which was substituted bromine at either the *ortho*, *meta* or *para* position on the aromatic ring (compounds **44b**, **44c** and **44d**), the *meta* position substituted compound **44c** showed the greatest activity with an ED_{50} value of 1.82 µg/ml (6.29 µM). Changing substituent from bromine to either chlorine or a hydroxyl group, the *ortho* position substitution resulted in the greatest activity (compound **44f**, **FM 57** and compound **44l**). Between, compound **44f** and **44l** the latter showed the greater activity with an ED_{50} of 0.77 µg/ml (3.40 µM). The order of activity against *T.brucei* of compounds that were *ortho* substituted on the aromatic ring was OH > Cl > Br > H.

Considering the thioesters with one substituent on the aromatic ring (compounds **44a-d**, **44f-h, 44l-n, 44q** and **44v)**, compound **44c** and **44l** showed greater activity against *T.brucei* with ED_{50} values of 1.82 µg/ml (6.29 µM) and 0.77 µg/ml (3.4 µM), respectively. Compound **44l** was more active than compound **44c**. For compounds that had more than one substituent (compounds **44i-k**, **44o-p**, **44r-u**, **44w**, compounds **44o** and **44r** showed the greatest activity and had ED_{50} values of 2.15 µg/ml (8.88 µM) and 1.50 µg/ml (5.85 µM). Compound **44r** was more active than compound **44o**. Considering all of the compounds that had one or more substituents, regardless of their nature, compound **44l** was the most active.

Amongst the hydroxylated aldehyde-derived thiosemicarbazone thioesters, compound **44l** showed better activity as stated previously. Compared to its corresponding fused bicyclic thiosemicarbazone thioester (compound **44z**), it showed greater activity against *T.brucei.*

A Comparison of compound **44l** with other singly hydroxylated (**44l**, **44r**, **44m**, **44n** and **44s)** and dihydroxylated compounds (**44o**, **44p** and **44r**), compound **44l** showed the greatest activity.

Within the *meta* alkoxylated aldehyde-derived thiosemicarbazone thioester series, compound **44r** showed the greatest activity against *T.brucei* with an ED_{50} of 1.50 µg/ml (5.85 µM). Changing the position of the hydroxyl group from *ortho* to *para* resulted in a loss of activity [compound **44s**; ED_{50} 5.51 µg/ml (21.52 µM)] .

4.4.2.3 *In vitro* testing of the *N*-substituted ferrocenic thiosemicarbazones against falcipains-2 & 3 and chloroquine resistant W2 strain

The results of the biological evaluation of *N*-substitued ferrocenic thiosemicarbazones are presented in Table 4.9. The piperazine-based *N*-substituted thiosemicarbazone **41a** and **41b** showed better inhibition of both falcipains 2 and 3 (FP-2 and FP-3) and the parasite chloroquine resistant W2 strain compared to the corresponding ferrocene methyl-based compounds **42b** and **42d**.

Within the group of ferrocene methyl-based thiosemicarbazones, the aldehyde-derived compounds **42e** and **42c** showed better inhibition of falcipains (2 and 3) compared to the corresponding ketones, **42b** and **42d**.

In the singly hydroxylated ferrocene methyl-based thiosemicarbazone, compound **42g** showed better activity against the falcipains-2 and W2 strain (IC_{50} values of 19.4 µM and 9.23 µM, respectively), whereas compound **42f** showed better activity against falcipains-3 compared to others. Inserting another hydroxyl group at the *ortho* position (compound **42i** increased activity against falcipains and the parasite W2 strain. Among both mono and dihydroxylated compounds, compound **42i** showed better activity on both falcipains and W2 strain.

Table 4.9: *In vitro* activities of *N*-substituted ferrocenic thiosemicarbazones against falcipains (FP-2 and FP-3) and the chloroquine resistant W2 strain.

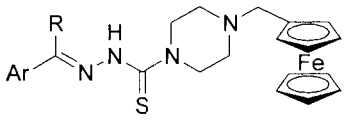

41 a-b

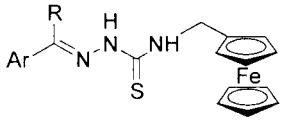

42 a-o

Cmpd	Ar	R	FP-2 IC_{50} in µM	FP-3 IC_{50} in µM	W2 IC_{50} in µM	Cmpd	Ar	R	FP-2 IC_{50} in µM	FP-3 IC_{50} in µM	W2 IC_{50} in µM
E 64	-	-	0.0095	0.056	2.482	**42d**		CH_3	287.5	95.23	>20
41a	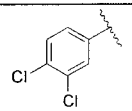	CH_3	14.35	18.55	9.515	**42e**	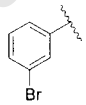	H	29.05	55.72	>20
41b	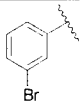	CH_3	17.34	13.85	10.15	**42f**		H	26.11	47	17.9
42a		H	47.21	99.83	15.72	**42g**		H	19.4	99.94	9.234
42b	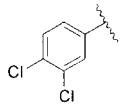	CH_3	61.71	69.69	>20	**42h**	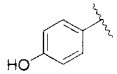	H	34.93	87.65	10.06
42c	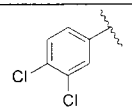	H	32.47	54.17	>20	**42i**	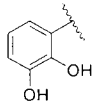	H	14.19	42.40	9.837

Table 4.9: *in vitro* activities of *N*-substituted ferrocenic thiosemicarbazones against falcipains (FP-2 and FP-3) and the parasite W2 strain (continued).

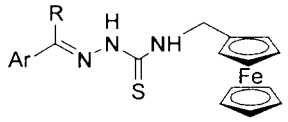

42a-o

Cmpd	Ar	R	FP-2 IC_{50} in µM	FP-3 IC_{50} in µM	W2 IC_{50} in µM	Cmpd	Ar	R	FP-2 IC_{50} in µM	FP-3 IC_{50} in µM	W2 IC_{50} in µM
42j	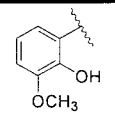	H	12.27	7.618	>20	**42m**	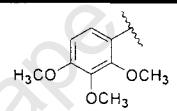	H	46.01	54.01	>20
42k	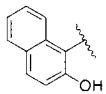	H	22.4	29.04	14.41	**42n**	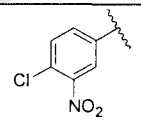	H	15.84	22.26	>20
42l	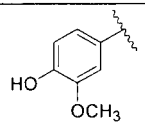	H	20.17	70.66	13.09	**42o**			36.20	31.02	0.1149

Note: Control drug E64: IC_{50}= 0.0095 µM (FP-2), IC_{50}= 0.056 µM (FP-3), IC_{50}= 2.482 µM (W2)

Within all the *N*-substituted thiosemicarbazones, compound **42o** showed the greatest activity against parasite chloroquine resistant W2 strain, with an IC_{50} of 0.11 μM while compound **42j** showed the greatest activity against both falcipains 2 and 3 with IC_{50} values of 12.27 μM and 7.62 μM, respectively.

4.4.3 Discussion

The bipyridyl thiosemicarbazone thioester **44y** showed the greatest activity on both K1 and 3D7 chloroquine strains. These types of compounds are known to be potential iron chelators and excellent parasiticidal agents.[15] Their mechanism of action as iron chelators appears to be complex. It has been proposed that since they are tridentate chelating agents, compound **44y** may be acting by inhibiting ribonucleotide reductase, an enzyme essential for DNA synthesis.[16,17] In addition, tridentate chelating thiosemicarbazones have been also proposed to act by inhibiting dihydrofolate reductase.[18,19]

In general, thiosemicarbazones are known to act on parasites in two ways, either by inhibiting metal-dependent enzymes or by forming lethal complexes which are directly toxic to the parasite. For example, there is evidence that copper complexes of thiosemicarbazones produce significant oxidative stress by binding endogenous reducing agents such as glutathione.[20]

The activity of **44y** is consistent with that previously observed for thiosemicarbazones in which the pyridine moiety of 2-acetylpyridine thiosemicarbazone analogues resulted in enhancement of the activity of this series of compounds against *P.falciparum*.[5,14] This result suggests that compounds that share structural features with 2-acetylpyridine thiosemicarbazone should offer excellent anti-malarial activity.

In the testing against *T.brucei*, compound **44x** and **44y** were found to be the most active. This class of compounds can also chelate iron and other endogenous metals which makes the mechanism complicated. Nevertheless the cysteine protease from *T.brucei* (rhodesain) could be a potential target.

In the series of *N*-substituted thiosemicarbazones, compound **42o** was found to be the most active (IC_{50} value of 0.11 μM) against the chloroquine resistant W2 strain compared to the rest. With the pyridine moiety in its structure, this compound shares some structural features with 2-acetylpyridine thiosemicarbazone, a well-studied tridentate metal chelator.[5] One may assume that these two compounds act similarly on *P.falciparum* by a metal chelation mechanism. If this compound acts by parasite iron chelation, then the lipophilic character of the ferrocenyl moiety is very important.

Lipophilicity is an important physical property of iron chelators since the iron which is chelated most likely resides within the parasitic compartment of the malaria-infected red blood cell (RBC). The drug has to pass through the RBC parasite and membranes to get to its target site and would need to display high selectivity for iron compared to other endogenous transition metals. A correlation between the degree of lipophilicity of an iron chelator and its anti-plasmodial activity has been demonstrated.[21]

It had been proven that the combination of an *ortho* hydroxyl substituent on the aromatic ring (e.g. 2-hydroxy-1-naphthaldehyde) of various thiosemicarbazides resulted in novel tridentate hybrid chelators.[22] Since Compound **42j** displayed these features, it may also be considered as a tridentate hybrid chelator. Related to the concept of a tridentate chelator, 2-acetylpyridine thiosemicarbazone, compound **42j** may also exert its anti-malarial activity through metal chelation. However, this hypothesis has yet to be proven experimentally. The ferrocenyl moiety, also present in compound **42j**, may play the same role as explained above for compound **42o**.

In this series of *ortho* hydroxyl thiosemicarbazones, substituents other than methoxy at the *ortho* position of the hydroxyl thiosemicarbazones (compounds **42i**; **42f** and **42k**) did not show greater activity than compound **42j** against falcipains (2 and 3). The Structure Activity Relationship studies

within this class of compounds clearly showed the preferred substitution of a methoxy group for anti-falcipain activity.

Being metal chelators, thiosemicarbazones synthesized in this Msc thesis, could mechanistically also act as metal-interactive cysteine protease inhibitors. In other words the free thiosemicarbazone ligand may not show inhibition of a protease. However, in the presence of endogenous metals, the resulting complex may then act as the inhibitor. This is because of the metal-binding properties (especially as a thiolate) of thiols. Given that the cysteine protease active site thiol exists in the thiolate form due to polarization by a histidine residue in close proximity, this is a likely mechanism. For example Sweeney et al have reported[23] on the metal-interactive cysteine protease inhibition of metal chelating biguanides. They found that the metal salt (Fe^{+3}) alone caused less inhibition (24 % inhibition) of falcipain at 20 μM and metformin, a biguanide metal chelator, alone did not cause any inhibition at the same concentration. However, the Fe^{+3}-metformin complex at 20 μM caused 80 % inhibition of falcipain and increasing the concentration at 40 μM, the inhibition had also increased to 90 %.

Most compounds showed selective toxicity towards the parasites relative to mammalian cells. However, compounds **44x** and **44y** showed major toxicity to mammalin cells. Toxicity may arise from unselective chelation of endogenous metals owing to these compounds being strong tridentate metal chelators.

4.4.4 Comparison of biological activities and electrochemical behaviour of *N*-substituted ferrocenic thiosemicarbazones

The combined data, both biological and electrochemical, are depicted in Table 4.10 below without their control drugs for reasons of clarity.

Table 4.10: *In vitro* anti-malarial activity and electrochemical data of *N*-substituted ferrocenic thiosemicarbazone compounds.

Compd	FP-2	FP-3	W2	$E_{1/2}$*
	IC_{50} µM	IC_{50} µM	IC_{50} µM	mV
41a	14.350	18.550	9.515	19 & 160
41b	17.340	13.850	10.150	22 &200
42a	47.210	99.830	15.720	17
42b	61.710	69.690	>20.000	21
42c	32.470	54.170	>20.000	14
42d	287.500	95.230	>20.000	10
42e	29.050	55.720	>20.000	13
42f	26.110	47.000	17.900	15
42g	19.400	99.940	9.234	12
42h	34.930	87.650	10.060	13
42i	14.190	42.400	9.837	26
42j	12.270	7.618	>20.000	8
42k	22.400	29.040	14.410	19
42l	20.170	70.660	13.090	13
42m	46.010	54.010	>20.000	9
42n	15.840	22.260	>20.000	17
42o	36.200	31.020	0.1149	8

* relative to $E_{1/2}$ for Fc / Fc^+ couple under same conditions (see Experimental)

The important point to note in considering the data presented in Table 4.10 is that even if the control drugs are not available, the smaller the value of IC_{50} the more active the compound and the smaller the $E_{1/2}$ values the easier the compound is to oxidize relative to the Fc/Fc^+ couple.

Considering the malaria enzymes falcipain-2 (FP-2) and falcipain-3 (FP-3),

compound **42j** was the most active, with IC_{50} values of 12.270 μM and 7.618 μM, respectively. Looking at the half-wave potential ($E_{1/2}$) value (which is an indication of the ease of oxidation or reduction of compound), the smaller the value the easier the compound is to oxidize relative to Fc/ Fc^+ couple. The most active compound **42j** was shown to be easily oxidizable with $E_{1/2}$ of 8 mV.

For piperazine-based ferrocenic thiosemicarbazones (**41a** and **41b**) the more active compound (**41a**) against both the malaria enzyme FP-2 (IC_{50} value of 14.35 μM) and the malaria parasite W2 strain (IC_{50} value of 9.515 μM) showed more facile oxidation, with $E_{1/2}$ values of (P1) 19 mV and (P2) 160 mV compared to **41b** [$E_{1/2}$ of (P1) 22 and (P2) 200], but was less active against malaria enzyme FP-3. This potential correlation between electrochemical behaviour and activities against FP-2 and W2 strain suggests that the more active against both malaria enzyme FP-2 and malaria parasite W2 strain, the easier this piperazine-based ferrocenic thiosemicarbazone is to oxidize. However, this conclusion is tentative since it is based on two examples only; further examples will give a more definitive conclusion.

Of the remaining *N*-substituted ferrocenic thiosemicarbazones, compounds **42j** and **42o** were the most easily oxidizable compounds, with equal $E_{1/2}$ values of 8 mV. Derivation of any overall correlation between the biological results and the electrochemical behaviour of the remaining *N*-substituted ferrocenic thiosemicarbazone compounds would come from an analysis of the scatter plots shown in Fig. 4.13.

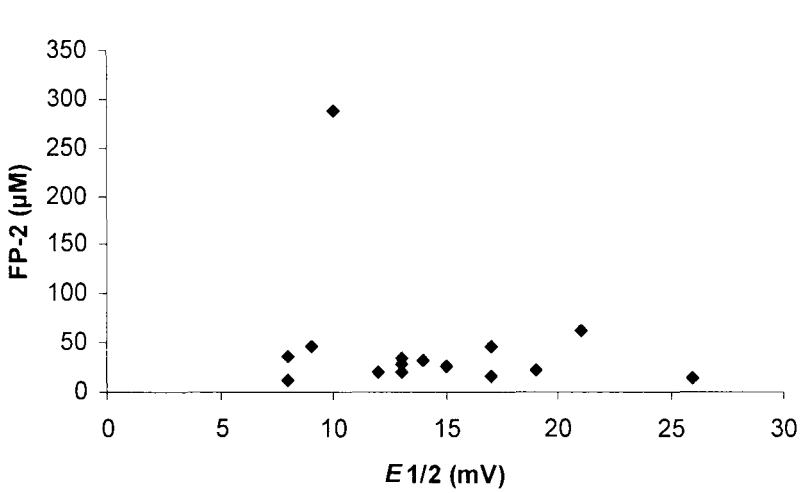

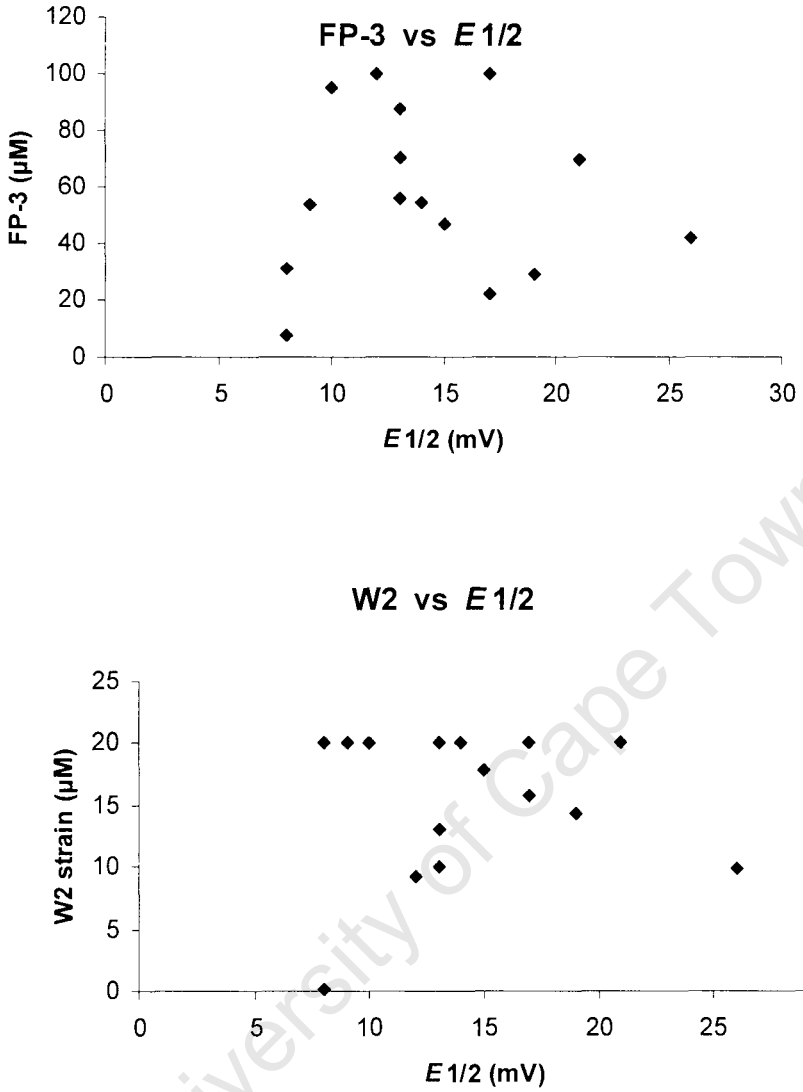

Figure 4.13: Scatter plots of IC_{50} for FP-2, FP-3 and W2 (µM) versus $E_{1/2}$(mV).

It has been shown that [24]:

a) The more the points tend to cluster around a straight line, the stronger the linear relationship between the two variables (the higher the correlation).

b) If the line around which the points tends to cluster runs from lower

left to upper right, the relationship between the two variables is positive (direct).

c) If the line around which the points tend to cluster runs from upper left to lower right, the relationship between the variables is negative (inverse).

d) If there exists a random scatter of points, there is no relationship between the two variables (very low or zero correlation).

e) Very low or zero correlation could result from a non-linear relationship between the variables.

From the perceptive view on these three plots, it is clear that there is no correlation between the biological data of the remaining *N*-substituted ferrocenic thiosemicarbazones and their electrochemical behaviour, because the points are randomly scattered . It could be that a larger and broader series of compounds and/or organisms/parasites (e.g. *T. brucei*) would shed more light, but that is beyond the scope of the current investigation.

4.4.5 CONCLUSION

In summary, ferrocenic metal chelators have been synthesized and SAR studies have been conducted. Ferrocenic metal chelator compounds have been designed based on the chelating thiosemicarbazone moiety. These thiosemicarbazones are known to have activity against multiple targets in parasites[14] and the lipophilic character of the ferrocenyl moiety is known to be crucial to the effectiveness of some reported compounds.[25]

The intermediate thiosemicarbazone thioesters were tested against *P.*

falciparum strains K1 and 3D7, and compound **44y** was particularly effective against both the chloroquine resistant K1 strain and the chloroquine sensitive 3D7 strain. The activity of this compound was attributed to its metal chelating ability. However, this compound was toxic to mammalian cells at a concentration close to the one at which it was killing the parasites. Thus selectivity was absent. Interestingly, a number of compounds (**44a-h**, **44k-m**, **44s** and **44u-v**) displaying greater potency against the chloroquine resistant K1 strain than against the chloroquine sensitive 3D7 strain were identified. This preferential potency suggests that compounds (**44a-h**, **44k-m**, **44s** and **44u-v**) are not well recognized by the chloroquine resistance mechanism. Coupled with the observed generally lower toxicity towards mammalian cells, these compounds warrant further investigation vis-à-vis detailed Structure-Activity Relationships, combination studies with chloroquine in resistant strains of the malaria parasite and mechanism of action studies.

Amongst the intermediates tested against *T. brucei*, compounds **44y** and **44x** were found to be the most active. Their activities could bee attributed to the metal-interactive cysteine protease (rhodesain) inhibition mechanism of action.

Within the *N*-substituted ferrocenic thiosemicarbazone series, two compounds were found to be active (compounds **42o** and **42j**). Compound **42o** was active against chloroquine resistant W2 strain and compound **42j** against falcipains (2 & 3). Their activities were attributed in both cases to their tridentate metal chelating ability. An additional factor is the presence of the lipophilic ferrocene moiety which presumably increases the potential to cross the parasite membranes and thereby access the parasite targets.

The electrochemical behaviour of the *N*-substituted ferrocenic thiosemicarbazone compounds was studied. Amongst the two piperazine-based ferrocenic thiosemicarbazones, compound **41a** was found marginally

more active against both FP-2 and malaria parasite W2 strain than compound **41b**; and the former compound showed more facile oxidation of the ferrocenyl group than the latter (recognizing that the difference in $E_{1/2}$ values here is not much larger than the uncertainty of the measurements). Thus it could be concluded that there is correlation between the activity against the malaria parasite enzyme FP-2 and malaria parasite W2 strain with the electrochemical behaviour of the piperazine-based ferrocenic thiosemicarbazones. However, this conclusion is tentative since it is based on two examples only.

The overall analysis for the remaining ferrocenic thiosemicarbazones presented in scatter plots, showed no correlation between the biological results and the electrochemical behaviour of these compounds.

REFERENCES

[1] Audrieth, LF; Scott, ES; Kippur, PS, *J. Org. Chem.*, **1954**, *19*, 733.

[2] West, DX; Carson, CS; Bouck, KJ; Liberta, AE, *Transition Met. Chem.*, **1991**, *16*, 271.

[3] a) Smith, DR; Marenthal, M; Tipton, J, *J. Org. Chem.*, **1952**, *217*, 294.
b) Yoon, NM; Brown, HC, *J. Am. Chem. Soc.*, **1968**, *90*, 2927.

[4] Blackie, M.A.L.B.; New Mono and Bimetallic Chloroquine Derivatives: Synthesis and Evaluation as Antiparasitic Agents; PhD thesis, UCT, **2002.**

[5] Klayman, DI; Bartosevich, JF; Griffin, TS; Mason, CJ; Scovill, JP, *J. Med. Chem.*, **1979**, *22*, 855.

[6] Kounaves, SP, Voltammetric Techniques: In Handbook of Instrumental Techniques for Analytical Chemistry, Prentice Hall, 1997

[7] http://www.chemistry.nmsu.edu/studntres/chem435/Lab4/intro.html

[8] Bard, AJ; Faulkner, L, " Electrochemical Methods: Fundamentals and Applications", Wiley, New York, **1980**.

[9] Kissinger, PT; Heineman, WR, " Laboratory Techniques in Electroanalytical Chemistry," Marcel Dekker, New York, **1984**.

[10] Hobart, HW; Lynne, LM; John, AD Jr; Franck, AS Jr, Introduction to electroanalytical methods of analysis: In Intrumental Methods of Analysis 7th ed., pp 656, **1988**.

[11] Kissinger, PT; Heineman, WR, *J. Chem. Educ.*, **1983**, *60*, 702.

[12] Gary, AM, *J. Chem. Educ.*, **1983**, *60*, 637.

[13] Klayman, DL; Scovill, JP; Bartosevich, JF; Bruce, J, *J. Med. Chem.*, **1983**, *26*, 35.

[14] Greenbaum, DC; Mackey, Z; Hansell, E; Doyle, P; Gut, J; Caffrey, CR; Lehrman, J; Rosenthal, PJ; McKerrow, JH; Chibale, K, *J. Med. Chem.*, **2004**, *47*, 3212.

[15] Kirshner, S; Wei, YK; Francis, D; bergman, JG, *J. Med. Chem.*, **1966**, *9*, 369.

[16] Finch, RA; Liu, M; Grill, SP; Rose, WC; Loomis, R; Vasquez, KM; Cheng, Y; Sartorelli, AC, *Biochem. Pharmacol.*, **2000**, *59*, 983.

[17] Li, J; Zheng, LM; King, I; Doyle, TW; Chen, SH, *Curr. Med. Chem.*, **2001**, *8*, 121.

[18] Lebrun, E; Tu, YX; van Rapenbusch, R; Banijamali, AR; Foye, WO, *Biochim. Biophys. Acta*, **1990**, *1034*, 81.

[19] Choi, IH; Kim, C, *Arch. Pharm. Res.*, **2002**, *25*, 807.

[20] Byrnes, RW; Mohan, M; Antholine, WE; Xu, RX; Petering, DH, *Biochem.*, **1990**, *29*, 7046.

[21] Pradines, B; Polain, JM; Ramiandrasoa, F; Fusai, T; Mosnier, J; Rogier, C; Daries, W; Baret, E; Kunesch, G; le Bras, J; Parzy, DJ, *Antimicrob. Chemother*, **2002**, *50*, 177.

[22] Lovejoy, DB; Richardson, DR, *Blood*, **2002**, *100*, 666.

[23] Sweeney, D; Raymer, ML; Lockwood, TD, *Biochem. Pharmacol.*, **2003**, *66*, 663.

[24] www.stats.gla.ac.uk/steps/glossary/presenting_data.html

[25] Jaouen, G, *Chem. Br.*, **2001**, *37*, 36.

CHAPTER 5
EXPERIMENTAL SECTION

5.1 General

Reactions were monitored by Thin-Layer Chromatography (TLC) using coated silica gel plates, detection by an ultra-violet lamp.

Proton nuclear magnetic resonance (^{1}H NMR) spectra were recorded at ambient temperature using the following instruments: Varian mercury (300 MHz) or Varian Unity Spectrometer (400 MHz) and TMS was used as an internal standard. The chemical shifts (δ) are given in parts per million relative to TMS (δ=0.00). Carbon-13 nuclear magnetic resonance (^{13}C NMR) spectra were recorded at 75 MHz or 100 MHz with the same internal standard. Dimethyl Sulfoxide (DMSO) was used in the determination of all the spectra unless stated otherwise.

Mass spectra were recorded by means of a low resolution mass spectroscopy apparatus from the Division of Pharmacology at the University of Cape town and high resolution mass spectroscopy from Wits University.

Infrared spectra were measured in solution using chloroform on a satellite FT-IR spectrophotometer. Micro (elemental) analysis was performed using a fisons EA 1108 CHNS-O instrument. Melting points were determined using a Reicher- Jung Thermovar (temperature range 0-350 °C) on cover slips and are uncorrected.

Cyclic voltametry (CV) was carried out using a BAS-100W electrochemical analyzer and a one–compartment three–electrode system, comprising a Ag/Ag^+ reference electrode (0.01 M $AgNO_3$ and 0.1 M Bu_4NClO_4 in acetonitrile), a platinum wire as the auxiliary electrode and a platinum disc

as the working electrode. The supporting electrolyte was a solution of 0.1 M tetrabutylammonium perchlorate in dried acetonitrile. All measurements were carried out on concentrations of 2–3 mM of the ligands at a scan rate of 100 mV s^{-1}, unless otherwise stated. The potentials *E* were recorded without IR compensation.

All potentials reported are relative to the half–wave potential ($E_{1/2}$) of a reference ferrocene/ ferrocenium couple run under the same conditions (*ca.* 0.07 V). The experiments were performed under an atmosphere of nitrogen at room temperature. The solutions were deoxygenated by bubbling nitrogen through the solution for 2 min prior to the CV run. The platinum disc electrode was polished after every run.

5.2 Synthesis of thiosemicarbazide thioesters 43

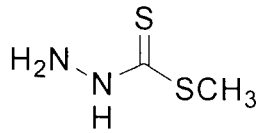

A solution of KOH (19.8 g, 0.3 mol) in 24 ml H_2O and iPrOH (20 ml) were stirred in an ice-bath for 20 min. 17.1 ml (0.3 mol) of hydrazine hydrate was added to the solution, which was kept < 10 °C. Ice- cold CS_2 (18.2 ml, 0.3 mol) was added dropwise to the reaction mixture and it was stirred for 120 min. during which the solution turned yellow. Cold CH_3I (18.7 ml, 0.3 mol) was added dropwise and a white precipitate formed. The reaction mixture was stirred for a further 150 min. and the white precipitate was collected with the aid of a filter dam, washed with ice- cold water (100 ml), collected and dried over $MgSO_4$; to afford white crystals (18.66 g, 50 %); δ_H ($CDCl_3$, 400 MHz) 8.64 (1H, br s, -N*H*CS-), 4.44 (2H, br s, NH_2NHCS-), 2.64 (3H, s, SCH_3).

5.3 Synthesis of the ferrocene carboxaldehyde oxime 46

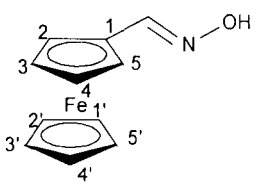

Ferrocene carboxaldehyde **45** (5.0 g, 23.35 mmol) was placed in a round bottomed flask with $NH_2OH.HCl$ (2.11 g, 30.36 mmol) in 25 mL EtOH. A solution of NaOH (2.43 g, 60.73 mmol) in

deionised H_2O (15 mL) was added. The mixture was refluxed for 120 min. 10 mL deionised H_2O was then added. The mixture was neutralized with $NaHCO_3$ the product extracted into CH_2Cl_2 and dried over Na_2SO_4. The solvent was then removed under reduced pressure to afford a deep red crystalline solid after crystallization from chloroform and hexane (4.80 g, 80 %); R_f (EtOAc:Hex 1:4) 0.23; δ_H (400 MHz; $CDCl_3$) 8.03 (1H, s, C*H*=N), 7.54 (1H, br s, O*H*), 4.52 (2H, s, 2Cp-*H*), 4.34 (2H, s, 2Cp-*H*), 4.21 (5H, s, 5Cp'-*H*); δ_C (100 MHz, $CDCl_3$) 149.7 (C=N), 71.7, 70.2 (2C), 69.2 (5C), 67.8 (2C).

5.4 Synthesis of the ferrocenylmethylamine 47

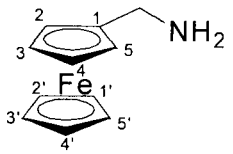

Ferrocene carboxaldehyde oxime **46**(1.0 g, 3.88 mmol) was placed in a 50 mL round bottomed flask. Anhydrous THF (20 ml) was added followed by $LiAlH_4$ (0.29 g, 7.75 mmol). The mixture was refluxed under an atmosphere of nitrogen for 6 h. The mixture was allowed to cool to room temperature before diluting with Et_2O (10 ml) and adding brine (10 ml). The product was extracted into the organic phase and the aqueous layer was washed with 20×30 ml of Et_2O. The organic extracts were combined and dried over K_2CO_3. The solvent was removed under reduced pressure and the residue purified by chromatography on SiO_2 (eluent EtOAc: Hex 1:4 then 15 % CH_3OH:CH_2Cl_2) affording a red oil (0.71 g, 76 %); R_f (CH_3OH–CH_2Cl_2 3:2) 0.2; δ_H (400 MHz, $CDCl_3$) 4.13 (9H, s, 4Cp-*H* & 5Cp'-*H*), 3.54 (2H, s, -C*H*$_2$-N-); δ_C (100 MHz, $CDCl_3$) 91.2, 68.3 (2C), 67.6 (5C), 67.1 (2C), 41.0.

5.5 Synthesis of ferrocenyl methane piperazine 48

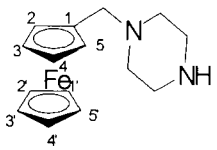

Ferrocene carboxaldehyde **45** (1.0 g, 4.67 mmol) and piperazine (0.6 g, 7.0 mmol) were allowed to stir in anhydrous MeOH (10 ml) for 4 h. $NaCNBH_3$ (0.62 g, 9.82 mmol) was then added and the reaction mixture allowed to stir for a further 2 h. The solvent was removed under reduced pressure and the residue dissolved in a solution of

1N HCl (20 ml). The mixture was washed three times with Et_2O (10 ml) and the aqueous layer was neutralized with Na_2CO_3 (1 N). The product was extracted into DCM and dried over Na_2SO_4. Solvent removal from the filtrate and subsequent purification on SiO_2 (eluent DCM:MeOH 1:9 then 30 % MeOH:DCM) afforded the product as an orange powder (0.53 g, 53 %); R_f (DCM:MeOH 1:9) 0.4; δ_H (300 MHz, $CDCl_3$) 6.25 (1H, br s, N*H*), 4.18 (2H, s, 2Cp-*H*), 4.10 (7H, s, 2Cp-*H* & 5Cp'-*H*), 3.40(2H, s, -CH_2-N-), 3.15 (4H, t, *J* 4.8, -N-[CH_2-CH_2]$_2$-N-), 2.65(4H, t, *J* 4.8, N-[CH$_2$-CH_2]$_2$-N-).

5.6 Synthesis of compounds thiosemicarbazone thioesters 44a - z

Synthesis of *methyl 3-[1-(2-pyridyl)ethylidene]hydrazine carbodithioate* 44a

A solution of methyl hydrazinecarbodithioate **43** (1.0 eq., 4.09 mmol) and 3'-acetophenone (1.0 eq., 4.09 mmol) in 10 ml iPrOH was mechanically stirred at room temperature. The product starts to precipitate out. The reaction mixture was stirred for an additional 2 h and cooled overnight. Crystals were collected, washed with cold iPrOH and air-dried. Yield 3.25 mmol (0.99 g, 80 %).

The same procedure described above was used to make **44b-z** from the appropriate carbonyl (ketone and/or aldehyde compound).

Methyl -3(3-bromophenyl) hydrazinecarbodithioate 44a

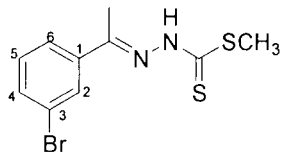

Beige crystalline product; m.p.127-128 °C;
R_f (EtOAc:Hex 1:9) 0.20; ν_{max} ($CHCl_3$/cm^{-1}) 3026 (N-H), 1423 (N=C), 1210 (C=S), 756, 663 (C-H, Ar); δ_H (300 MHz, $CDCl_3$) 9.95 (1H, br s, N*H*), 7.96 (1H, s, H-2), 7.74 (1H, d, *J* 8.0, H-6), 7.53 (1H, d, *J* 8.0, H-4), 7.27 (1H, t, *J* 8.0, H-5), 2.66 (3H, s, SCH_3), 2.28 (3H, s, CH_3); δ_C (100 MHz, $CDCl_3$) 202.2 (C=S), 147.1, 139.2, 133.2, 130.3, 129.8, 125.3, 123.1, 18.1 (S*C*H$_3$), 13.20 (*C*H$_3$);

LR-MS *m/z* 303 $(M)^+$; Found: C, 39.86; H, 3.32; N, 9.30; S, 20.6 Calcd for $C_{10}H_{11}BrN_2S_2$: C, 39.61; H, 3.66; N, 9.24; S, 21.95.

***Methyl 3-(2- bromobenzylidine) hydrazine carbodithioate* 44b**

2-bromobenzaldehyde (1.0 eq, 2.75 mmol) was used and the product was obtained as a yellow powder. Yield 1.95 mmol (565 mg, 71 %); m.p:174-177 °C;

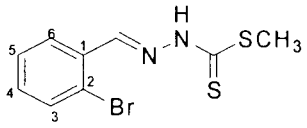

R_f (EtOAc:Hex 1:4) 0.50; $\nu_{max.}(CHCl_3/cm^{-1})$ 3020 (N-H),1427 (N=C), 1213 (C=S), 760, 670 (C-H, Ar); δ_H (400 MHz, DMSO-d_6) 13.41 (1H, br s, N*H*), 8.60 (1H, s, C*H*=N), 7.92 (1H, dd, *J* 2.0 & 8.0, H-6), 7.69 (1H, dd, *J* 1.2 & 8.0, H-3), 7.46 (1H, td, *J* 1.2 & 8.0, H-5), 7.38 (1H, td, *J* 2.0 & 8.0, H-4), 2.52 (3H, s, SC*H*$_3$); δ_C (75 MHz, DMSO-d_6) 199.0 (C=S), 144.7, 133.3, 132.3, 128.2, 127.1 (2C), 124.1, 16.7 (S*C*H$_3$); LR-MS *m/z* 289 $(M)^+$; Found: C, 37.75; H, 2.77; N, 9.80; S, 22.54 Calcd for $C_9H_9BrN_2S_2$: C, 37.38; H, 3.14; N, 9.69; S, 22.17.

***Methyl 3-(3-bromobenzylidine) hydrazine carbodithioate* 44c**

3-bromobenzaldehyde (1.0 eq, 2.78 mmol) was used and the product was obtained as a white powder. Yield 1.97 mmol (570 mg, 71 %); m.p:178-180 °C; R_f (EtOAc:Hex 1:4) 0.45; $\nu_{max}.(CHCl_3/cm^{-1})$ 3020 (N-H), 1426 (N=C), 1213 (C=S), 770, 666 (C-H, Ar); δ_H (400 MHz, DMSO-d_6) 13.34 (1H, br s, N*H*), 8.19 (1H, s, C*H*=N), 7.88 (1H, s, H-2), 7.69 (1H, d, *J* 8.0, H-6), 7.51 (1H, d, *J* 8.0, H-4), 7.40 (1H, t, *J* 8.0, H-5), 2.51 (3H, s, SC*H*$_3$); δ_C (100 MHz, DMSO-d_6) 198.9 (C=S), 144.5, 135.8, 133.1, 131.1, 129.3, 126.5, 122.2, 16.7 (S*C*H$_3$); LR-MS *m/z* 289 $(M)^+$; Found: C, 37.69; H, 2.85; N, 9.77; S, 22.60 Calcd for $C_9H_9BrN_2S_2$: C, 37.38; H, 3.14; N, 9.69; S, 22.17.

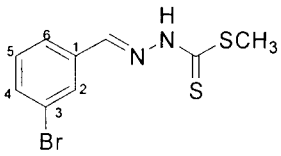

***Methyl 3-(4- bromobenzylidine) hydrazine carbodithioate* 44d**

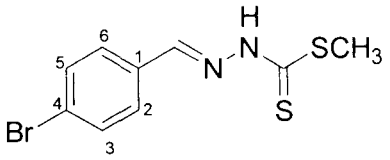

3-bromobenzaldehyde (1.0 eq, 2.70 mmol) was used and the product was obtained as a white powder. Yield 1.56 mmol (450 mg, 57 %); m.p:197-200 °C; R_f (EtOAc:Hex 1:9) 0.26; $\nu_{max.}$($CHCl_3$/cm^{-1}) 3020 (N-H), 1427 (N=C), 1213 (C=S), 767, 667 (C-H, Ar); δ_H (400 MHz, DMSO-d_6) 13.22 (1H, br s, N*H*), 8.20 (1H, s, C*H*=N), 7.64 (4H, m, H-2, H-3, H-4 & H-6), 2.51 (3H, s, SCH_3); δ_C (75 MHz, DMSO-d_6) 198.6 (C=S), 145.0, 132.6, 131.9 (2C), 129.1 (2C), 124.0, 16.7 (SCH_3); LR-MS *m/z* 289 $(M)^+$; Found: C, 37.68; H, 2.99; N, 9.91; S, 23.36 Calcd for $C_9H_9BrN_2S_2$: C, 37.38; H, 3.14; N, 9.69; S, 22.17.

***Methyl 3-(benzylidine) hydrazine carbodithioate* 44e**

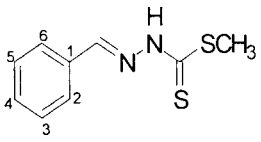

Benzaldehyde (1.0 eq, 4.71 mmol) was used and the product was obtained as a white powder. Yield 3.32 mmol (700 mg, 71 %); m.p:156-158 °C; R_f (EtOAc:Hex 1:4) 0.40; $\nu_{max.}$($CHCl_3$/cm^{-1}) 3013 (N-H), 1473, 1430 (N=C), 1217 (C=S), 770, 667 (C_H, Ar); δ_H (400 MHz, DMSO-d_6) 13.25 (1H, br s, N*H*), 8.23 (1H, s, C*H*=N), 7.70 (2H, dd, *J* 2.4 & 7.2, H-2 & H-6), 7.46-7.45 (3H, m, H-3, H-4, H-5), 2.51 (3H, s, SCH_3); δ_C (75 MHz, DMSO-d_6) 198.4 (C=S), 146.3, 133.4, 130.7, 128.9 (2C), 127.3 (2C), 16.7 (SCH_3); LR-MS *m/z* 211 $(M+H)^+$; Found: C, 51.67; H, 4.76; N, 13.61; S, 31.05 Calcd for $C_9H_{10}N_2S_2$: C, 51.40; H, 4.79; N, 13.32; S, 30.44.

***Methyl 3-(2- chlorobenzylidine) hydrazine carbodithioate* 44f**

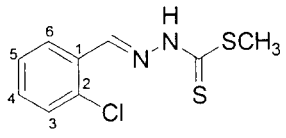

2-chlorobenzaldehyde (1.0 eq, 3.55 mmol) was used and the product was obtained as a yellow powder. Yield 2.29 mmol (560 mg, 63 %); m.p:168-170 °C; R_f (EtOAc:Hex 1:4) 0.60; $\nu_{max.}$ ($CHCl_3$/cm^{-1}) 3013 (N-H), 1423 (N=C), 1213 (C=S), 763, 670 (C-H, Ar); δ_H (400 MHz, DMSO-d_6) 13.38 (1H, br s, N*H*), 8.63 (1H, s,

C*H*=N), 7.95 (1H, dd, *J* 2.0 & 7.6, H-3), 7.53 (1H, dd, *J* 1.2 & 7.9, H-6), 7.48-7.40 (2H, m, H-4 & H-5), 2.52 (3H, s, SCH_3); δ_C (100 MHz, DMSO-d_6) 198.99 (C=S), 142.3, 133.7, 132.0, 130.7, 130.0, 127.7, 126.8, 16.7 (SCH_3); LR-MS *m/z* 245 $(M)^+$; Found: C, 44.42; H, 3.25; N, 11.42; S, 25.68 calcd for $C_9H_9ClN_2S_2$: C, 44.16; H, 3.71; N, 11.45; S, 26.20.

***Methyl 3-(3- chlorobenzylidine) hydrazine carbodithioate* 44g**

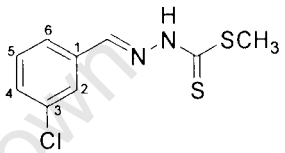

3-chlorobenzaldehyde (1.0 eq, 3.66 mmol) was used and the product was obtained as a white powder. Yield 2.33 mmol (570 mg, 64 %); m.p:157-158 °C; R_f (EtOAc:Hex 1:4) 0.40; ν_{max} ($CHCl_3$/cm^{-1}) 3007 (N-H), 1427 (N=C), 1220 (C=S), 760, 663 (C-H, Ar); δ_H (400 MHz, DMSO-d_6) 13.28 (1H, br s, N*H*), 8.21 (1H, s, C*H*=N), 7.74 (1H, d, *J* 2.0, H-2), 7.65 (1H, dt, *J* 2.0 & 7.0, H-4 or H-6), 7.5-7.4 (2H, m, H-5 & H-4 or H-6), 2.52 (3H, s, SCH_3); δ_C (75 MHz, DMSO-d_6) 198.91 (C=S), 144.5, 135.6, 133.7, 130.8, 130.3, 126.4, 126.1, 16.7 (SCH_3); LR-MS *m/z* 245 $(M)^+$; Found: C, 44.41; H, 3.47; N, 11.52; S, 26.35 Calcd for $C_9H_9ClN_2S_2$: C, 44.16; H, 3.71; N, 11.45; S, 26.20.

***Methyl 3-(4- chlorobenzylidine) hydrazine carbodithioate* 44h**

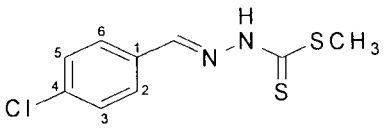

4-chlorobenzaldehyde (1.0 eq, 3.66 mmol) was used and the product was obtained as a white powder. Yield 2.91 mmol (715 mg, 80 %); m.p:187-190 °C; R_f (EtOAc:Hex 1:4) 0.35; ν_{max} ($CHCl_3$/cm^{-1}) 3020 (N-H), 1473, 1423 (N=C), 1213 (C=S), 767, 670 (C-H, Ar); δ_H (400 MHz, DMSO-d_6) 13.28 (1H, br s, N*H*) 8.21 (1H, s, C*H*=N), 7.72 (2H, d, *J* 8.5, H-2 & H-6), 7.51 (2H, d, *J* 8.5, H-3 & H-5), 2.51 (3H, s, SCH_3); δ_C (75 MHz, DMSO-d_6) 198.6 (C=S), 144.9, 135.1, 132.3, 129.0 (2C), 128.9 (2C), 16.7 (SCH_3); LR-MS *m/z* 245 $(M)^+$; Found: C,

44.57; H, 3.85; N, 11.62; S, 26.58 Calcd for $C_9H_9ClN_2S_2$: C, 44.16; H, 3.71; N, 11.46; S, 26.20.

***Methyl –3(3,4- dichlorophenyl) hydrazine carbodithioate* 44i**

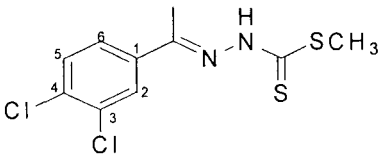

3',4'-acetophenone (1.0 eq, 4.09 mmol) was used and the product was obtained as white crystals. Yield 3.75 mmol (1.10 g, 92 %); m.p.150-152 °C; R_f (EtOAc:Hex 1:9) 0.20; ν_{max} ($CHCl_3$/cm^{-1}) 3020 (N-H), 1423 (N=C), 1213 (C=S), 753, 666 (C-H, Ar); δ_H (300 MHz, $CDCl_3$) 9.91(1H, br s, N*H*); 7.91(1H, d, *J* 2.0, H-2), 7.62 (1H, dd, *J* 2.0 & 8.7, H-6), 7.42 (1H, d, *J* 8.7, H-5), 2.62 (3H, *SCH*$_3$); 2.23 (3H, s, C*H*$_3$);. δ_C (75 MHz, $CDCl_3$) 201.2 (C=S), 145.9, 136.9, 134.3, 133.0, 130.6, 128.4, 125.6, 17.8 (S*C*H$_3$), 12.8 (*C*H$_3$); LR-MS m/z 293 $(M)^+$, Found: C, 41.37; H, 3.27; N, 9.67; S, 22.34 calcd for $C_{10}H_{10}Cl_2N_2S_2$: C, 40.96; H, 3.44; N, 9.55; S, 21.80.

***Methyl 3-(3,4-dichlorobenzylidine) hydrazine carbodithioate* 44j**

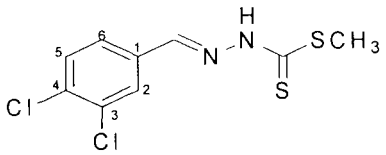

3,4-dichlorobenzaldehyde (1.0 eq, 2.85 mmol) was used and the product was obtained as a white powder. Yield 2.51 mmol (700 mg, 88 %); m.p:195-196 °C; R_f (EtOAc:Hex 1:9) 0.20; ν_{max}($CHCl_3$/cm^{-1}) 3007 (N-H), 1433 (N=C), 1217 (C=S), 767, 663; δ_H (400 MHz, DMSO-d_6) 13.39 (1H, br s, N*H*); 8.18 (1H, s, C*H*=N), 7.89 (1H, d, *J* 1.7, H-2), 7.73-7.65 (2H, m, H-5 & H-6), 2.51 (3H, s, SC*H*$_3$); δ_C (100 MHz, DMSO-d_6) 199.1 (C=S), 143.5, 134.2, 132.9, 131.8, 131.2, 128.7, 127.0, 16.7 (S*C*H$_3$); LR-MS *m/z* 279 $(M)^+$; Found: C, 39.06; H, 2.66; N, 10.07; S, 22.88 Calcd for $C_9H_8Cl_2N_2S_2$: C, 38.71; H, 2.89; N, 10.03; S, 22.97.

***Methyl 3-(4-chloro-3-nitrobenzylidine) hydrazine carbodithioate* 44k**

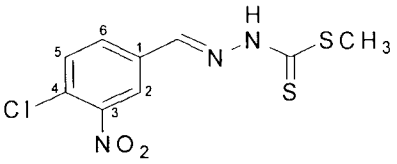

4-chloro-3-nitrobenzaldehyde (1.0 eq, 2.74 mmol) was used and the product was obtained as a yellow powder. Yield 2.42 mmol (700 mg, 88 %); m.p:188-190 °C; R_f (EtOAc:Hex 1:4) 0.23; ν_{max} .($CHCl_3$/cm^{-1}) 3013 (N-H), 1417 (N=C), 1217 (C=S), 747, 663 (C-H, Ar); δ_H (400 MHz, DMSO-d_6) 13.43 (1H, br s, N*H*), 8.34 (1H, d, *J* 2.0, H-2), 8.26 (1H, s, C*H*=N), 8.01 (1H, dd, *J* 2.0 & 8.5, H-6), 7.84 (1H, d, *J* 8.5, H-5), 2.52 (3H, s, SCH_3); δ_C (75 MHz, DMSO-d_6) 199.4 (C=S), 147.9 , 142.8, 134.1, 132.3, 131.5, 126.3, 123.9, 16.8 (SCH_3); LR-MS *m/z* 290 $(M+H)^+$; Found: C, 37.51; H, 2.57; N, 14.63; S, 22.26 Calcd for $C_9H_8ClN_3O_2S_2$: C, 37.31; H, 2.78; N, 14.50; S, 22.13.

***Methyl 3-(2-hydroxybenzylidine) hydrazine carbodithioate* 44l**

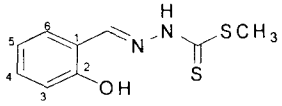

Salicylaldehyde (1.0 eq, 4.17 mmol) was used and the product was obtained as a yellow powder. Yield 3.51 mmol (795 mg, 84 %); m.p:194-196 °C; R_f (EtOAc:Hex 1:4) 0.30; ν_{max} ($CHCl_3$/cm^{-1}) 3013 (N-H), 1430 (N=C), 1213 (C=S), 770, 666 (C-H, Ar); δ_H (400 MHz, DMSO-d_6) 13.28 (1H, br s, N*H*), 10.18 (1H, br s, O*H*), 8.51 (1H, s, C*H*=N), 7.63 (1H, dd, *J* 2.0 & 7.6, H-6), 7.28 (1H, td, *J* 2.0 & 8.5, H-4), 6.88 (2H, m, H-3 & H-5), 2.5 (3H, s, SCH_3); δ_C (75 MHz, DMSO-d_6) 197.4 (C=S), 157.2, 145.0, 132.4, 127.7, 119.9, 119.1, 116.5, 16.9 (SCH_3); LR-MS *m/z* 227 $(M+H)^+$; Found: C, 48.09; H,4.80; N, 12.61; S, 28.62 Calcd for $C_9H_{10}N_2OS_2$: C, 47.76; H, 4.45; N, 12.28 ; S, 28.34.

***Methyl 3-(3-hydroxybenzylidine) hydrazine carbodithioate* 44m**

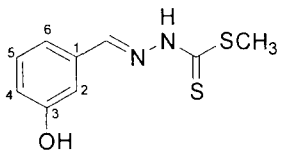

3-hydroxybenzaldehyde (1.0 eq, 4.21 mmol) was used and the product was obtained as a light yellow powder.

Yield 3.98 mmol (900 mg, 94 %); m.p:174-176 °C; R_f (EtOAc:Hex 2:3) 0.40; ν_{max} ($CHCl_3$/cm^{-1}) 3020 (N-H), 1423 (N=C), 1210 (C=S), 760, 663 (C-H, Ar); δ_H (300 MHz, DMSO-d_6) 13.24 (1H, br s, N*H*), 9.68 (1H, br s, O*H*), 8.18 (1H, s, C*H*=N), 7.28 (1H, t, *J* 8.0, H-5), 7.19 (1H, t, *J* 2.0, H-2), 7.13 (1H, dd, *J* 2.0 & 8.0, H-6), 6.9 (1H, dd, *J* 2.0& 8.0, H-4), 2.55 (3H, s, SCH_3); δ_C (75 MHz, DMSO-d_6) 198.4 (C=S), 157.7, 146.8, 134.8, 130.3, 119.5, 118.3, 118.1, 16.9 (SCH_3); LR-MS *m/z* 227 $(M+H)^+$; Found: C, 47.82; H, 4.33; N, 12.35; S, 28.24 Calcd for $C_9H_{10}N_2OS_2$: C, 47.76; H, 4.45 N, 12.38; S, 28.34.

***Methyl 3-(4-hydroxybenzylidine) hydrazine carbodithioate* 44n**

4-hydroxybenzaldehyde (1.0 eq, 4.21 mmol) was used and the product was obtained as a light yellow powder. Yield 3.99 mmol (910 mg, 95 %); m.p:180-182 °C; R_f (EtOAc-Hex, 2:3) 0.40; ν_{max} ($CHCl_3$/cm^{-1}) 3022 (N-H),1426 (N=C), 1212 (C=S), 761, 667 (C-H, Ar); δ_H (300 MHz, DMSO-d_6) 13.13 (1H, br s, N*H*), 10.07 (1H, br s, O*H*), 8.17 (1H, s, C*H*=N), 7.59 (2H, d, *J* 8.5 , H-2 & H-6), 6.88 (2H, d, *J* 8.5, H-3 & H-5), 2.53 (3H, s, SCH_3); δ_C (75 MHz, DMSO-d_6) 197.3 (C=S), 160.1, 147.1, 129.6 (2C), 124.5, 116.1 (2C), 16.7 (SCH_3); LR-MS *m/z* 227 $(M+H)^+$; Found: C, 47.38; H, 4.50; N, 12.36; S, 28.10 calcd for $C_9H_{10}N_2OS_2 \cdot 0.1H_2O$: C, 47.76; H, 4.46; N, 12.38; S, 28.34.

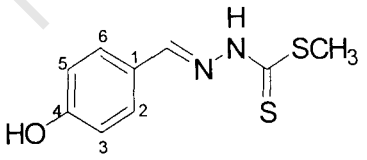

***Methyl 3-(2,4-dihydroxybenzylidine) hydrazine carbodithioate* 44o**

2,4-dihydroxybenzaldehyde (1.0 eq, 3.73 mmol) was used and the product was obtained as a light yellow powder. Yield 2.79 mmol (678 mg, 75 %); m.p:208-210 °C; R_f (Hex:EtOac 2:3) 0.50; ν_{max} ($CHCl_3$/cm^{-1}) 3020 (N-H), 1423 (N=C), 1210 (C=S), 757, 667 (C-H, Ar); δ_H (300 MHz, DMSO-d_6) 13.19 (1H, br s, N*H*), 10.23 (1H, br s, O*H*), 10.03 (1H, br s, O*H*), 8.42 (1H, s, C*H*=N), 7.47 (1H, d, *J* 8.2, H-6), 6.39 (1H, d, *J* 8.2, H-5), 6.36 (1H, s, H-3), 2.55 (3H, s, SCH_3); δ_C (75

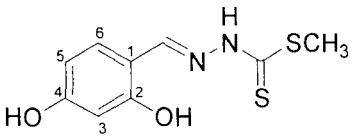

MHz, DMSO-d_6) 195.8 (C=S), 161.5, 159.1, 146.4, 130.2, 110.6, 108.5, 102.6, 16.9 (SCH_3); LR-MS *m/z* 243 $(M+H)^+$; Found: C, 44.73; H, 3.76; N, 11. 55; S, 26.92 Calcd for $C_9H_{10}N_2O_2S_2$: C, 44.61; H, 4.16; N, 11.56; S, 26.47.

***Methyl 3-(2,3-dihydroxybenzylidine) hydrazine carbodithioate* 44p**

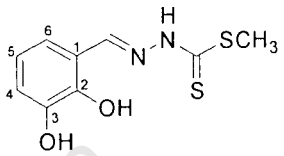

2,3-dihydroxybenzaldehyde (1.0 eq, 3.73 mmol) was used and the product was obtained as a yellow powder. Yield 2.13 mmol (515 mg, 57 %); m.p: 203-205 °C; R_f (EtOAc:Hex 2:3) 0.23; ν_{max} .($CHCl_3/cm^{-1}$) 3014 (N-H), 1429 (N=C), 1216 (C=S), 757, 667 (C-H, Ar); δ_H (300 MHz, DMSO-d_6) 13.35 (1H, br s, N*H*), 9.53 (2H, br s, O*H*), 8.54 (1H, s, C*H*=N); 7.13 (1H, dd, *J* 1.5 & 8.0, H-4), 6.90 (1H, dd, *J* 1.5 & 8.0, H-6), 6.74 (1H, t, *J* 8.0, H-5), 2.57 (3H, s, SCH_3); δ_C (75 MHz, DMSO-d_6) 197.0 (C=S), 146.0, 145.7, 145.6, 119.4, 119.3, 118.0, 117.6, 16.7 (SCH_3); LR-MS *m/z* 243 $(M+H)^+$; Found: C, 44. 94; H, 3.91; N, 11.59; S, 25.99 Clacd for $C_9H_{10}N_2O_2S_2$: C, 44.61; H, 4.16; N, 11.56; S, 26.47.

***Methyl 3-(-3-methoxybenzylidine) hydrazine carbodithioate* 44q**

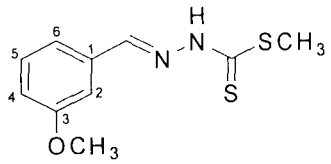

4-hydroxybenzaldehyde (1.0 eq, 3.78 mmol) was used and the product was obtained as a beige powder. Yield 3.20 mmol (770 mg, 85 %); m.p:148-149 °C; R_f (EtOAc:Hex 2:3) 0.20; ν_{max} ($CHCl_3/cm^{-1}$) 3013 (NH), 1433 (N=C), 1217 (C=S), 770, 667 (C-H, Ar); δ_H (400 MHz, DMSO-d_6) 13.27 (1H, br s, N*H*), 8.19 (1H, s, C*H*=N), 7.36 (1H, t, *J* 8.0, H-5), 7.28 (1H, dd, *J* 1.2 & 8.0, H-6), 7.24 (1H, t, *J* 1.2, H-2), 7.04 (1H, dd, *J* 1.2 & 8.0, H-4), 3.78 (3H, s, OCH_3), 2.51 (3H, s, SCH_3); δ_C (75 MHz, DMSO-d_6) 198.4 (C=S), 159.5, 146.1, 134.8, 130.1, 120.0, 116.6, 111.9, 55.1, 16.70 (SCH_3); LR-MS *m/z* 241$(M+H)^+$; Found: C, 50.43; H, 5.10; N, 11.75; S, 26.76 calcd for $C_{10}H_{12}N_2OS_2 \cdot 0.1H_2O$: C, 49.97; H, 5.03; N, 11.66; S, 26.68.

***Methyl 3-(2-hydroxy-3-methoxybenzylidine) hydrazine carbodithioate* 44r**

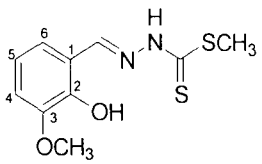

2-hydroxy-3-methoxybenzaldehyde (1.0 eq, 3.28 mmol) was used and the product was obtained as a beige powder. Yield 2.08 mmol (535 mg, 64 %); m.p:187-190 °C; R_f (EtOAc:Hex 2:3) 0.50; ν_{max} ($CHCl_3$/cm^{-1}) 3013 (N-H), 1427 (N=C), 1213 (C=S), 760, 670 (C-H, Ar); δ_H (400 MHz, DMSO-d_6) 13.27 (1H, br s, N*H*), 9.60 (1H, br s, O*H*), 8.54 (1H, s, C*H*=N), 7.25 (1H, dd, *J* 1.2 & 8.0, H-6), 7.03 (1H, dd, *J* 1.2 & 8.0, H-4), 6.82 (1H, t, *J* 8.0, H-5), 3.80 (3H, s, OCH_3), 2.52 (3H, s, SCH_3); δ_C (100 MHz, DMSO-d_6) 197.3 (C=S), 148.0, 146.9, 144.4, 119.4, 119.3, 118.5, 113.9, 55.9, 16.7 (S*C*H_3); LR-MS *m/z* 257 $(M+H)^+$; Found: C, 46.52; H, 4.76; N, 10.92; S, 24.84 Calcd for $C_{10}H_{12}N_2O_2S_2 \cdot 0.1H_2O$: C, 46.85; H, 4.72; N, 10.93; S, 25.02..

***Methyl 3-(4-hydroxy-3-methoxybenzylidine) hydrazine carbodithioate* 44s**

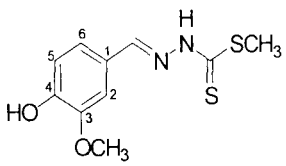

4-hydroxy-3-methoxybenzaldehyde (1.0 eq, 3.28 mmol) was used and the product was obtained as a light yellow powder. Yield 2.54 mmol (650 mg, 77 %); m.p:167-169 °C; R_f (EtOAc:Hex 2:3) 0.50; ν_{max}($CHCl_3$/cm^{-1}) 3013 (N-H), 1477, 1427 (N=C), 1217 (C=S), 760, 667 (C-H, Ar); δ_H (400 MHz, DMSO-d_6) 13.12 (1H, br s, N*H*), 9.64 (1H, br s, O*H*), 8.11 (1H, s, C*H*=N), 7.25 (1H, d, *J* 2.0, H-2), 7.13 (1H, dd, *J* 2.0. & 8.3, H-6), 6.84 (1H, d, *J* 8.3 , H-5), 3.79 (3H, s, OCH_3), 2.49 (3H, s, SCH_3); δ_C (100 MHz, DMSO-d_6) 197.0 (C=S), 149.7, 147.9, 146.8, 124.6, 122.2, 115.7, 109.9, 55.5, 16.6 (S*C*H_3); LR-MS *m/z* 257 $(M+H)^+$; Found: C, 47.21; H, 4.67; N, 11.05; S, 25.43 Calcd for $C_{10}H_{12}N_2O_2S_2$: C, 46.85; H, 4.72; N, 10.93; S, 25.02.

***Methyl 3-(3,4-dimethoxybenzylidine) hydrazine carbodithioate* 44t**

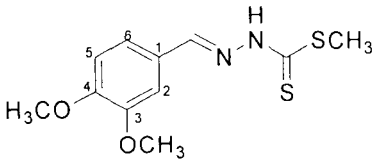

3,4-dimethoxybenzaldehyde (1.0 eq, 3.01 mmol) was used and the product was obtained as a yellow powder. Yield 2.33 mmol (630 mg, 77 %); m.p:180-183 °C; R_f (EtOAc:Hex 2:3) 0.50; $\nu_{max.}$($CHCl_3$/cm^{-1}) 3020 (N-H), 1423 (N=C), 1213 (C=S), 760, 670 (C-H, Ar); δ_H (400 MHz, DMSO-d_6) 13.15 (1H, br s, N*H*), 8.15 (1H, s, C*H*=N), 7.28 (1H, d, *J* 2.0, H-2), 7.24 (1H, dd, *J* 2.0 & 8.3, H-6), 7.02 (1H, d, *J* 8.3, H-5), 3.79 (3H, s, OCH_3), 3.78 (3H, s, OCH_3), 2.51 (3H, s, SCH_3); δ_C (75 MHz, DMSO-d_6) 197.4 (C=S), 151.3, 149.1, 146.4, 126.1, 122.1, 111.7, 108.9, 55.6 55.4, 16.7 (SCH_3); LR-MS *m/z* 271 $(M+H)^+$; Found: C, 49.25; H, 5.27; N, 10.39; S, 23.70 calcd for $C_{11}H_{15}N_3O_2S_2$: C, 48.86; H, 5.2; N, 10.36; S, 23.72.

***Methyl 3-(2,3,4-trimethoxybenzylidine) hydrazine carbodithioate* 44u**

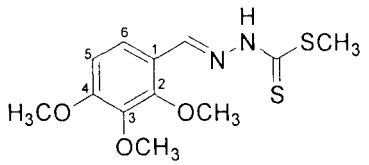

2,3,4-methoxybenzaldehyde (1.0 eq, 2.54 mmol) was used and the product was obtained as a white powder. Yield 2.09 mmol (630 mg, 82 %); m.p:162-164 °C; R_f (Hex:EtOAc 2:3) 0.60; ν_{max} ($CHCl_3$/cm^{-1}) 3013 (N-H), 1473, 1420 (N=C), 1210 (C=S), 763, 667 (C-H, Ar); δ_H (400 MHz, DMSO-d_6) 13.12 (1H, br s, N*H*), 8.42 (1H, s, C*H*=N), 7.5 (1H, d, *J* 8.9, H-6), 6.9 (1H, d, *J* 8.9, H-5), 3.83 (3H, s, OCH_3), 3.81 (3H, s, OCH_3), 3.75 (3H, s, OCH_3), 2.49 (3H, s, SCH_3); δ_C (75 MHz, DMSO-d_6) 197.3 (C=S), 155.8, 155.2, 142.5, 142.6, 120.7, 119.5, 108.9, 61.8, 60.4, 56.0, 16.6 (SCH_3); LR-MS *m/z* 301 $(M+H)^+$; Found: C, 48.34; H, 5.32; N, 9.44; S, 21.06 Calcd for $C_{12}H_{16}N_2O_2S_2$: C, 47.98; H, 5.37; N, 9.33; S, 21.35.

***Methyl 3-(4-dimethylaminobenzylidine) hydrazine carbodithioate* 44v**

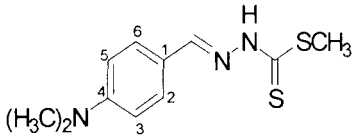

4-dimethylaminobenzaldehyde (1.0 eq, 3.35 mmol) was used and the product was obtained as an orange powder. Yield 3.16 mmol (800 mg, 94 %); m.p:179-182 °C; R_f (EtOAc:Hex 2:3) 0.50;. $\nu_{max.}$($CHCl_3$/cm^{-1}) 3020 (N-H),1430 (N=C), 1213 (C=S), 753, 667 (C-H, Ar);. δ_H (400 MHz, DMSO-d_6) 13.03 (1H, br s, N*H*), 8.09 (1H, s, C*H*=N), 7.51 (2H, d, *J* 8.7, H-2 & H-6), 6.73 (2H, d, *J* 8.7, H-3 & H-5), 2.96 (6H, s, (CH_3)$_2$-N-), 2.49 (3H, s, SCH_3); δ_C (100 MHz, DMSO-d_6) 195.9 (C=S), 151.9, 147.3, 128.8 (2C), 120.3, 111.7 (2C), 70.1 (2C), 16.6 (SCH_3); LR-MS *m/z* 254 $(M+H)^+$; Found: C, 51.77; H, 6.00; N, 16.47; S, 25.12 Calcd for $C_{11}H_{15}N_3S_2 \cdot 0.1H_2O$: C, 52.14; H, 5.97; N, 16.58; S, 25.31.

***Methyl 3-(2,6-dinitrobenzylidine) hydrazine carbodithioate* 44w**

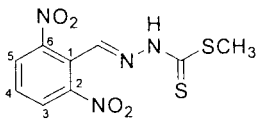

2,6-dinitrobenzaldehyde (1.0 eq, 2.60 mmol) was used and the product was obtained as a yellow powder. Yield 2.40 mmol (720 mg, 92 %); m.p:171-173 °C; R_f (EtOAc:hex 2:3) 0.5; ν_{max} ($CHCl_3$/cm^{-1}) 3013 (N-H), 1427 (N=C), 1213 (C=S), 767, 670 (C-H, Ar); δ_H (400 MHz, DMSO-d_6) 13.54 (1H, br s, N*H*), 8.55 (1H, s, C*H*=N), 8.37 (2H, d, *J* 8.1, H-3 & H-5), 7.90 (1H, t, *J* 8.1, H-4), 2.47 (3H, s, SCH_3); δ_C (75 MHz, DMSO-d_6) 200.0 (C=S), 149.1, 139.1 (2C), 131.7, 128.7 (2C), 122.7, 16.9 (SCH_3); LR-MS *m/z* 301 $(M+H)^+$; Found: C, 36.46; H, 2.57; N, 18.68; S, 21.82 Calcd for $C_9H_8N_4O_4S_2$: C, 35.99; H, 2.69; N, 18.66; S, 21.35.

***Methyl 3-[1-(2-pyridyl) ethylidene]hydrazine carbodithioate* 44x**

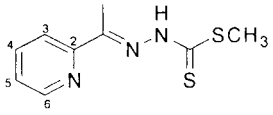

2-acetypyridine (1.0 eq, 16.36 mmol) was used and the product was obtained as Orange crystalline. The product was revealed by ^{1}H NMR and ^{13}C NMR as two isomers (*E* and *Z*). Yield 10.53 mmol (2.37 g, 64 %)

m.p.122-124 °C; R_f (CH_3OH) 0.60; ν_{max} ($CHCl_3/cm^{-1}$) 3013 (NH), 1426 (N=C), 1216 (C=S), 760, 670 (C-H, Ar); δ_H (300 MHz, $CDCl_3$) 15.85 (1H, br s, N*H* *ZE*), 9.95 (1H, br s, N*H* *ZE*), 8.74 (1H, dd, *J* 1.8 & 4.8, H-6 *ZE*), 8.59 (1H, dd, *J* 1.8 & 4.8, H-6 *ZE*), 8.18 (1H, d, *J* 7.9, H-3 *ZE*), 7.89 (1H, td, *J* 1.8 & 7.9, H-4 *ZE*), 7.71 (1H, td, *J* 1.8 &7.9, H-4 *ZE*), 7.59 (1H, d, *J* 7.9, H-3 *ZE*), 7.39 (1H, m, H-5 *ZE*), 7.29 (1H, m, H-5 *ZE*), 2.67 (3H, s, SC*H*$_3$ *ZE*), 2.64 (3H, s, SC*H*$_3$ *ZE*), 2.45 (3H, s, C*H*$_3$ *ZE*), 2.44 (3H, s, C*H*$_3$ *ZE*); δ_C (100 MHz, $CDCl_3$) 201.6 (C=S *ZE*), 201.0(C=S *ZE*), 154.1, 152.4, 149.6 , 148.5, 147.8, 140.3, 137.6, 124.2, 124.2, 123.8, 120.8, 21.9(S*C*H$_3$ *ZE*), 17.71(*C*H$_3$ *ZE*), 17.1(*C*H$_3$ *ZE*), 11.1(S*C*H$_3$ *ZE*); LR-MS *m/z* 226 $(M+H)^+$; Found: C, 47.81; H, 4.89; N, 18.62; S, 27.75 Calcd for $C_9H_{11}N_3S_2$: C, 47.97; H, 4.92; N, 18.65; S, 28.46.

***Methyl 3-(2-dipyridinyl methylene) hydrazine carbodithioate* 44y**

Di-(2-pyridyl) ketone (1.0 eq, 2.71 mmol) was used and the product was obtained as an orange powder. Yield 2.32 mmol (670 mg, 86 %); m.p:152-153 °C; R_f (100 % CH_3OH) 0.60;. $\nu_{max.}$($CHCl_3/cm^{-1}$) 2993 (N-H), 1427 (N=C), 1217 (C=S), 770, 666 (C-H, Ar); δ_H (300 MHz, DMSO-d_6) 15.27 (1H, br s, N*H*), 8.80-8.78 (1H, m, Ar-*H*), 8.62-8.60 (1H, m, Ar-*H*), 8.06 (1H, d, *J* 8.2, Ar-*H*), 7.87-7.79 (2H, m, Ar-*H*), 7.73 (1H, d, *J* 7.9, Ar-*H*), 7.42- 7.34 (2H, m, Ar-*H*), 2.66 (3H, s, SC*H*$_3$); δ_C (100 MHz, DMSO-d_6) 202.1 (C=S), 155.3, 151.0, 148.2, 147.9, 137.0, 136.9, 127.2, 124.3, 124.1, 123.7, 113.0, 17.3 (S*C*H$_3$); LR-MS *m/z* 289 $(M+H)^+$; Found: C, 54.38; H, 3.85; N, 19.61; S, 21.76 Calcd for $C_{13}H_{12}N_4S_2$: C, 54.14; H, 4.19; N, 19.43; S, 22.24.

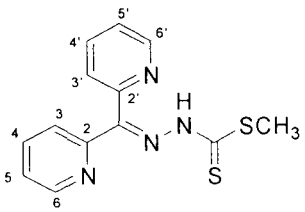

***Methyl 3-[1(2-hydroxynaphtanyl) methylene] hydrazine carbodithioate* 44z**

2-hydroxy-1-naphthaldehyde (1.0 eq, 2.90 mmol) was used and the product was obtained as a brown powder. Yield 2.68 mmol (740 mg, 92 %); m.p: 212-

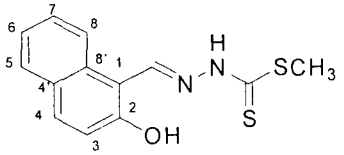

213 °C; R_f (EtOAc:Hex, 1:9) 0.20; $\nu_{max.}$($CHCl_3$/cm^{-1}) 3013 (N-H), 1430 (N=C), 1213 (C=S), 757, 660 (C-H, Ar); δ_H (300 MHz, DMSO-d_6) 13.36 (1H, br s, N*H*), 11.06 (1H, br s, O*H*), 9.20 (1H, s, C*H*=N), 8.77 (1H, d, *J* 8.5, H-4), 7.95-7.88 (2H, m, Ar-*H*), 7.58 (1H, t, *J* 7.9, Ar-*H*), 7.39 (1H, t, *J* 7.9, Ar-*H*), 7.24 (1H, d, *J* 8.5, H-3), 2.60 (3H,s, SCH_3); δ_C (100 MHz, DMSO-d_6) 196.2 (C=S), 158.1, 147.7, 133.6, 131.2, 128.8, 128.1, 128.1, 123.6, 123.1, 118.2, 109.3, 16.9 (S*C*H_3); LR-MS *m/z* 277 $(M+H)^+$; Found: C, 56.13; H, 4.41; N, 10.13; S, 23.04 Calcd for $C_{13}H_{12}N_2OS_2 \cdot 0.1H_2O$: C, 56.49; H, 4.38; N, 10.14; S, 23.20.

5.7 General procedure (GP) for the synthesis of *N*-substituted thiosemicarbazones

Selected methyl 3-hydrazine carbodithioates (1.0 eq, 0.443 mmol) suspended in warm MeOH (EtOH). 1.0 eq (0.443 mmol) of the appropriate amine **47** and /or **48** was added and the mixture was stirred under reflux condition for 24 h. The product precipitated from hot solution as reaction progressed. The precipitates were collected and dried in vacuo.

Compound 41a

1[1-(3,4-dichlorophenyl)ethylidine]piperazine ferrocenylmethyl thiosemicarbazone

The conditions employed for the preparation of this compound were those described in **GP** for the synthesis of thiosemicarbazones. 0.32 mmol 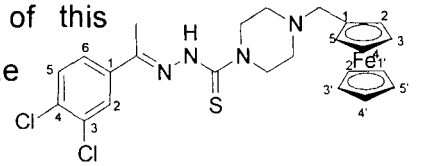 of the methyl 3-hydrazine carbodithioate **44i** and ferrocenyl methyl piperazine **48** were used. 0.12 mmol (63 mg, 44 %) of a beige powder were obtained; m.p: 162–164 °C; R_f (EtOAc:DCM 4:1) 0.30; ν_{max} ($CHCl_3$/cm^{-1}) 3421, 3020 (N-H), 1653, 1517 (C=N), 1432 (C=C), 1216 (C=S); δ_H (400 MHz, DMSO-d_6) 7.92 (1H, d, *J* 2.0,

H-2), 7.72 (1H, dd, *J* 2.0 & 8.4, H-6), 7.65 (1H, d, *J* 8.4, H-5), 4.16 (2H, s, Cp-*H*), 4.12 (5H, s, Cp'-*H*), 4.10 (2H, s, 2Cp-*H*), 3.79 (4H, t, *J* 4.8, N-(C*H*$_2$-CH$_2$)$_2$-N), 3.36 (2H, s, N-C*H*$_2$-Cp), 2.38 (4H, t, *J* 4.8, N-(CH$_2$-C*H*$_2$)$_2$-N), 2.25 (3H, s, C*H*$_3$); δ_C (75 MHz, DMSO-d$_6$) 184.0 (C=S), 144.1, 137.5, 133.4, 132.9, 130.5, 127.8, 125.1, 82.9, 70.2 (2C), 68.6 (5C), 68.3 (2C), 58.0 (2C), 52.28 (2C), 51.7, 12.49 (*C*H$_3$); HRMS (FAB) *m/z* 528.7 $(M-H)^+$; Found: C, 54.97; H, 5.48; N, 10.76; S, 5.88 Calcd for $C_{24}H_{26}Cl_2FeN_4S$: C, 54.44; H, 4.94; N, 10.57; S, 6.04; E(P1) $_{1/2}$= 19mV, E(P2) $_{1/2}$= 160mV.

Compound 41b

1-[1-(3-bromophenyl)ethylidine]piperazine ferrocenylmethyl thiosemicarbazone

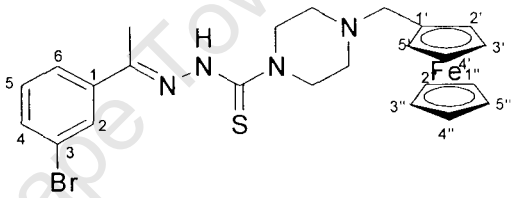

The conditions employed for the preparation of this compound were those described in **GP** for the synthesis of thiosemicarbazones. Using 0.33 mmol of the methyl 3-hydrazine carbodithioate **44a** and ferrocenyl methyl piperazine **48**, 0.09 mmol of the product was obtained as a beige powder (50 mg, 26 %); m.p: 58 – 61 °C;

R_f (EtOAc:Hex 2:3) 0.30; ν_{max} ($CHCl_3$/cm^{-1}) 3428, 3010 (N-H), 1642, 1520 (C=N), 1433 (C=C), 1216 (C=S); δ_H (300 MHz, $CDCl_3$) 8.33 (1H, br s, N-*H*), 7.82 (1H, s, H-2), 7.55 (2H, d, *J* 7.8, H-6), 7.50 (1H, d, *J* 7.8, H-4), 7.23 (1H, t, *J* 7.8, H-5), 4.19 (2H, s, 2Cp-*H*), 4.17 (7H, s, 2Cp-*H* & 5Cp'-*H*), 4.08 (4H, t, *J* 4.8, N-(C*H*$_2$-CH$_2$)$_2$-N), 3.45 (2H, N-C*H*$_2$-Cp), 2.57 (4H, t, *J* 4.8, N-(CH$_2$-C*H*$_2$)$_2$-N), 2.19 (3H, s, C*H*$_3$); δ_C (75 MHz, $CDCl_3$) 182.1 (C=S), 145.1, 139.6, 132.2, 129.9, 129.0, 124.6, 122.8, 81.9, 70.3 (2C), 68.5 (5C), 68.3 (2C), 58.0 (2C), 52.3 (2C), 51.6, 12.6 (*C*H$_3$); LR-MS *m/z* 539 $(M)^+$; Found: C, 51.29; H, 5.53; N, 9.21; S, 5.07 Calcd for $C_{24}H_{27}BrFeN_4S.H_2O$: C, 51.72; H, 5.24; N, 10.05; S, 5.75; E(P1) $_{1/2}$= 22 mV, E(P2) $_{1/2}$=200 mV.

Compound 42a

1(1-methylidinephenyl) ferrocenylmethyl thiosemicarbazone

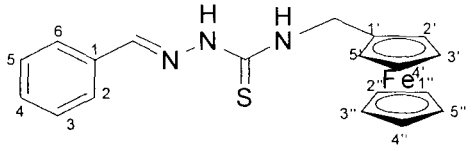

The conditions employed for the preparation of this compound were those described in **GP** for the synthesis of thiosemicarbazones. Using 0.95 mmol of methyl 3-hydrazine carbodithioate **44f** and ferrocene methanamine **47**, 0.26 mmol of the product were obtained as a red powder (97 mg, 27 %); m.p: 143-146 °C; R_f (EtOAc:Hex 1:4) 0.50; ν_{max} (KBr/cm^{-1}) 3314, 3075 (N-H), 1650, 1547 (C=N), 1483, 1444 (C=C), 1284 (C=S); δ_H (300 MHz, DMSO-d_6) 8.52 (1H, t, *J* 6.0, S=C-N*H*), 8.11 (1H, s, C*H*=N), 7.76 (2H, dd, *J* 2.0 & 8.4, H-2 & H-6), 7.41-7.37 (3H, m, H-3, H-4 & H-5), 4.51 (2H, d, *J* 6.0, N-CH_2-Cp), . 4.33 (2H, t, *J* 2.0, 2Cp-*H*), 4.21 (5H, s, 5Cp'-*H*), 4.11 (2H, t, *J* 2.0, 2Cp-*H*); δ_C (75 MHz, DMSO-d_6) 176.6(C=S), 142.2, 134.2, 129.8, 128.6, 127.0, 85.7, 68.2 (2C), 68.2 (5C), 67.2 (2C), 42.1 (*C*H$_3$); LR-MS *m/z* 377 $(M)^+$; Found: C, 59.82; H, 4.77; N, 11.00; S, 8.54 Calcd for $C_{19}H_{19}FeN_3S$: C, 60.53; H, 5.07; N,11.14; S, 8.50;

$E_{1/2}$= 17mV.

Compound 42b

1-[1-(3,4-dichlorophenyl)ethylidine] ferrocenylmethyl thiosemicarbazone

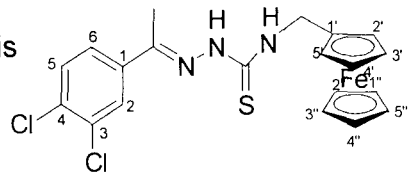

The conditions employed for the preparation of this compound were those described in **GP** for the synthesis of thiosemicarbazones. Using 0.34 mmol methyl 3- hydrazine carbodithioate **44i** and ferrocene methanamine **47**, 0.26 mmol of the product were obtained as a beige powder (122 mg, 76 %); m.p:172-175 °C; R_f (EtOAc:Hex 1:4) 0.40; ν_{max} ($CHCl_3$/cm^{-1}) 3443, 3020 (N-H), 1646, 1527 (C=N), 1424 (C=C), 1216 (C=S); δ_H (400 MHz, $CDCl_3$) 8.64 (1H, br s, N-N*H*), 7.79 (2H, br s, S=C-N*H* & H-2), 7.51 (1H, d, *J* 8.0, H-6), 7.45 (1H, d, *J* 8.0, H-5), 4.55 (2H, s, N-CH_2-Cp), 4.33 (2H, s, 2Cp-*H*), 4.24 (7H, s, 2Cp-*H* & 5Cp'-*H*), 2.27 (3H, s, C*H*$_3$); δ_C (100 MHz, $CDCl_3$) 177.1 (C=S), 144.5, 137.4, 133.9, 133.1, 130.6, 128.1, 125.4, 84.2, 68.5 (2C), 68.2 (5C), 67.8 (2C), 43.8, 13.5 (*C*H$_3$); LR-MS

m/z 459 $(M- H)^+$; Found: C, 52.01; H, 4.05; N, 9.17; S, 6.63 Calcd for $C_{20}H_{19}Cl_2FeN_3S$: C, 52.19; H, 4.16; N, 9.13; S, 6.96;

$E_{1/2}$= 21mV.

Compound 42c

1-[1-(3,4--dichlorophenyl)methylidine]ferrocenylmethyl thiosemicarbazone

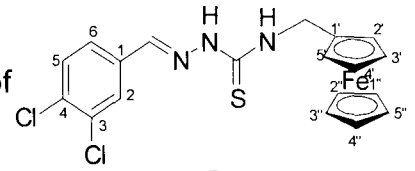

The conditions employed for the preparation of this compound were those described in **GP** for the synthesis of thiosemicarbazones. Using 0.72 mmol of methyl 3-hydrazine carbodithioate **44j** and ferrocene methanamine **47**, 0.32 mmol of the product were obtained as a beige powder (140 mg, 44 %); m.p: 178-180 °C; R_f (EtOAc:Hex 1:4) 0.20; ν_{max} (KBr/cm^{-1}) 3370 (N-H), 1650, 1531 (C=N), 1446 (C=C), 1233 (C=S); δ_H (300 MHz, DMSO-d_6) 11.64 (1H, br s, N-N*H*), 8.74 (1H, t, *J* 6.0, S=C-N*H*), 8.14 (1H, d, *J* 2.0, H-2), 8.03 (1H, s, C*H*=N), 7.74 (1H, dd, *J* 2.0 & 8.4, H-6), 7.67 (1H, d, *J* 8.4, H-5), 4.52 (2H, d, *J* 6.0, N-CH_2-Cp), 4.33 (2H, t, *J* 2.0, 2Cp-*H*), 4.20 (5H, s, 5Cp'-*H*), 4.10 (2H, t, *J* 2.0, 2Cp-*H*); δ_C (75 MHz, DMSO-d_6) 176.7 (C=S), 139.4, 135.0, 131.8, 131.7, 130.8, 128.1, 127.4, 85.7, 68.5 (2C), 68.2 (5C), 67.2 (2C), 42.1 (CH_3); LR-MS *m/z* 444.9 $(M +H)^+$; Found: C, 50.9; H, 3.76; N, 9.13; S, 6.97 Calcd for $C_{19}H_{17}Cl_2FeN_3S$: C, 51.41; H, 3.85; N, 9.46; S, 7.22; $E_{1/2}$= 14 mV.

Compound 42d

1-[1-(3-bromophenyl)ethylidine]ferrocenyl methyl thiosemicarbazone

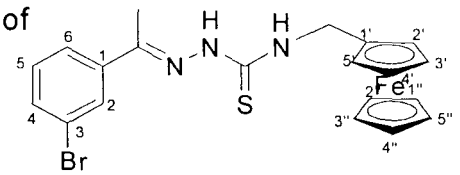

The conditions employed for the preparation of this compound were those described in **GP** for the synthesis of thiosemicarbazones. Using 0.33 mmol of methyl 3-hydrazine carbodithioate **44a** and ferrocene methanamine **47**, 0.12 mmol of the product were obtained as a yellow powder (60 mg, 38 %);

m.p:117-119 °C; R_f (EtOAc:Hex 1:4) 0.30; ν_{max} ($CHCl_3$/cm^{-1}) 3431, 3020 (N-H), 1650, 1524 (C=N), 1465 (C=C), 1218 (C=S); δ_H (400 MHz, $CDCl_3$) 8.72 (1H, br s, N-N*H*), 7.86 (2H, br s, S=C-N*H* & H-2), 7.63 (1H, d, *J* 7.8, H-6), 7.54 (1H, d, *J* 7.8, H-4), 7.23 (1H, t, *J* 7.8 , H-5), 4.53 (2H, s, N-CH_2-Cp), 4.32 (2H, s, 2Cp-*H*), 4.20 (7H, s, 2Cp-*H* & 5Cp'-*H*), 2.28 (3H, s, CH_3); δ_C (100 MHz, $CDCl_3$) 177.2 (C=S), 145.5, 139.6, 132.6, 130.1, 129.3, 124.9, 122.9, 84.3, 68.6 (2C), 68.2 (5C), 67.7 (2C), 43.8, 13.9(*C*H_3); LR-MS *m/z* 471 $(M+H)^+$; Found: C, 51.07; H, 3.92; N, 8.54; S, 6.31 Calcd for $C_{20}H_{20}BrFeN_3S$: C, 51.08; H, 4.28; N, 8.93; S, 6.82; $E_{1/2}$= 10 mV.

Compound 42e

1-[1-(3-bromophenyl)methylidine] ferrocenylmethyl thiosemicarbazone

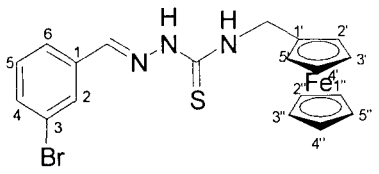

The conditions employed for the preparation of this compound were those described in **GP** for the synthesis of thiosemicarbazones. Using 0.69 mmol of methyl 3-hydrazine carbodithioate **44c** and ferrocene methanamine **47**, 0.15 mmol of the product were obtained as a dark-brown powder (68mg, 22%); m.p:168-171 °C; R_f (EtOAc:Hex 1:4) 0.50; ν_{max} (KBr/cm^{-1}) 3370 (N-H), 1655, 1531 (C=N), 1446 (C=C), 1233 (C=S); δ_H (300 MHz, DMSO-d_6) 11.57 (1H, br s, N-N*H*), 8.65 (1H, t, *J* 6.0, S=C-N*H*), 8.07 (1H, t, *J* 2.0, H-2), 8.05 (1H, s, C*H*=N), 7.71 (1H, dd, *J* 2.0 & 7.5, H-6), 7.58 (1H, dd, *J* 2.0 & 7.5, H-4), 7.36 (1H, t, *J* 7.5, H-5), 4.52 (2H, d, *J* 6.0, N-CH_2-Cp), 4.33 (2H, t, *J* 2.0, 2Cp-*H*), 4.21 (5H, s, 5Cp'-*H*), 4.11 (2H, t, *J* 2.0, 2Cp-*H*); δ_C (100 MHz, DMSO-d_6) 176.7 (C=S), 140.5, 136.6, 132.3, 130.7, 128.8, 126.7, 122.2, 85.7, 68.4 (2C), 68.2 (5C), 67.3 (2C), 41.1 (*C*H_3); LR-MS *m/z* 456 $(M)^+$; Found: C, 49.88; H, 3.72; N, 9.05; S, 7.11 Calcd for $C_{19}H_{18}BrFeN_3S$: C, 50.04; H, 3.97; N, 9.20; S, 7.02; $E_{1/2}$= 13mV.

Compound 42f

1-[1-(2-hydroxyphenyl)methylidine] ferrocenylmethyl thiosemicarbazone

The conditions employed for the preparation of this compound were those described in **GP** for the synthesis of thiosemicarbazones. 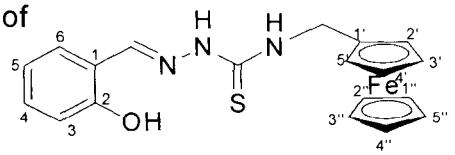
Using 0.88 mmol of methyl 3-hydrazine carbodithioate **44l** and ferrocene methanamine **47**, 0.27 mmol of the product were obtained as a brown powder (107 mg, 31 %); m.p:59-62 °C; R_f (EtOAc:Hex 1:4) 0.30; ν_{max} (KBr/cm^{-1}) 3370- 3118 (OH/N-H), 1650, 1531 (C=N), 1446 (C=C), 1233 (C=S); δ_H (300 MHz, DMSO-d_6) 11.44 (1H, br s, N-N*H*), 9.91 (1H, br s, O*H*), 8.42 (1H, s, C*H*=N), 8.40 (1H, t, *J* 6.0, S=C-N*H*), 7.87 (1H, dd, *J* 2.0 & 7.8, H-6), 7.24 (1H, td, *J* 2.0 & 7,6, H-4), 6.86– 6.79 (2H, m, H-3 & H-5), 4.49 (2H, d, *J* 6.0, N-CH_2-Cp), 4.32 (2H, t, *J* 2.0, 2Cp-*H*), 4.20 (5H, s, 5Cp'-*H*), 4.11 (2H, t, *J* 2.0, 2Cp-*H*); δ_C (100 MHz, DMSO-d_6) 176.2 (C=S), 156.4, 144.8, 139.5, 131.1, 126.3, 119.2, 116.1, 85.8, 68.2 (2C), 67.9 (5C), 67.30 (2C), 42.09 (*C*H$_3$); LR-MS *m/z* 393 (M+H)$^+$; Found: C, 55.32; H, 4.66; N, 9.81; S, 7.40 Calcd for $C_{19}H_{19}FeN_3OS.H_2O$: C, 55.66; H, 5.16; N, 10.25; S, 7.82; $E_{1/2}$= 15 mV.

Compound 42g

1-[1-(3-hydroxyphenyl)methylidine] ferrocenylmethyl thiosemicarbazone

The conditions employed for the preparation of this compound were those described in **GP** for the synthesis of thiosemicarbazones. 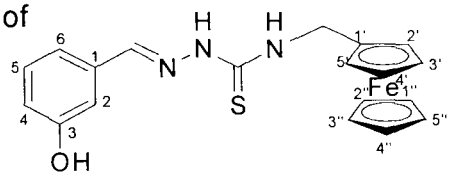
Using 0.88 mmol of methyl 3-hydrazine carbodithioate **44m** and ferrocene methanamine **47**, 0.46 mmol of the product were obtained as a yellow powder (182 mg, 52 %); m.p:166-169 °C; R_f (EtOAc:Hex 2:3) 0.50; ν_{max} (KBr/cm^{-1}) 3370-3118 (OH/N-H), 1650, 1531 (C=N), 1446 (C=C), 1233 (C=S); δ_H (300 MHz, DMSO-d_6) 11.44 (1H, br s, N-N*H*), 9.53 (1H, br s, O*H*), 8.40 (1H, t, *J* 6.0, S=C-N*H*), 7.99 (1H, s, C*H*=N), 7.17 (1H, t, *J*

7.5, H-5), 7.15 (1H, d, *J* 7.5, H-4), 7.12 (1H, t, *J* 2.0, H-2), 6.80 (1H, dd, *J* 2.0 & 7.5, H-6), 4.48 (2H, d, *J* 6.0, N-CH_2-Cp), 4.31 (2H, t, *J* 2.0, 2Cp-*H*), 4.19 (5H, s, 5Cp'-*H*), 4.10 (2H, t, *J* 2.0, 2Cp-*H*); δ_C (100 MHz, DMSO-d_6) 176.5 (C=S), 157.6, 142.6, 135.3, 129.6, 118.2, 117.1, 113.5, 85.7, 68.23 (2C), 68.13 (5C), 67.32 (2C), 42.13 (*C*H_3); LR-MS *m/z* 393 $(M+H)^+$; Found: C, 55.94; H, 4.47; N, 10.26; S, 7.72 Calcd for $C_{19}H_{19}FeN_3OS$. 0.75 H_2O: C, 56.27; H, 5.09; N, 10.36; S, 7.90; $E_{1/2}$= 12 mV.

Compound 42h

1-[1-(4-hydroxyphenyl)methylidine] ferrocenylmethyl thiosemicarbazone

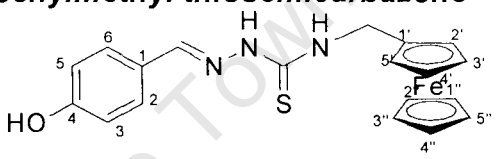

The conditions employed for the preparation of this compound were those described in **GP** for the synthesis of thiosemicarbazones. Using 0.88 mmol of methyl 3-hydrazine carbodithioate **44n** and ferrocene methanamine **47**, 0.05 mmol of the product were obtained as a brown powder (20 mg, 6 %); m.p: 186-189 °C; R_f (EtOAc:Hex 2:3) 0.30; ν_{max} (KBr/cm^{-1}) 3370- 3118 (OH/N-H), 1650, 1531 (C=N), 1446 (C=C), 1233 (C=S); δ_H (300 MHz, DMSO-d_6) 11.20 (1H, br s, N-N*H*), 9.77 (1H, br s, O*H*), 8.36 (1H, t, *J* 6.0, S=C-N*H*), 8.01 (1H, s, C*H*=N), 7.61 (2H, d, *J* 8.7, H-2 & H-6), 6.80 (2H, d, *J* 8.7, H-3 & H-5), 4.49 (2H, d, *J* 6.0, N-CH_2-Cp), 4.32 (2H, t, *J* 2.0, 2Cp-*H*), 4.21 (5H, s, 5Cp'-*H*), 4.12 (2H, t, *J* 2.0, 2Cp-*H*); δ_C (100 MHz, DMSO-d_6) 176.2 (C=S), 159.3, 142.8, 128.8 (2C), 125.0, 115.6 (2C), 85.9, 68.2 (2C), 68.1 (5C), 67.3 (2C), 42.0 (*C*H_3); LR-MS *m/z* 393 $(M+H)^+$; Found: C, 57.55; H, 5.18; N, 10.44; S, 8.86 Calcd for $C_{19}H_{19}FeN_3OS$: C, 58.02; H, 4.86; N, 10.68; S, 8.15;

$E_{1/2}$= 13 mV.

Compound 42i

1-[1-(2,3-dihydroxyphenyl)methylidine]ferrocenylmethyl thiosemicarbazone

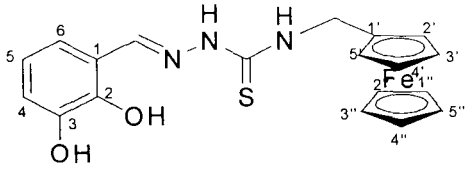

The conditions employed for the preparation of this compound were those described in **GP** for the synthesis of thiosemicarbazones. Using 0.83 mmol of the methyl 3-hydrazine carbodithioate **44p** and ferrocene methanamine **47**, 0.11 mmol of the product were obtained as an orange powder (45 mg, 13 %); m.p: 195-197 °C; R_f (EtOAc:Hex 2:3) 0.20; ν_{max} (KBr/cm^{-1}) 3370 - 3118 (OH/N-H), 1650, 1531 (C=N), 1446 (C=C), 1233 (C=S); δ_H (400 MHz, DMSO-d_6) 11.43 (1H, br s, N-N*H*), 9.47 (1H, br s, O*H*), 8.91 (1H, br s, O*H*), 8.40 (1H, s, C*H*=N), 8.35 (1H, t, *J* 6.0, S=C-N*H*), 7.30 (1H, dd, *J* 2.0 & 8.0, H-6), 6.78 (1H, dd, *J* 2.0 & 8.0, H-4), 6.62 (1H, t, *J* 8.0, H-5), 4.46 (2H, d, *J* 6.0, N-CH_2-Cp), 4.29 (2H, t, *J* 2.0, 2Cp-*H*), 4.18 (5H, s, 5Cp'-*H*), 4.09 (2H, t, *J* 2.0, 2Cp-*H*); δ_C (100 MHz, DMSO-d_6) 176.3 (C=S), 145.6, 145.3, 140.2, 120.9, 118.9, 116.6, 116.4, 85.8, 68.2 (2C), 68.1 (5C), 67.3 (2C), 42.1; LR-MS *m/z* 409 $(M)^+$; Found: C, 56.11 ; H, 4.32; N, 10.68; S, 8.00 Calcd for $C_{19}H_{19}FeN_3O_2S$: C, 55.75; H, 4.67; N, 10.26; S, 7.83; $E_{1/2}$= 26 mV.

Compound 42j

1-[1-(2-hydroxy-3-methoxyphenyl)methylidine] ferrocenylmethyl thiosemicarbazone

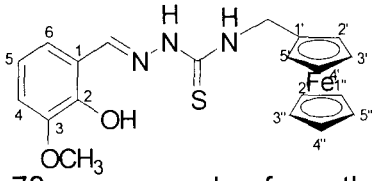

The conditions employed for the preparation of this compound were those described in **GP** for the synthesis of thiosemicarbazones. Using 0.78 mmol of methyl-3-hydrazine carbodithioate **44r** and ferrocene methanamine **47**, 0.19 mmol of the product were obtained as a yellow powder (80 mg, 24 %); m.p: 214-215 °C; R_f (EtOAc:Hex 2:3) 0.40; ν_{max} (KBr/cm^{-1}) 3370-3118 (OH/N-H), 1645, 1531 (C=N), 1446 (C=C), 1233 (C=S); δ_H (400 MHz, DMSO-d_6) 11.46 (1H, br s, N-N*H*), 9.18 (1H, br s, O*H*), 8.43 (1H, s, C*H*=N), 8.38 (1H, t, *J* 6.0, S=C-N*H*), 7.47 (1H, d,

J 7.9, H-6), 6.95 (1H, d, *J* 7.9, H-4), 6.75 (1H, t, *J* 7.9, H-5), 4.49 (2H, d, *J* 6.0, N-CH_2-Cp), 4.29 (2H, t, *J* 2.0, Cp-*H*), 4.18 (5H, s, Cp'-*H*), 4.09 (2H, t, *J* 2.0, Cp-*H*), 3.78 (3H, s, OCH_3); δ_C (100 MHz, DMSO-d_6) 176.4 (C=S), 148.0, 146.0, 139.4, 120.7, 119.0, 117.7, 112.9, 85.8, 68.2 (2C), 68.1 (5C), 67.3 (2C), 55.9, 42.1 (CH_3); HRMS (FAB) *m/z* 424 (M+H)$^+$; Found: C, 56.39; H, 4.99; N, 9.96; S, 7.54 Calcd for $C_{20}H_{21}FeN_3O_2S$: C, 56.75; H, 5.00; N, 9.92; S, 7.57;

$E_{1/2}$= 8 mV.

Compound 42k

1-[1-(2-hydroxy-1-naphtyl)methylidine] ferrocenylmethyl thiosemicarbazone

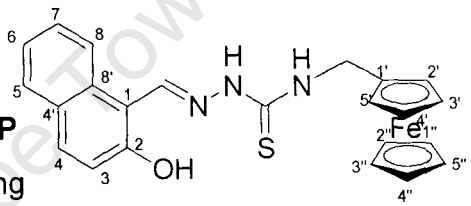

The conditions employed for the preparation of this compound were those described in **GP** for the synthesis of thiosemicarbazones. Using 0.72 mmol of methyl 3-hydrazine carbodithioate **44z** and ferrocene methanamine **47**, 0.06 mmol of the product were obtained as a green powder (28mg, 8%); m.p:110-112 °C; R_f (EtOAc:Hex 2:3) 0.40; ν_{max} (KBr/cm^{-1}) 3370-3118 (OH/N-H), 1645, 1531 (C=N), 1446 (C=C), 1233 (C=S); δ_H (400 MHz, DMSO-d_6), 9.11 (1H, s, C*H*=N), 8.06 (1H, d, *J* 8.4, H-4), 7.72 (1H, d, *J* 9.3, H-5), 7.63 (1H, d, *J* 9.3, H-8), 7.41 (1H, t, *J* 9.3, H-7), 7.18 (1H, t, *J* 9.3, H-6), 6.77 (1H, d, *J* 8.4, H-3), 4.49 (2H, d, *J* 6.0, N-CH_2-Cp), 4.32 (2H, t, *J* 2.0, 2Cp-*H*), 4.21 (5H, s, 5Cp'-*H*), 4.12 (2H, t, *J* 2.0, 2Cp-*H*); δ_C (100 MHz, DMSO-d_6) 178.6 (C=S), 159.0, 137.9, 135.1, 129.6, 128.6, 126.4, 125.9 (2C), 122.8, 119.1, 106.3, 85.9, 69.3 (2C), 68.7 (5C), 68.0 (2C), 50.4; HRMS (FAB) *m/z* 443 (M+H)$^+$; Found: C, 60.45; H, 4.71; N, 9.02; S, 6.98 Calcd for $C_{23}H_{21}FeN_3OS$ .H_2O: C, 60.1; H, 5.03; N, 9.13; S, 6.95; $E_{1/2}$= 19 mV.

Compound 42l

1-[1-(4-hydroxy-3-methoxyphenyl)methylidine] ferrocenylmethyl thiosemicarbazone

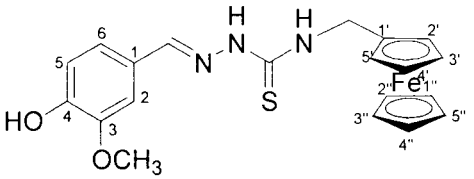

The conditions employed for the preparation of this compound were those described in **GP** for the synthesis of thiosemicarbazones. Using 0.78 mmol of methyl 3-hydrazine carbodithioate **44s** and ferrocene methanamine **47**, 0.22 mmol of the product were obtained as a brown powder (95 mg, 28 %); mp:188- 191 °C; R_f (EtOAc:Hex 2:3) 0.45; ν_{max} (KBr/cm^{-1}) 3370-3118 (OH/N-H), 1645, 1531 (C=N), 1446 (C=C), 1233 (C=S); δ_H (400 MHz, DMSO-d_6) 11.36 (1H, br s, N-N*H*), 9.37 (1H, br s, O*H*), 8.35 (1H, t, *J* 6.0, S=C-N*H*), 8.00 (1H, s, C*H*=N), 7.38 (1H, d, *J* 2.0, H-2), 7.09 (1H, dd, *J* 2.0 & 8.0, H-6), 6.79 (1H, d, *J* 8.0, H-5), 4.47 (2H, d, *J* 6.0, N-CH_2-Cp), 4.28 (2H, t, *J* 2.0, 2Cp-*H*), 4.21 (5H, s, 5Cp'-*H*), 4.10 (2H, t, *J* 2.0, 2Cp-*H*), 3.75 (3H, s, OCH_3); δ_C (100 MHz, DMSO-d_6) 176.2 (C=S), 148.9, 148.0, 143.0, 125.4, 122.0, 115.4,109.6, 86.1, 68.2 (2C), 67.9 (5C), 67.3 (2C), 55.7, 41.9 (*C*H$_3$); HRMS (FAB) *m/z* 423 (M)$^+$; Found: C, 56.16; H, 4.86; N, 9.74; S, 7.33 Calcd for $C_{20}H_{21}FeN_3O_2S$: C, 56.75; H, 5.00; N, 9.92; S, 7.57; $E_{1/2}$= 13 mV.

Compound 42m

1-[1-(2,3,4-methoxyphenyl)methylidine] ferrocenylmethyl thiosemicarbazone

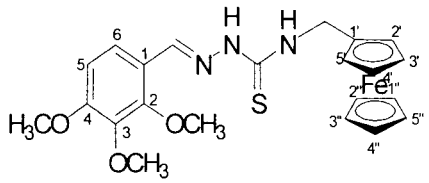

The conditions employed for the preparation of this compound were those described in **GP** for the synthesis of thiosemicarbazones. using 0.67 mmol of methyl 3-hydrazine carbodithioate **44u** and ferrocene methanamine **47**, 0.15 mmol of the product were obtained as an orange powder (72mg, 23%); m.p:61-63 °C; R_f (EtOAc:Hex 1:4) 0.20; ν_{max} (KBr/cm^{-1}) 3370 (N-H), 1645, 1531 (C=N), 1446 (C=C), 1233 (C=S); δ_H (300 MHz, DMSO-d_6) 11.4 (1H, br s, N-N*H*), 8.38 (1H, t, *J* 6.0, S=C-N*H*), 8.30 (1H, s, C*H*=N), 7.75 (1H, d, *J* 8.7, H-6), 6.86 (1H, d, *J* 8.7, H-

5), 4.46 (2H, d, *J* 6.0, N-C*H*$_2$-Cp), 4.29 (2H, t, *J* 2.0, 2Cp-*H*), 4.19 (5H, s, 5Cp'-*H*), 4.09 (2H, t, *J* 2.0, 2Cp-*H*), 3.80 (3H, s, OC*H*$_3$), 3.78 (3H, s, OC*H*$_3$), 3.73 (3H, s, OC*H*$_3$); δ_C (100 MHz, DMSO-d_6) 176.3 (C=S), 155.0, 152.7, 141.6, 138.4, 120.6, 120.2, 108.6, 85.9, 68.2 (2C), 68.1 (5C), 67.3 (2C), 61.8, 60.4, 56.0, 42.0 (*C*H$_3$); HRMS (FAB) *m/z* 467; Found: C, 56.57; H, 5.35; N, 9.10; S, 7.10 Calcd for $C_{22}H_{25}FeN_3O_3S$. H_2O: C, 54.48; H, 5.19; N, 8.65; S, 6.59, $E_{1/2}$= 9mV.

Compound 42n

1[1-(4-chloro-3-nitrophenyl)methylidine]ferrocenylmethyl thiosemicarbazone

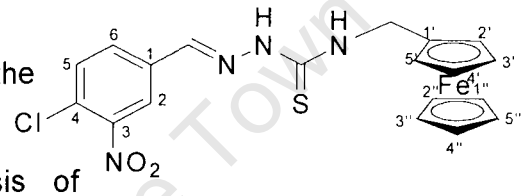

The conditions employed for the preparation of this compound were those described in **GP** for the synthesis of thiosemicarbazones. Using 0.69 mmol of methyl 3-hydrazine carbodithioate **44k** and ferrocene methanamine **47**, 0.27 mmol of the product were obtained as a beige powder (121 mg, 39 %); m.p:182-185 °C; R_f (EtOAc:Hex 2:3) 0.40; ν_{max} (KBr/cm^{-1}) 3370 (N-H), 1650, 1531 (C=N), 1446 (C=C), 1233 (C=S); δ_H (300 MHz, DMSO-d_6) 11.72 (1H, br s, N-N*H*), 8.80 (1H, t, *J* 6.0, S=C-N*H*), 8.48 (1H, d, *J* 2.0, H-2), 8.10 (1H, s, C*H*=N), 8.09 (1H, dd, *J* 2.0 & 8.4, H-6), 7.81 (1H, d, *J* 8.4, H-5), 4.53 (2H, d, *J* 6.0, N-C*H*$_2$-Cp), 4.33 (2H, t, *J* 2.0, 2Cp-*H*), 4.19 (5H, s, 5Cp'-*H*), 4.09 (2H, t, *J* 2.0, 2Cp-*H*); δ_C (75 MHz, DMSO-d_6) 176.8 (C=S), 148.1, 138.4, 134.9, 131.7, 131.6, 124.8, 122.8, 85.5, 68.4 (2C), 68.2 (5C), 67.2 (2C), 42.1 (*C*H$_3$); LR-MS *m/z* 456 $(M+H)^+$; Found: C, 49.99; H, 3.46; N, 11.94; S, 7.64 Calcd for $C_{19}H_{17}ClFeN_3SO$: C, 50.15; H, 3.76; N, 12.26; S, 7.02; $E_{1/2}$= 17mV.

Compound 42o

1(2-bipyridinyl) ferrocenylmethyl thiosemicarbazone

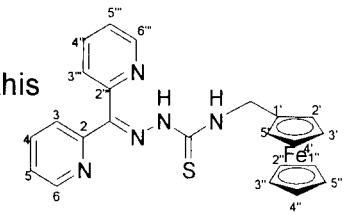

The conditions employed for the preparation of this compound were those described in **GP** for the synthesis

of thiosemicarbazones. Using 0.69 mmol of methyl 3-hydrazine carbodithioate **44y** and ferrocene methanamine **47**, 0.37 mmol of the product were obtained as a light green powder (170 mg, 54 %); m.p:169-172 °C; R_f (100 % MeOH) 0.45; ν_{max} (KBr/cm^{-1}) 3370 (N-H), 1650, 1531 (C=N), 1446 (C=C), 1233 (C=S); δ_H (300 MHz, DMSO-d_6) 13.43 (1H, br s, N-N*H*), 8.85-8.82 (2H, m, S=C-N*H* & pyridine-*H*), 8.58–8.56 (1H, m, pyridine-*H*), 8.16 (1H, dt, *J* 0.9 & 7.8, pyridine-*H*), 8.01-7.90 (2H, m, pyridine-*H*), 7.60-7.55 (1H, m, pyridine-*H*), 7.47–7.43 (2H, m, pyridine-*H*), 4.53 (2H, d, *J* 6.0, N-CH_2-Cp), 4.32 (2H, t, *J* 2.0, 2Cp-*H*), 4.17 (5H, s, 5Cp'-*H*), 4.11 (2H, t, *J* 2.0, 2Cp-*H*); δ_C (100 MHz, DMSO-d_6) 176.9 (C=S), 155.1, 151.1, 148.6, 148.4, 148.1, 141.3, 137.5, 137.0, 126.9, 124.7, 123.84, 85.2, 68.2 (2C), 68,1 (5C), 67.3 (2C), 42.6 (*C*H_3); LC-MS *m/z* 455 $(M+H)^+$; Found: C, 59.72; H, 4.42; N, 15.54; S, 7.41 Calcd for $C_{23}H_{21}FeN_5S$. 0.5 H_2O: C, 59.66; H, 4.78; N,15.11; S, 6.91; $E_{1/2}$= 8mV.